UNIVERSIDAD DE CHILE
FACULTAD DE CIENCIAS FÍSICAS Y MATEMÁTICAS
DEPARTAMENTO DE INGENIERÍA DE MINAS

NUMERICAL MODELING OF THREADBAR UNDER DYNAMIC LOADING

TESIS PARA OPTAR AL GRADO DE DOCTOR EN
INGENIERÍA DE MINAS

LINA YESENIA MARULANDA CARDONA

PROFESOR GUIA:
JAVIER VALLEJOS MASSA

MIEMBROS DE LA COMISIÓN:
MAURICIO SARRAZÍN ARELLANO
CHARLIE LI
KIMIE SUZUKI MORALES

SANTIAGO DE CHILE
2021

ABSTRACT OF THE THESIS SUBMITED FOR THE DEGREE OF: Doctor in Mining Engineering

AUTHOR: Yesenia Marulanda

DATE: September 2021

ADVISOR: Javier Vallejos

NUMERICAL MODELING OF THREADBAR UNDER DYNAMIC LOADING

The prevention or mitigation of the effects of rockburst in rock masses subjected to high levels of stress, is one of the most challenging problems for the field of study of rock mechanics.

Although the use of bolts is a main requirement when designing / installing a reinforcement system for underground mines, the design and selection guidelines of these that are used today are limited, since the choice of an element or another is often based on empirical knowledge and field observations.

In this context, the use of laboratory scale test to represent in-situ conditions has become a useful tool to quantify the deformation and energy absorption of support elements and systems, providing the possibility for a comparative analysis of the performance between different types of fortification and retention elements, as well as their behavior under static and / or dynamic load.

However, it is observed that, for practical reasons, most laboratory tests involve a high cost in preparation and validation. The challenge then is focused on how to obtain reliable results that can be used in the design of fortification systems for underground excavations. Numeric modeling appears as an alternative that, in addition to complementing laboratory results, it can be used to explain the process of deformation and energy absorption of tested support elements.

An FDM numerical model is proposed considering that is necessary to implement different boundary shapes, different kinds of boundary conditions, and regions containing a number of different materials in order to represent the explicit dynamic response of reinforcement elements tested in laboratory.

The main result is the accurately representation of the dynamic response of grout and threadbar (bolt) by varying the test conditions.

Grout results are presented in terms of σ_1 Vs σ_3 taking values between 40-60 and 3-11 MPa respectively and τ Vs σ_n between 16-21 and 11-23 MPa. Obtained results are compared with appropriate failure envelopes showing good agreement.

Bolt results are mainly presented in terms of load capacity Vs displacement and absorbed energy Vs displacement. Results from initial model was compared and calibrated with information extracted from the existing literature and available laboratory results. After parametric analysis the relation between absorbed energy, displacement and characteristics of the bolt was established.

RESUMEN DE LA TESIS PARA OPTAR AL GRADO DE: Doctor En Ingeniería de Minas

AUTOR: Yesenia Marulanda

FECHA: Septiembre 2021

PROFESOR GUIA: Javier Vallejos

MODELAMIENTO NUMERICO DE BARRA HELICOIDAL SOMETIDA A CARGA DINAMICA

La prevención o mitigación de los efectos producto de estallidos de roca en macizos rocosos sometidos a altos niveles de esfuerzo, es uno de los problemas más desafiantes para el campo de estudio de la mecánica de rocas.

Si bien el uso de pernos es un requerimiento principal a la hora de diseñar un sistema de fortificación para minas subterráneas, las pautas de diseño y selección de estos que se usan en la actualidad se encuentran limitadas, pues la elección de un elemento u otro a menudo se basa en el conocimiento empírico y las observaciones de campo.

En este contexto, el uso de ensayos de laboratorio para representar las condiciones in-situ se ha convertido en una herramienta útil para cuantificar la deformación y capacidad de absorción de energía de elementos/sistemas de fortificación, generando la posibilidad de desarrollar un análisis comparativo entre los diferentes tipos de elementos de fortificación y retención, así como también su desempeño bajo carga estática y/o dinámica.

Sin embargo, se observa que, por razones prácticas, la mayoría de los ensayos de laboratorio involucran un alto costo en preparación y validación. El desafío se enfoca entonces en cómo obtener resultados fiables que puedan ser usados en el diseño de sistemas de fortificación para excavaciones subterráneas. El modelamiento numérico aparece como una alternativa que, en conjunto con resultados de laboratorio, puede ser usado para explicar la respuesta dinámica de elementos de refuerzo

Se propone un modelo numérico FDM considerando que es necesario implementar diferentes superficies, diferentes condiciones de borde y regiones que representan materiales diferentes para representar la respuesta dinámica explícita de los elementos de refuerzo ensayados en laboratorio.

El resultado principal es la representación precisa de la respuesta dinámica de la lechada y la barra helicoidal (perno) al variar las condiciones del ensayo.

Los resultados de la lechada se presentan en términos de σ_1 Vs σ_3 tomando valores entre 40-60 y 3-11 MPa respectivamente y τ Vs σ_n entre 16-21 y 11-23 MPa. Los resultados obtenidos se comparan algunas envolventes de falla mostrando buena relación.

Los resultados de los pernos se presentan principalmente en términos de capacidad de carga Vs desplazamiento y energía absorbida Vs desplazamiento. Los resultados del modelo inicial se compararon y calibraron con información extraída de la literatura existente y los resultados de laboratorio disponibles. Luego del análisis paramétrico se estableció la relación entre energía absorbida, desplazamiento y características del ensayo.

Acknowledgements

Firstly, I would like to acknowledge to the major sponsors of the research, CONICYT/PIA Project AFB180004 of the Advanced Mining Technology Center (AMTC), Advanced Human Capital Attraction and Insertion Program of the National Commission for Scientific and Technological Research (CONICYT) and the Geomechanical and Mining Design Laboratory of the University of Chile.

Besides, I would like to thank to Itasca Chile who, in agreement with the Department of Mining Engineering (DIMIN), supplied the software licenses that allowed the development of the project.

The other member of the research team includes my supervisor, Dr. Javier Vallejos, who supervised this thesis, providing much-needed direction, technical review and support, as well as co-authoring result products.

I can't be more grateful with all the staff members of the "ofish" for the continuous laughs and jokes. You guys made easier all this difficult journey

Finally, tremendous thanks to my husband Pablo, for trying to keep me on track when I had my doubts, an also for his constant love and support, which made this work possible.

To Tinto.

"What counts is not necessarily the size of the dog in the fight; it's the size of the fight in the dog."

General Dwight D. Eisenhower

Table of Contents

List of Figures

List of tables

List of equations

1 Introduction

1.1 Motivation

As the depth of mining developments and definitive mining excavations increases, failure processes in hard rock induced by stress redistribution in areas far from the excavations and around them become unavoidable.

In some cases, the rock mass fails violently, leading to seismic events caused by sliding along planes of weakness or by shear rupture. In other cases, the rock mass fractures gradually or suddenly, causing damage to the walls of the excavation. Either a remote fault or around the excavation or a combination of these mechanisms can lead to a rock burst.

In order to mitigate the damage caused by rock burst, various elements of dynamic reinforcement, support and retention have been developed and used in mining operations. Regarding the rock support design, commonly adopted methods, ranging from analytical, empirical, numerical, to observational methods (Cai & Kaiser, 2018).

Kaiser and Cai (2013a, b) point out that the commonly adopted methodologies are flawed and should be reviewed.

Recently, Stacey (2016) suggests that is not satisfactory to follow conventional design approaches for fortification design and proposed a risk-consequence approach in which design decisions are made based on quantifying risk measures.

Both determination of the demand that will be imposed on the support during a rockburst event and support system absorption energy capacity are issue to be solved as lack of accurate estimates reduces confidence in the selected support design. Therefore, control of rockburst effects continues to challenge the underground mining, motivating more research and / or improvements in dynamic fortification systems capacity.

After identifying the deficiencies of the design methodologies used during the last decades, there has been an increase in the use of laboratory test results as a support tool in the analysis and design of the fortification systems necessary to ensure excavations stability.

However, the execution of laboratory testing programs implies a high cost in terms of time and validation, which implies that only a limited number of them have been successfully completed. In this context, numerical modeling is a tool that allows representing the process and improving laboratory tests, which has become increasingly relevant.

In this thesis a numerical model that simulates the response of threadbar (dynamic rockbolt most used in Chilean underground mining) under dynamic impact testing is developed. It is expected that the proposed model will serve as a tool in the calibration and execution of laboratory tests.

1.1 Scope, objectives and methodology

When talking about the dynamic response of rock support elements, research can be separated in four study areas:

1. Studying the causes and origins of seismic events as well as their propagation through the ground and the mechanisms under which their energy is transferred to the support system. Such an analysis can be useful to define guidelines for mining activities in order to minimize the occurrences and consequences of rock bursts. Also, this study can reveal important design criteria for rock support elements, e.g., the velocity of ejected rocks or their mass. This study is limited to fault-slip burst.
2. Dynamic testing of support elements. Tests are important in order to determine accurately the mechanical properties of various support elements. Better knowledge of these properties will allow engineers to design an optimal and safe support system for a given situation from results obtained in laboratory tests.
3. Developing new support elements. There is always a need for better and economically more interesting support systems. Improvements can come from the analysis of experimental tests or simply the development of new technologies.
4. Modeling the response of rock support elements. With the permanently growing potential of computational methods, numerical simulation of tunnel stability is now very common. However, in order to predict the dynamic stability of a reinforced excavation, a model for each support element is required. Such a model has to be simple enough to reduce calculation time but robust enough to obtain reliable results close to the real response of the modeled element.

The present research is indirectly related with item 2 and concerns directly with item 4, applied particularly to the threadbar.

The main objective of the research is to develop a numerical model that simulates the explicit mechanical response of the threadbar under to dynamic loads based on input parameters typical of impact laboratory tests. For this, the project has been separated into 3 stages, with different specific objectives and results for each one:

1. **Modeling parameters establishment for the correct simulation of the behavior of the independent elements of the model**. In this stage, the specific objective is to establish the modeling parameters for dynamic tests and fortification elements simulation, which allow to determine optimally the energy requirements of the element / test system and obtain a response according to the expected results.

   The methodology in this stage of the research consists in principle in establishing the parameters that will define the three fundamental components of the numerical model:

   - A grid of finite differences.
   - Constitutive behavior and properties of the materials to be represented in the model.
   - Initial and boundary conditions.

The grid defines the geometry of the test to be represented, to define it, the real dimensions of the equipment, main components and the elements tested in laboratory testing.

The constitutive behavior and the properties associated with the materials present in the tests (steel, grout), determine the type of response that the model will present when simulating the dynamic impact test (in terms of load and deformation). These will be assigned from the collected bibliography, in the case of grout the properties are mainly controlled by the water: cement ratio and the radial confinement that acts on the outer surface of the grout ring (Hyett et al., 1992).

In the case of the bolt, its properties will depend mainly on its diameter, the dynamic resistance of the steel and its confinement. In the case of the interfaces to be defined, their resistance will depend mainly on their normal and shear stiffness, defined from the calibration of the published results.

The initial and boundary conditions define the condition of the test equipment / reinforcement element system before the test is performed, that is, the condition before a change or disturbance is introduced in the initial configuration of the model.

After these conditions are defined in FLAC, the initial equilibrium state of the model is reached.

Code programming that simulates both the dynamic impact laboratory test and the results obtained when testing threadbar. The specific objective is formulating a FISH (programming language) code is that relates the de input parameters in order to present the response of the threadbar and each of the other components when subjected to dynamic loading.

Once the initial equilibrium state for the model is reached, using the FISH programming language, the instructions will be introduced that will allow to represent the dynamic test to be modeled, that is, a test where a mass falls from a given height impacting the lower end of the bolt embedded in cement grout (installed in a steel tube simulating the rock mass), causing it deformation and possible failure.

There are various models that describes dynamic structures under a certain applied force using resolution schemes in which the entire system is simplified to be described through a damped oscillator. In this sense, the equations that describe the testing process are well known, as is their solution.

However, the complexity of these systems lies in the way in which the components stiffness and damping conditions are applied.

To solve the numerical model, the test system will be divided into two scenarios. The first scenario will be the one where the mass in free fall is described (used in dynamic tests of laboratory) until it impacts on the lower part of the steel tube.

The second scenario of the model is the one of main interest for the research project, as it is the one that defines the behavior of the system after the impact occurs, when the mass begins to move along with the bolt, stretching or sliding it until reaching failure.

After the impact occurs, the model will be presented simplified as a free body diagram, therefore, the system can be represented by two differential equations, the first one describes the movement of the bolt and the second the movement of the grout. St-Pierre (2007) presented a similar scheme when he developed his analytical model for the cone bolt.

The equations of motion are solved using an explicit iterative numerical method over time combined with the FLAC3D unbalanced force criteria.

The stiffness of the rock bolt and the grout that are considered in the differential equations of motion are approximated by their equivalent stiffness for the systems connected in series (Rao & Yap, 2011). Furthermore, the viscous damping of the bolt and the grout will be proportional to their mass and stiffness, applying the commonly known classical damping (Rayleigh, 1877).

The properties the threadbar are well known and it is possible to define them from the catalogs presented by each of their manufacturers. However, steel is known to change its yield strength and maximum strength under dynamic load conditions.

According to Malvar and Crawford (1998), steel strength magnitudes can be estimated by the elastic properties of the steel through a dynamic increase factor (DIF) that is integrated into the model to simulate the behavior of the bolt in a real way.

Within the results of this stage, a numerical code will be delivered to run in FLAC3D, calibrated and validated with laboratory tests collected from the bibliography.

Perform a parametric analysis to define the threadbar response under different loading conditions. The specific objective of this stage is to define trends for threadbar according to their energy absorption capacity, defined from numerical modeling and dependent on its characteristics.

This objective has a direct relation with laboratory testing, as can serve as capacity guide for threadbar dynamic test configuration, supported by a scientific and empirical basis, as it will be defined from the numerical modeling of the bolt / test interaction.

Depending on how the test parameters are varied, linear trends are established from which it is possible to identify how much load and how much deformation the tested element reach.

1.2 Thesis outline

In addition to the present chapter where general overview of the scope, objectives and the problem that motivates the present investigation are described, the document will be formed by the following chapters:

Chapter 2 presents a detailed procedure and configuration of dynamic and static tests review, followed by an extensive review of dynamic tests results focusing on threadbar

published results. An analysis of the collected data is made and used as input for model calibration in chapter 3 and chapter 4.

Chapter 3 describes the first model developed to simulate the threadbar dynamic response. A procedure to calculate the parameters of the model is presented. Then both simulation results and experimental tests are compared.

Chapter 4 is dedicated to the second of two numerical models proposed to analyze the threadbar dynamic response. In this last model, the threadbar rib is modeled as 3D geometry in an external software and afterwards imported in FLAC3D. A parametric analysis is presented.

Chapter 5 summarizes the work done, presents conclusions and raises certain questions that need further investigation.

2 Dynamic laboratory testing and its simulation through numerical modeling. State of the art.

2.1 Laboratory tests

2.1.1 Static tests

Below is a brief summary of the state of the art as it relates to static tests carried out on bolts and meshes.

2.1.1.1 Bolts

In the existing literature, it is shown that several authors have been interested in determining the behavior of the bolt-grout interface, as a result a large number of experimental and theoretical investigations are available. This section describes and examines the most significant related studies conducted in recent years.

It is worth noting that the majority of published research on bolt performance has been directed at mining applications rather than civil engineering works (Stillborg, 1983). The reason is that, in general, civil engineering projects do not consider the use of bolts as the main support technique. Due to the prominent use of bolts in the mining industry, it is not surprising that most research and testing programs are in the context of mining.

Pull-out test

To test experimentally the anchoring capacity of rock and cable bolts, so-called pull-out tests are carried out both in the laboratory and in situ. In the laboratory, bolts are anchored to a rock sample or alternatively to an artificial sample (made of cement or concrete) whose mechanical properties are comparable to those of a typical rock.

Sheathed length is the distance over which the studs are grout cemented into steel tubes that have the same internal diameter as the drill diameters used in the field. Since the purpose of this test is to study the load transfer mechanism between the bolt and the surrounding media, the sheathed length should be short enough to avoid bolt failure.

The test consists of applying an axial tensile load to the bolt at the end that protrudes from the hole. The far end of the bar is free and thus, the axial force at this point is equal to zero. The load and displacement at the loaded end are recorded during the test. The scheme of a pull-out test is presented in Figure 1.

Test results are usually presented as a graph of load vs. displacement. If the bolt is instrumented over its length, it is possible to know the axial deformation and the axial load distribution in the embedment length.

The tests can be controlled in terms of displacement or axial load in order to determine the behavior of the bolt-grout interface. It is important to mention that the measurements that occur under the control of axial displacement are more reliable.

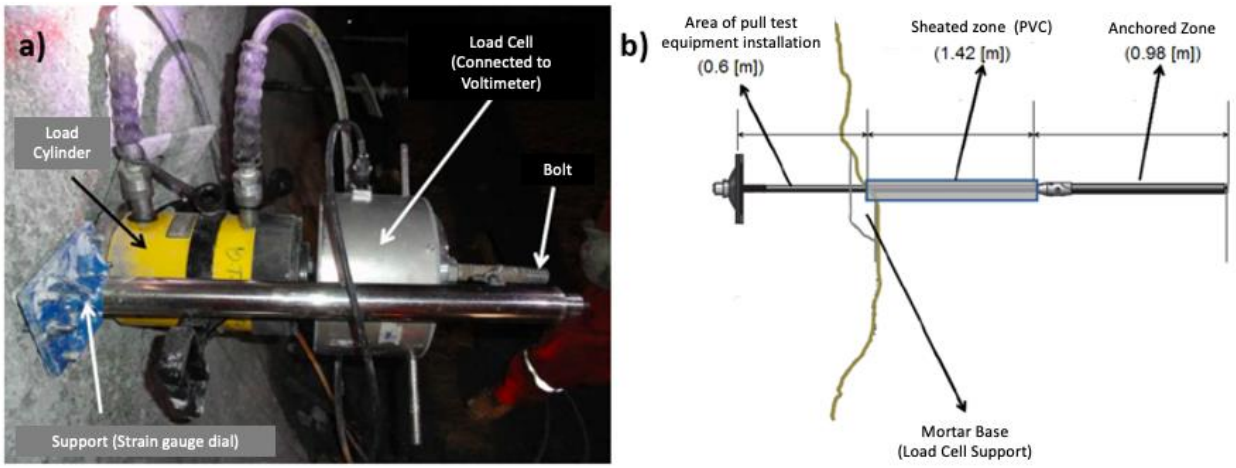

Figure 1 a) Pull test equipment. b) Bolt installation diagram **(Garay & Zepeda, 2012)**

The widespread use of laboratory pull tests has led to standardization in several countries. Regarding the on-site execution of such tests, the ISRM described a suggested method for rock bolts (ISRM, 1973). In practice, laboratory tests are preferred to in situ tests because they are more complete (study parameters can be easily changed and more measurements can be made), generally cheaper tests, and easier to control.

In addition, the standardization of the laboratory pull tests allows the comparison of the results obtained for different types of bolts. Sophisticated testing equipment has been developed since the 90s, allowing testing of the influence of a large number of parameters, such as confinement pressure, water-cement ratio of the grout or thickness of the grout ring.

On the other hand, in situ tests are useful to know if the use of a specific type of bolt is compatible with the mechanical properties of the surrounding medium and its degree of damage.

Table 1 presents a summary of the most relevant experimental studies of static tests performed on bolts that are available in the literature.

Table 1 Pull out test experimental studies summary.

Reference	Objective	Tests program
Farmer, 1975	First investigations on the distribution of stress along the anchoring of a grout bolt. Special emphasis on the importance of such a distribution in determining design parameters.	Pull laboratory test in 20 mm diameter steel bars cemented with resin in different materials (concrete, limestone and chalk).

Reference	Objective	Tests program
Dunham, 1976	Control the stress distributed along the bar. ERS gauges (electrical resistance strain gauges) were installed at different points of the bar and a back analysis of the shear stress was performed from the measured deformations	Pull test on 25 mm diameter corrugated steel bars cemented with resin in 36 mm diameter holes in sandstone blocks.
Benmokrane et al., 1995	Proposes a tri-linear model of loss of adhesion at the bolt-grout interface.	Pull out test to grout cemented bolts and cables, varying the cemented length.
Hyett et al., 1995	Proposes constitutive law for bond failure for grout bolts. To date, this work is considered a reference within the community. The new law defines the friction-expansion behavior at the bolt-grout interface.	Pull laboratory test. Tests performed using a modified Hoek cell, MHC, which allows to study the effect of the confining pressure on the adhesion capacity. the MHC has become a laboratory standard.
Li & Stillborg, 1999	Introduces the term disengagement front to designate the boundary between the disengaged and mated parts of the cemented length.	Pull test on bars with instrumentation
Hagan, 2004	Suggests that the confinement acting on the free face of the rock (due to the reaction force) can significantly change the stress field around the hole.	Pull test on resin cemented 21.7 mm diameter bolts, using two different test settings.
Moosavi et al., 2005	When comparing with the results of Hyett et al. (2015), both agree with the postulate that the slip between the cablebolt and the grout is mainly frictional in nature, hence the importance of radial pressure. From the experimental results, a non-linear relationship between confining pressure and adherence is presented.	Pull out test on three types of cemented bolts: 22 and 28 mm diameter Rebars and 20 mm diameter Dywidag. MHC was used.

2.1.2 Dynamic tests

2.1.1.2 Dynamic test facilities.

For around twenty-five years a number of testing facilities have been constructed by the mining industry in order to investigate the dynamic behaviour of reinforcement elements and surface support. These were mainly developed in Canada, Australia and South Africa.

Hadjigeorgiou and Potvin (2008) as well as Player et al., (2008) are among the authors who have presented overviews and results of dynamic testing of rock support.

The facilities work by using various loading mechanisms and boundary conditions, whilst
the testing principles of those facilities are similar. The dynamic load is simulated by the impact of an element with known momentum with another element (generally stationary). The mass used for producing direct impact can be guided in a variety of ways (Villaescusa et al.,2005a). See Table 2.

Table 2 Conditions for simulate dynamic load. Modified from (Villaescusa et al., 2005a)

Dynamic loading can come from	Direct impact could use
• Impact of a mass onto an element. • Impact of the structure/element onto a fixed element. • Impact of a mass onto a load transfer mechanism or energy dissipation element. • Impact from a mass directly onto the test structure/element and in particular shotcrete panel tests. • Impact from a mass onto a surface that spreads the load from the moving mass to the test structure/element.	• A free-falling mass. • A guided mass. • A thrown mass.

For the purpose of this document, dynamic testing procedure is defined as a test that allows a better understanding on how a reinforcement element behaves under rapid loading conditions. The test should replicate as closely as possible the loading conditions of a dynamic event in situ. This chapter aims at clarifying and consolidating the critical information on the most reported testing rigs.

WASM Western Australia School of Mines Dynamic Test Facility

The WASM dynamic test facility is the most recent and instrumented facility, developed at the Western Australia School of Mines in Kalgoorlie, Australia. The objective of this test is to quantify the force-displacement responses of the reinforcement elements (between the collar and anchorage zones separated by a discontinuity) subjected to dynamic loading.

Figure 2 represents the WASM dynamic testing rig, highlighting three main components: reinforcement system, the collar region, and the anchoring zone. At a mine, the last two represent an ejected rock block and a stable one, respectively. See Figure 3 for a detailed description of facility components.

Dynamic loading is applied to test samples through momentum transferring. Using this facility, not only tests on reinforcement systems but significant testing mesh programs have been made. In addition, soon there will be testing on fibrecrete panels, and the combination of mesh and reinforced system, using the same loading principles. (Player et al. 2008).

For bolt testing, the element is installed in a split steel tube. The drop mass and bolt sample are lifted by a beam to a predefined height. The beam and the mass, as well as the sample, freely fall and the beam is then stopped on to a reaction surface to rapidly decelerate while the momentum of the mass loads the collar of the reinforcement, see Figure 4. This type of loading has some similarity to the dynamic loading of a tendon installed in situ.

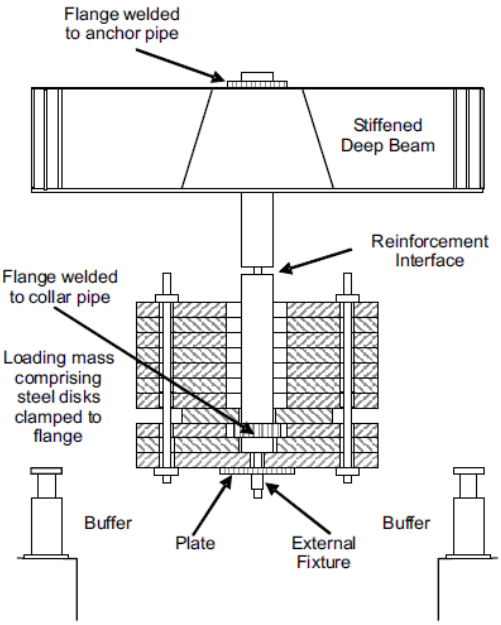

Figure 2 Schematic of testing arrangement showing the major components. Modified from (Villaescusa et al., 2005b)

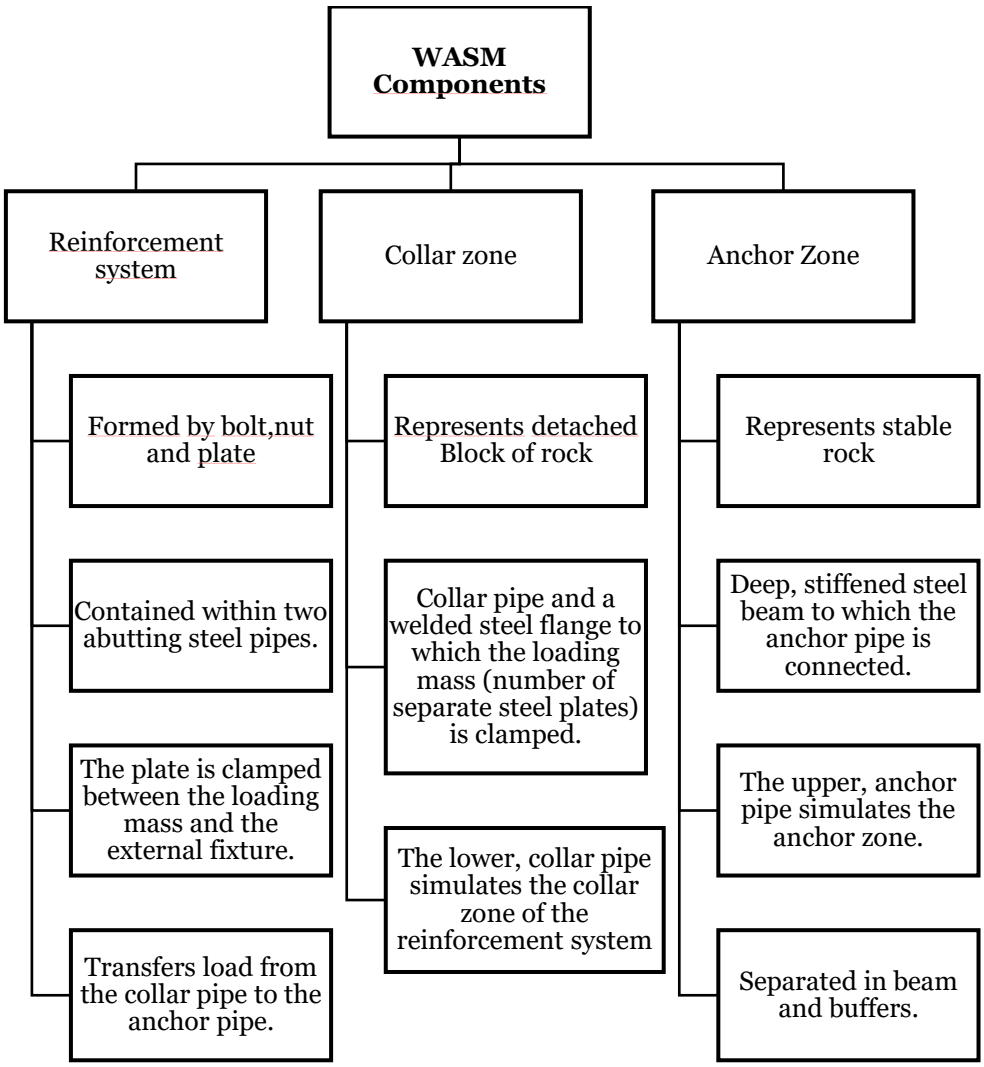

Figure 3 WASM test main component characteristics

Figure 4 WASM test procedure

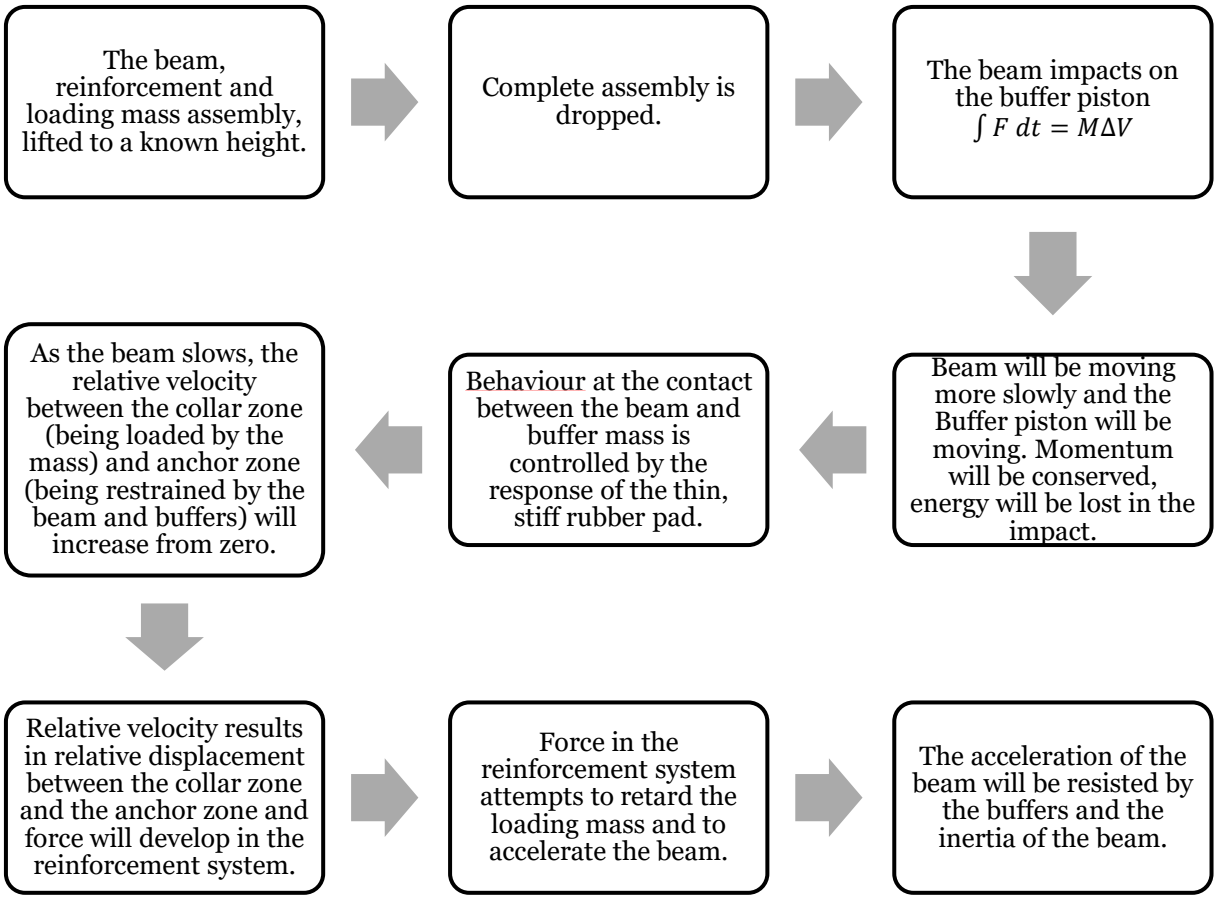

WASM facility is characterized by the capacity to calculate the energy absorbed by any component at any time during a test. Hence, instrumentation was designed or selected to measure and record force, displacement, acceleration and strain in small time increments of the following (Villaescusa et al. 2005a):

- **Reinforcement system:** bolt, surface hardware, collar and anchor.
- **Simulated ejected rock:** the integrated steel rings and lower pipe length.
- **Simulated rock mass:** the drop beam and upper pipe length.
- **Buffers:** the impact surface.

Instrumentation and data acquisition are described in Figure 5 and Figure 6.

The setup of WASM Dynamic Test Facility for a reinforcement system dynamic test is shown in Figure 7.

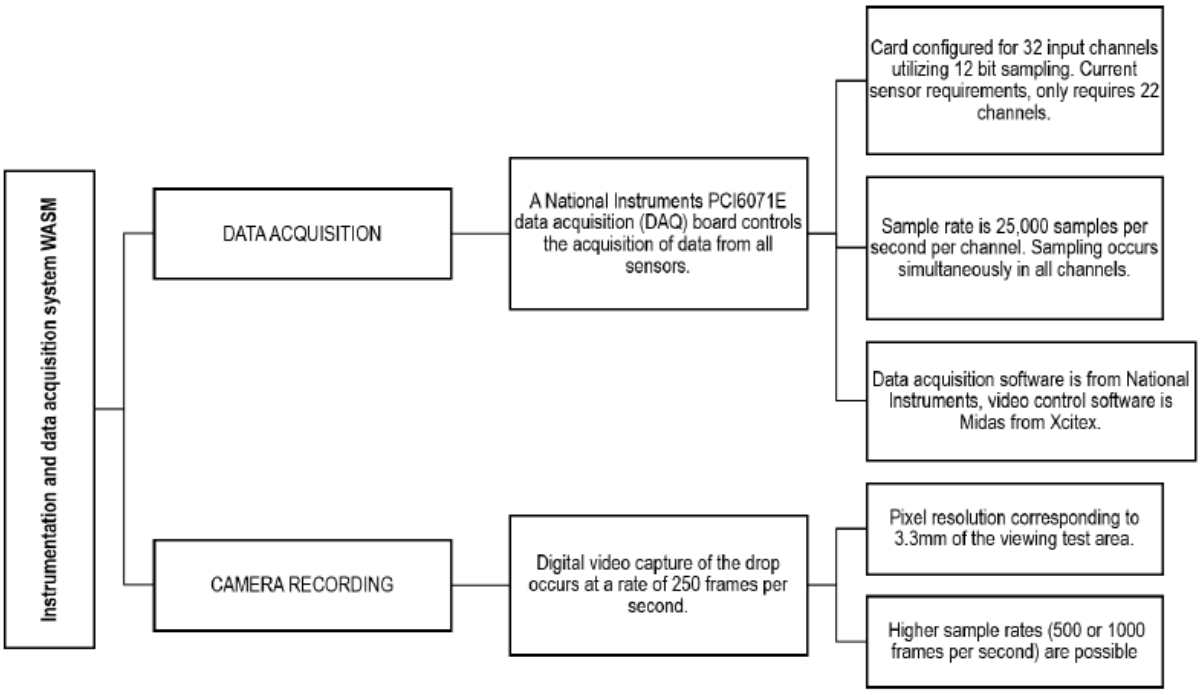

Figure 5 Instrumentation and data acquisition system WASM (1).

Noranda Technology Centre/CANMET dynamic test facility

Noranda Technology Centre Impact Test acility, now called CANMET – Mining and Mineral Sciences Laboratories, was developed at the CANMET Mining Sciences Laboratories in Ottawa, Canada and is primarily used to test rock bolts.

Each test is conducted by dropping a known mass, from a known height, onto a plate connected to a tendon grouted inside a steel tube. The energy input is controlled by the drop height and the mass. The setup of CANMET facility is shown in Figure 8.

The drop mass is attached to a release system located on the top part of the facility. Once released, the square shaped impact mass slides along the shaft of the bolt to impact on the surface plate. The latter is supported by the tendon installed in a test tube (Gaundreau et al., 2004). Test procedure of CANMET is described in Figure 9.

The test facility is well instrumented to monitor the displacement of (St-Pierre, 2007):

- The impact mass.
- Both extremities of the bolt.

And the forces:

- Applied to the bolt.
- Transferred to the test structure.

CANMET Instrumentation and data acquisition system are described in Figure 10.

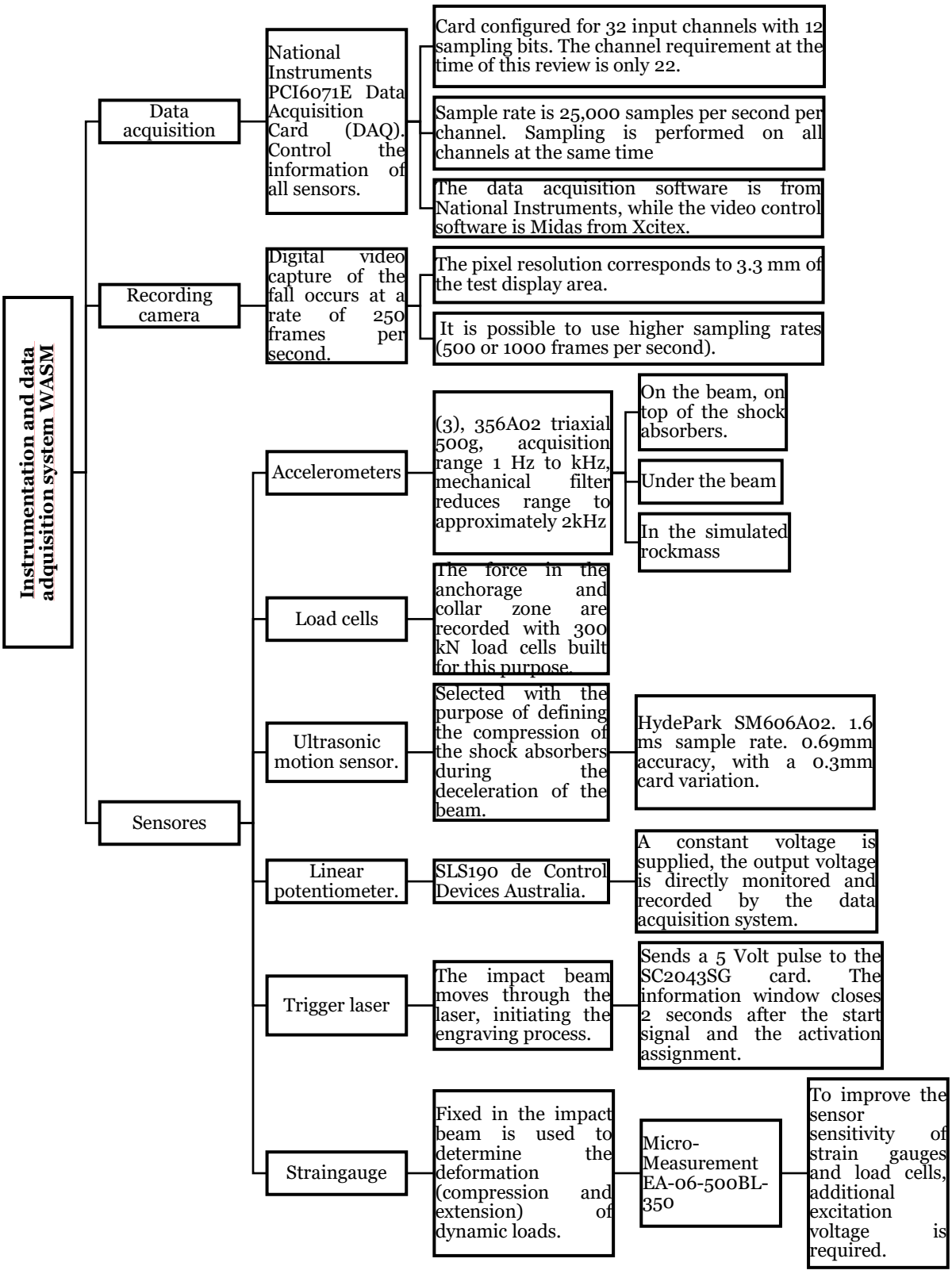

Figure 6 Instrumentation and data acquisition system WASM (2).

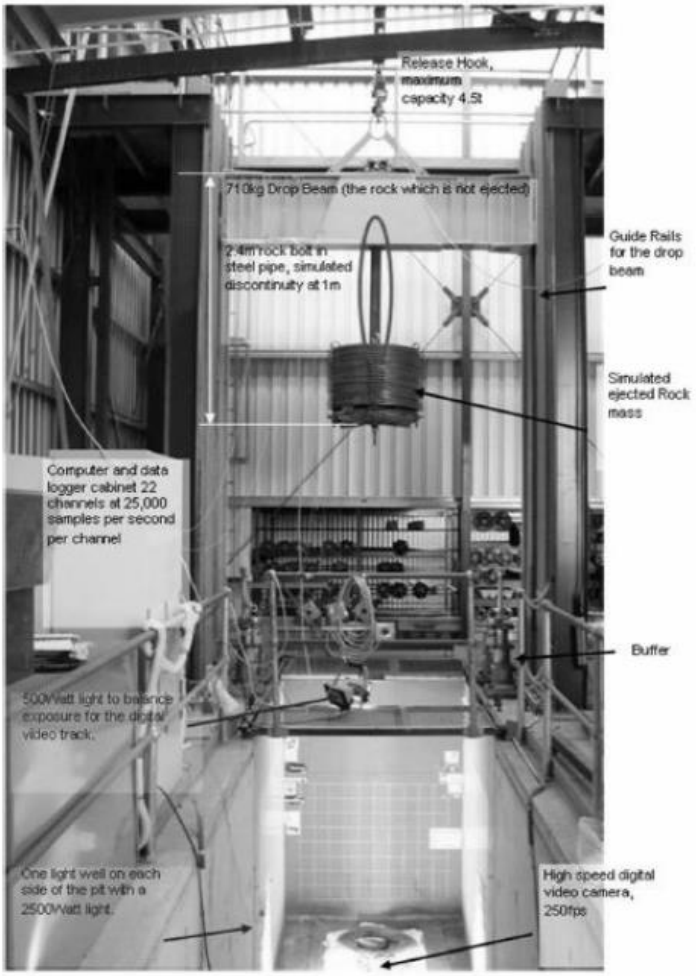

Figure 7 WASM test configuration. (Villaescusa et al., 2015)

Other dynamic test facilities

CSIR-TERRATEK

The test facility was built in 1978 at MiningTek in Johannesburg, South Africa, with equipment originally given by Terraket from the United States.

Inside a tube, the element to be tested is encapsulated, to which a clamping collar is attached at both ends and joined to a hydraulic system that pulls the collar of the previously shortened bolt or pushes its upper end at a certain speed (Villaescusa et al., 2005a). The equipment is presented in Figure 11.

Terratek unit was configured to test rock bolts in tension or shear and assess the performance of both. Instrumentation was limited to displacement, piston velocity and force at the load cell attached to the collar (Hadjigeorgiou & Potvin, 2011). Setup of the slow and dynamic tests is shown in Figure 12.

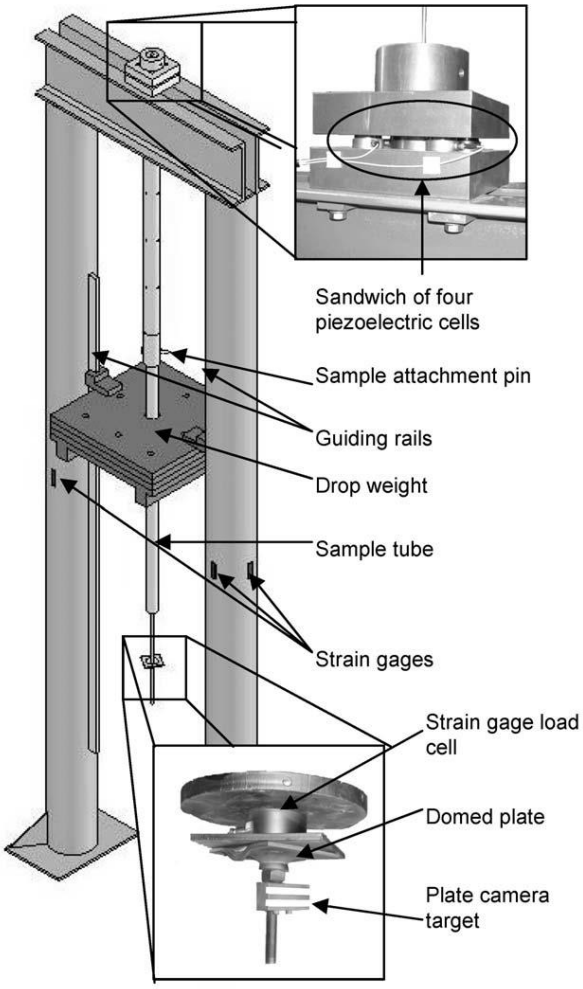

Figure 8 CANMET test configuration. Modified by St-Pierre,(2007).

The mass is lifted with an electromagnet, which in turn is raised using a pair of cranes mounted in parallel on top of the equipment.

By cutting power to the magnet, the mass falls freely on the bolt plate connected to the bar cemented within a steel tube.

The input energy is controlled by the fall height and the impact mass.

Figure 9 CANMET test procedure.

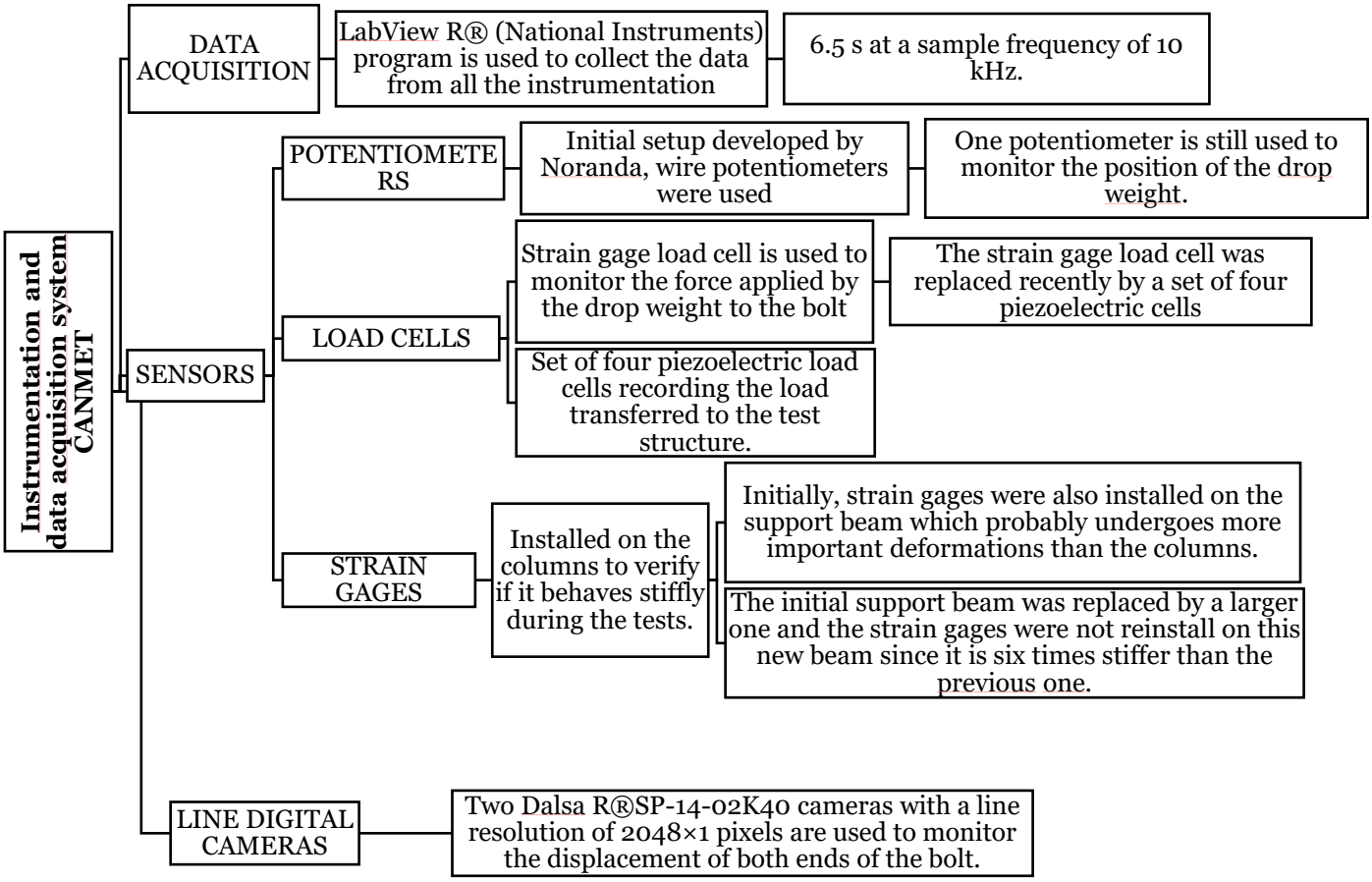

Figure 10 CANMET information acquisition system and instrumentation.

Figure 11 Terratek hydraulic equipment for dynamic tests. Taken from (Villaescusa et al., 2005a)

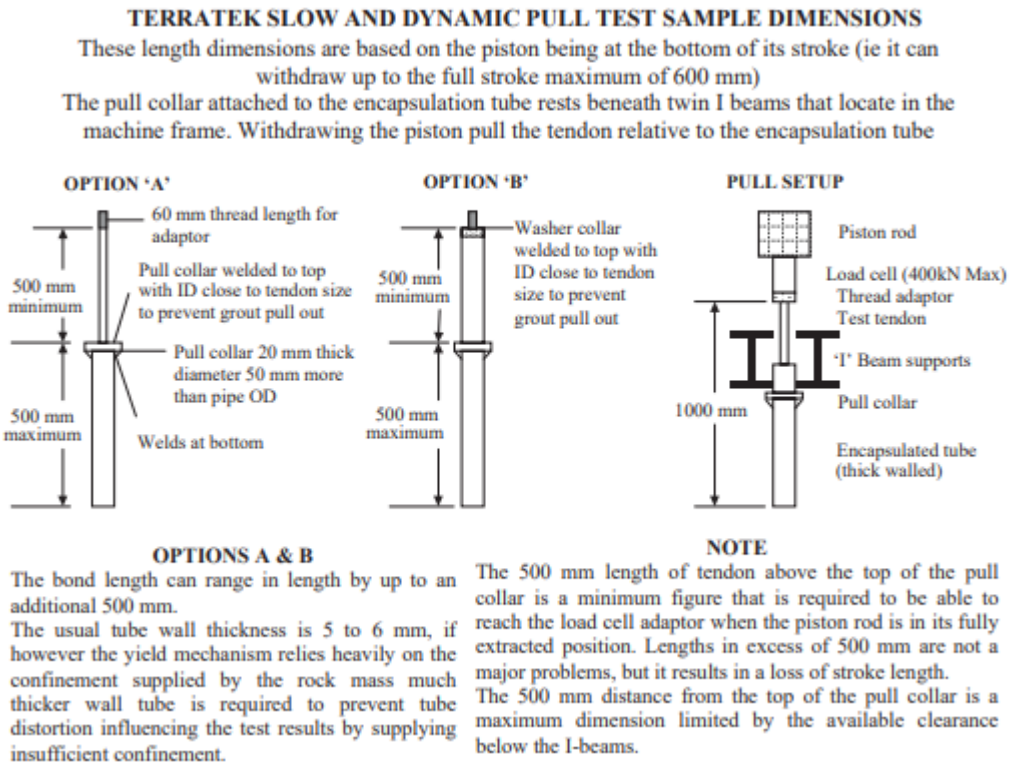

Figure 12 Terratek setup of slow and dynamic pull test. Taken from (Player et al., 2008)

CSIR impact facility

This development can be divided into two stages, the first is described in the GAP (Gold and Platinum) Research Project 221, which resulted in principle, in the design and construction of a dynamic test facility (using a falling mass free) with the ability to test support elements.

The second phase is reported in GAP 423, which describes the improvements made to the equipment in order to specifically test reinforcement elements. The proposals use the principle of a moving mass that impacts a fixed structure or element.

Both test rigs were designed and built by Steffen Robertson and Kirsten Consultants (SRK), with funding from the Mine Safety Advisory Committee (SIMRAC) (Hadjigeorgiou & Potvin, 2011) The equipment is currently in the CSIR facility in Johannesburg.

GAP 221

The objective of the project was to determine the performance of surface support systems (wire mesh, lacing and shotcrete) when subjected to simulated rockbursts, elements typically used in mining in South Africa.

The equipment used in these tests comprises a mass in free fall that provides the dynamic impulse, this impacts a structure formed by a pyramid of load distribution (concrete blocks encased with a steel element) that simulates the rock mass. This structure is supported by the containment system to be tested, which in turn is suspended to dynamic rock bolts (yielding rock bolts) (Human & Fernandes, 2004). See Figure 13.

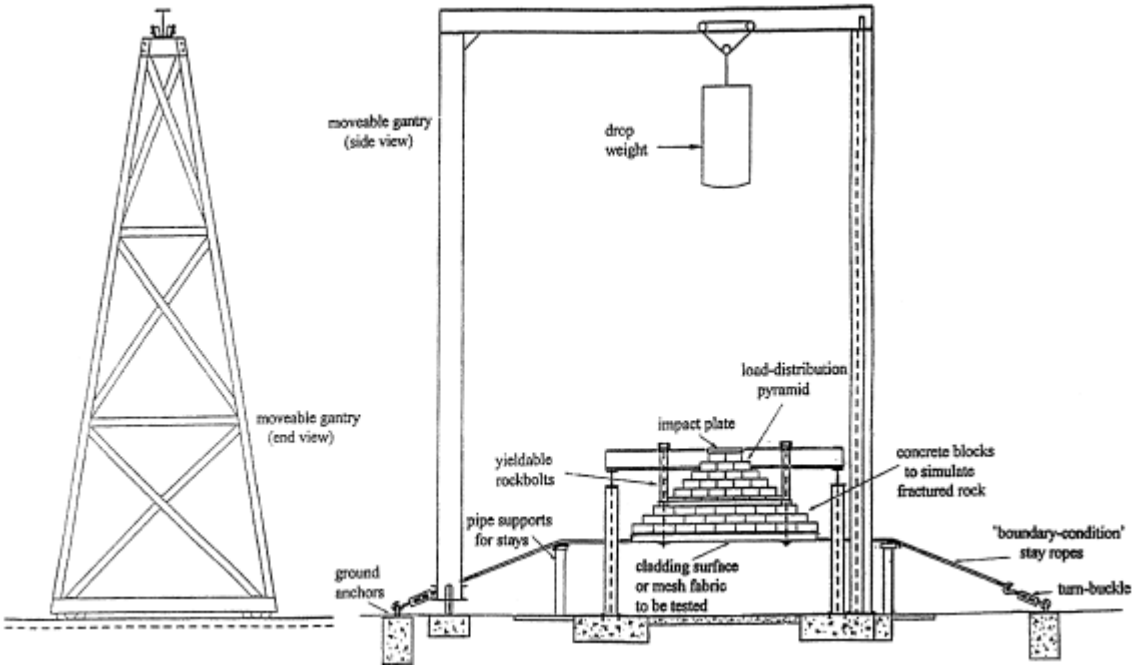

Figure 13 Dynamic testing equipment for CSIR retaining elements. Modified by Hadjigeorgiou & Potvin (2011)

The upper and lower layers of the distribution pyramid are restricted to prevent the ejection of concrete blocks, this ensures the transfer of load to the lower block and the surface retaining element. The sample to be tested hangs from support beams using dynamic bolts, ensuring that these do not fail during the tests, in this way it is possible to determine the behavior of the retention system.

SIMRAC 616 project

The SIMRAC stope support system testing facility was located at the Savuka satellite training center in the North West province of South Africa in 1999. The new facility is the result of modifications made to the CSIR equipment for support systems (Zhou & Zhao, 2011).

The two most important differences are the provision of a discontinuous surface, which would be subject to a dynamic load (Ortlepp, 2000), in addition the test facility is not it's not limited to testing one support unit at a time, it recognizes the possibility that in a rock collapse it occurs between support units, representing what is observed in reality (Human & Fernandes, 2004).

The equipment consists of two essential components, the collapsible roof that represents the fractured hangingwall of the stope and a 10 Ton solid steel cylinder that provides the dynamic energy impulse.

The dynamic load is applied on the collapsible roof by dropping the steel cylinder from the required height to impact a load distribution pyramid composed of steel-lined concrete blocks, a side view of the equipment is presented in Figure 14. The movement of the mass is not directed or restricted by some type of guide or rail, it falls freely (Ortlepp, 2000).

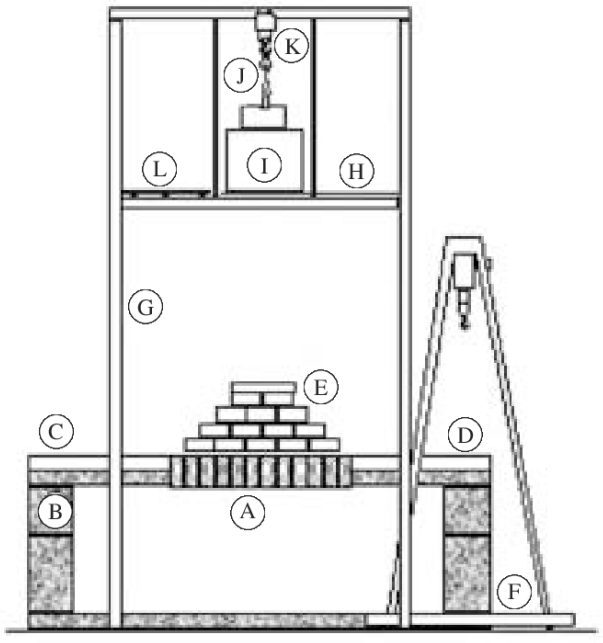

A – Collapsible roof
B – Corner column
C – Deck
D – Side beam
E – Load distribution pyramid
F – Portal crane
G – Main support column
H – Floor
I – Drop weight
J – Quick release shackle
K – 10 t hoist column
L – Berthing platform for drop weight

Figure 14 SIMRAC dynamic test equipment general section. Modified by Human & Fernandes (2004).

The compressed air crane that lifts the impact mass is attached to a mobile truck along an I-section beam, thus forming the upper part of the steel structure. This superstructure also supports a working floor 6.6 [m] from the lower deck.

The load distribution pyramid transfers the dynamic impulse to the simulated area of the 3 [m] x 3 [m], where the support system is installed and it supports three discontinuous and collapsible rows, consisting of 12 concrete blocks each. The concrete blocks that make up the three discontinuous beams in the center of the installation can move freely towards the inclined area under dynamic conditions during the test (Human & Fernandes, 2004).

This configuration simulates a rock structure where the weak planes are normal to the applied load. The blocks were assembled around four bars within a confining frame. Afterwards, the bars are tensioned and confinement is applied using the confinement frame, in this way the frame that supports the entire system can be removed (Hadjigeorgiou & Potvin, 2011).

The displacement is recorded and measured after each significant vertical movement for each of the blocks that make up the central beam, during the release of the horizontal restraining force. For recording and measurement, a monitoring frame is used that contains nine vertical telescopic bars in contact with nine specific points along the bottom of the assembly (Hadjigeorgiou & Potvin, Overview of dynamic testing of ground support, 2008). The vertical displacements and the horizontal restraining force are recorded and plotted (Ortlepp, 2000).

GAP 423

In 1997, a series of dynamic tests on wire mesh, lacing and shotcrete using impulsive loading were carried out. As an extension of this work, it was proposed to subject various types of bolts commonly used to dynamic tensile loads, the results of this test program and the equipment used are presented in the report called GAP 423 (Ortlepp & Stacey, 1998).

The equipment used makes it possible to test reinforcement elements and anchoring mechanisms, but it is not always possible to include the accessories that make up a complete fortification system in the tests (Villaescusa et al., 2005a).

The bars are cemented inside steel tubes or installed in holes developed in simulated rock inside steel tubes, the thickness of the tubes provides a confinement equivalent to that provided by the rock mass. Dynamic load is imposed using the impact of a mass on an oscillating beam. The equipment configuration is presented in Figure 15.

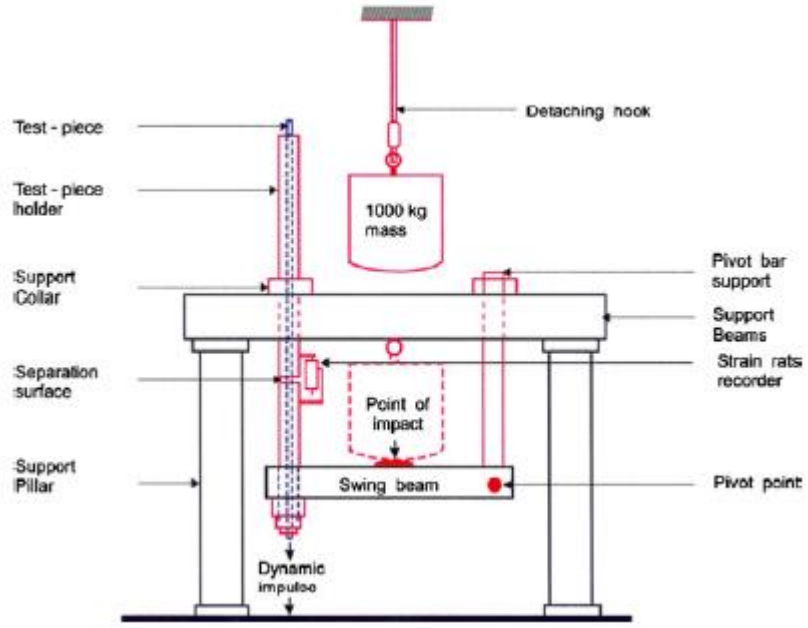

Figure 15 CSIR dynamic test facility for reinforcement elements. Modified by Ortlepp & Stacey (1998).

Although there are several reports that refer to the tests carried out with the equipment, the GAP 423 report is the one that presents a complete description of these.

GRC Dynamic test facilities

Two dynamic test facilities have been developed at the Creighton Mine in Canada, projects led by the Laurentian University Geomechanics Research Center (GRC) and funded by the Canadian Rockburst Research Program (Villaescusa et al., 2005a).

The facility in Figure 16 uses the impact of a mass in free fall on a support element, which can be a shotcrete panel, fibercrete or mesh and shotcrete.

A series of concrete beams were installed where the elements to be tested rest. The support plates (plate and bolt) are located on load cells, and can be tensioned from above, this tension allows to somehow replicate the underground environment. The applied tension was not reported. The load cells were installed between the concrete columns and the lower support plates, the equipment configuration is shown in Figure 16.

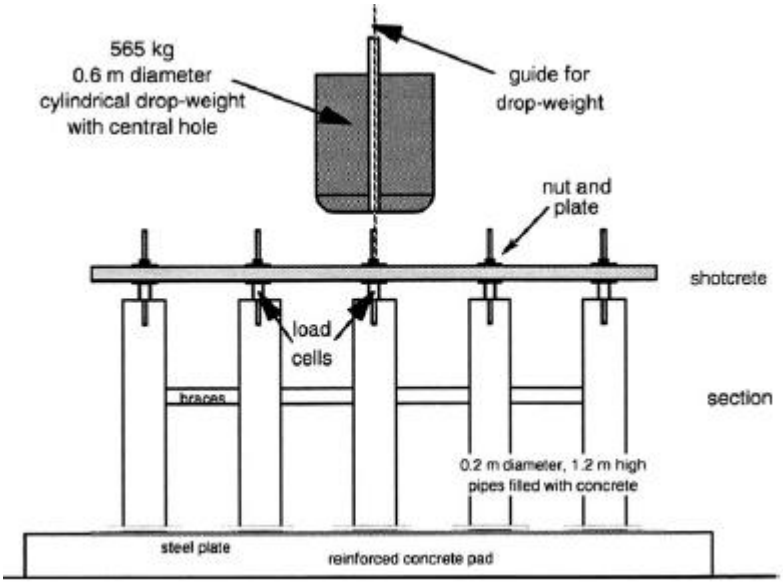

Figure 16 GRC dynamic test facility for shotcrete testing. Modified by Hadjigeorgiou & Potvin (2011).

The impact of the mass was monitored with accelerometers, load cells, and displacement measuring instruments.

The input energy of the GRC equipment is much lower than that of the CSIR equipment, because it uses the direct impact on the element to be tested and not on a load distribution mechanism. The test facility tests the performance of the support element when suffering a direct impact and not the interaction of the accessories (plate and bolt) with the fortification element (Hadjigeorgiou & Potvin, 2011).

The equipment in Figure 17 was used to demonstrate the influence of multiple impact loading, resulting in accumulation of plastic deformation in full-scale bolts. The tests were carried out on a shortened steel bar with shock absorbers, the bar is protected from the buckling product of the fall of the mass. The existing information about the results obtained and the configuration of the equipment is limited.

KBN dynamic test facility for rockbolts

The equipment was developed by the State Committee for Scientific Research (KBN) in Katowice, Poland. To design the equipment, it is assumed that a rock burst can be considered as the impact of a conventional weight on a bolt, which at one end with a washer and nut, and at its other end is fixed at the bottom of a drilling, see Figure 18.

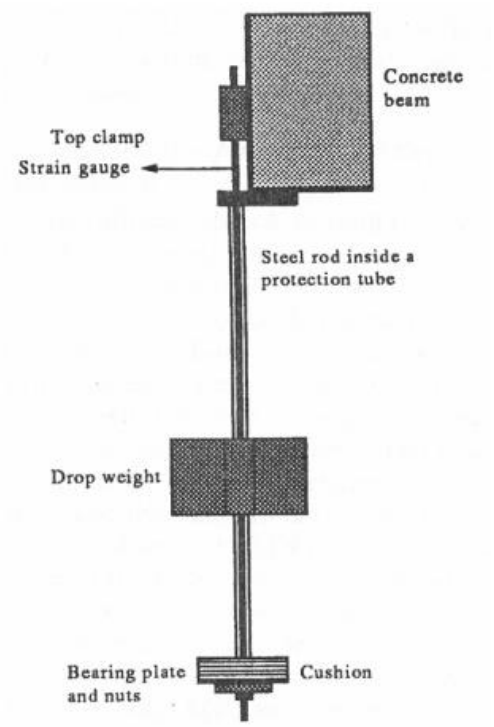

Figure 17 GRC mass drop test equipment. Modificado de Villaescusa et al., (2005a).

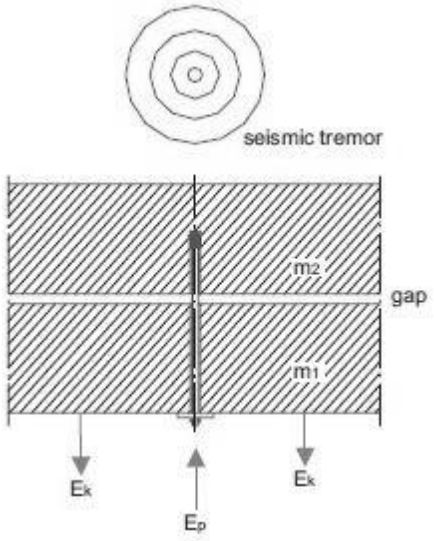

Figure 18 KBN load model **(Nierobisz, 2006)**.

For the KBN test proposal, it is assumed that when a seismic event occurs the bolt supports a defined weight of rock, which is hit by a mass $m_2 > m_1$. Therefore, the equipment is composed of a mass m_1 loading the bolt which is inserted in resin inside a steel cylinder (rock mass simulation). From a defined height, the impact mass m_2 is dropped until it collides with m_1; At this point the response of the bolt is observed, measuring the load and displacement. The equipment configuration is presented in Figure 19.

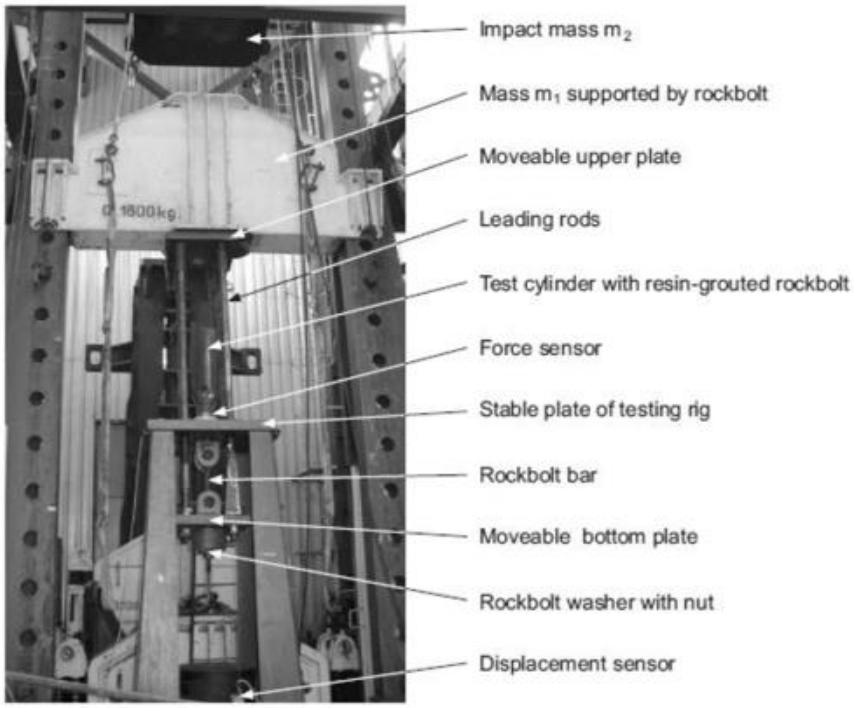

Figure 19 KBN dymanic impact test facility (Nierobisz 2006).

The bolt is cemented within the trial cylinder in accordance with the polish standard. The upper end of the bolt sits on a force sensor and the top plate of the equipment. The lower end of the bolt ends with a washer and is located on a movable lower plate with four rods that end with an upper plate where the mass m_1 is located. The load is transferred to the bolt through the middle of the bars to the movable bottom plate and then towards the nut and the ring pull (Nierobisz, 2006).

SRK Duraset Wedge-Block Loading Device/SRK

In order to be able to test grout bolts longer than 1.2 [m] in length in the laboratory, a special testing device was developed by Duraset in partnership with SRK Consulting in South Africa. The device consists of two thrust blocks with inclined faces guided by a wedge that separates them. The wedge converts the vertical displacement into horizontal, a schematic of the device can be seen in Figure 20. The SRK / Duraset displacement conversion device employs the SIMRAC test set.

Placing the sample in a horizontal position makes it possible to test bolts up to 5 [m] long. The hollow rod from which the sample holder is made has an outer diameter of 80 [mm] and an inner diameter of 50 [mm]. This characteristic is considered to adequately represent the compressibility presented by the partially relaxed rock surrounding a hard rock excavation (Hadjigeorgiou & Potvin, 2011).

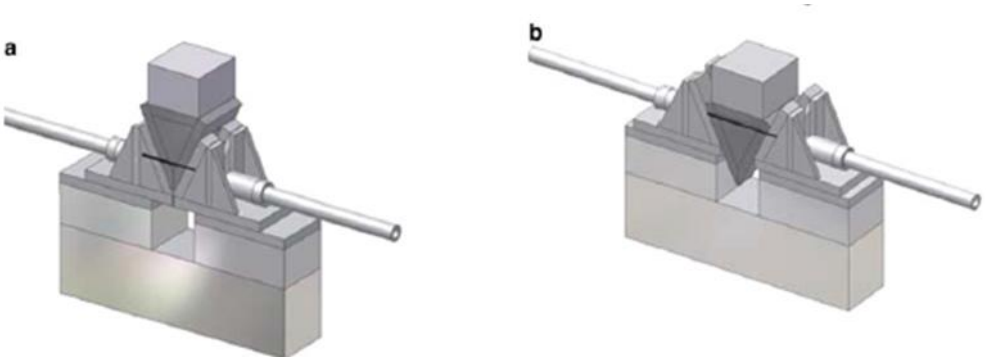

Figure 20 Block-wedge loading mechanism a) Before impact b) After impact (Ortlepp et al., 2005).

Bolt load and displacement are captured using electronic devices. The results can be analyzed to determine the energy consumed during the test or at the time of failure instead of a derived value.

The input energy can be applied quasi-statically with a compression machine, as shown in Figure 21, or dynamically with the impact of a mass, the height of the fall can be defined. This test characteristic can be used to study the effects of speed and / or moment transfer on the behavior of the bolt or the test itself (Ortlepp et al., 2005).

Figure 21 Block-wedge loading mechanism located under test facility (Ortlepp et al., 2005).

Dynamic test facilities comparison

In the previous section, a review of the characteristics, instrumentation and test procedure of the equipment for dynamic tests to reinforcement / retention elements / systems more documented in the bibliography was presented. In order to group and allow comparison between the mentioned equipment, Table 3 presents the following information for each of these:

- Test scale:
    - Input energy.
- Load mode:
    - Momentum transfer.
    - Direct impact.
    - Hydraulic load.
    - Direct impact on a dissipation element or on an energy transfer mechanism.
- Repeatability of the test.
- To be tested:
    - An element of the structure.
    - Complete structure.
- Analysis:
    - Reported advantages and limitations.

Similar comparisons have been made previously and are documented (Hadjigeorgiou & Potvin, 2008; 2011), in order to keep the information updated, a new data collection was carried out.

Table 4 presents a comparison of the advantages and disadvantages of the use of each of the facilities.

Table 3 Dynamic test facilities main characteristics.

Test facility	Location	Condition	Load mode	Impact length	Impact velocity	Impact mass	Impact height	Impact energy
WASM	Western Australian School of Mines. Kalgoorlie, Western Australia.	Operational	Momentum transfer	140 [ms]	Max 10 [m/s]	Max 4500 [kg]	Max 6 [m]	Max 265 [kJ]
CANMET - MMSL	Mining and Mineral Sciences Laboratories. Ottawa, Ontario, Canadá.	Operational	Direct impact on a reinforcement element.	50 [ms]-80 [ms]	Max 6.26 [m/s]	500 [kg]-3000 [kg]	0.5 [m] -2 [m]	Max 62 [kJ]
CSIR - TERRATEK	CSIR centre. Johannesburgo, Sudáfrica	Dismantled	Hydraulic load.	N/A	1.2 [m/s] – 3 [m/s] [1]	N/A		
CSIR – Support system[2]	CSIR centre. Johannesburgo, Sudáfrica	Dismantled	Direct impact on a distribution system.	-	Max 8 [m/s]	1048 [kg] o 2706 [kg]	Max 4 [m]	Max 70 [kJ]
SIMRAC[3]	Savuka Mine (AngloGold West Wits Operations Satellite training centre), Sudafrica.	Operational	Direct impact on a distribution system.	-	7.7 [m/s]	Max 10000 [kg]	Max 3 [m]	-

[1] The TERRATEK equipment does not use impact. Speed is determined from the restriction between the high and low pressure cylinders.
[2] Reported in GAP 221.
[3] Reported in GAP 616.

CSIR – Reinforcement elements[4]	CSIR centre. Johannesburgo, Sudáfrica	Dismantled	Direct impact on an oscillating beam.	-	Max 20 [m/s]	1048 [kg] o 2706 [kg]	Max 4 [m]	-
GRC- Support elements	Creighton mine. Sudbury, Ontario, Canadá	Dismantled	Direct impact on a support element.	25 [ms]	Max 7.7 [m/s]	48.494 [kg]	Max 0.3 [m]	Max 23 [kJ]
GRC- Mass impact test	LaurentianUniversity, Sudbury, Canada.	Dismantled	Direct impact on a fixed plate	-	-	18.36 [kg] o 48.494 [kg]	0.1 [m] o 0.3 [m]	-
KBN	Katowice, Polonia.	Operational	Direct impact on a fixed element.	-	-	m_1: 2000 [kg] o 2200 [kg] m_2: 4000 [kg] o 5000 [kg]	0.2 [m] o 0.7 [m]	Max 38 [kJ]
SRK/Duraset	Duraset Site, MiningTek. Johannesburgo, Sudáfrica	Operational	Direct impact on a transfer element.	-	Max 8.9 [m/s]	Max 10000 [kg]	0.4 [m] – 4 [m]	Max 390 [kJ]

Table 4 Advantages and limitations of existing dynamic test equipment

Test facility	Tested element			Advantages	Limitations
	Reinforcement	Support/Retaining	Accessories		
WASM	Bolts and cables up to 2.4 [m] long, achieving a creep displacement of 800 [mm] max. Longer elements can be	Mesh and shotcrete panels of 1 [m] x 1 [m].	-	• Ability to test elements on a full scale. • High input energy available to test complete fortification systems.	• Largest testing equipment • More expensive mining dynamic testing equipment. • The setup (preparation) of

[4] Reported in GAP 423.

Test facility	Tested element			Advantages	Limitations
	Reinforcement	**Support/Retaining**	**Accessories**		
	tested, but the required creep must be established.			• Ability to replicate a dynamic load. • Integration of the simulated rock mass with the reinforcement system. • The test tube provides confinement of the same order of magnitude as the rockmass. • Equipment designed with the ability to calculate the energy absorbed by various components at any time during a test.	an assay is time consuming. • Higher cost per test. $ 6000- $ 7000 US (2016).
CANMMET-MMSL	Bolts up to 2.1 [m] long	-	-	• Relatively quick and inexpensive equipment to build. • It is possible to test shortened or full-scale bolts. • Compared with WASM equipment, lower cost per test. $ 4000 - $ 6000 US (2016).	• The results do not consider the rigidity of the equipment, nor the energy losses. • Low impact energy. This creates the need for multiple impacts to generate bolt failure. Hence the difficulty in interpreting the results. • The calculation model is not accurate, the results do not represent the first the first maximum in the load applied to the reinforcing element. • There is no integration of the rockmass with the reinforcing element, all the load is transferred through the surface elements (accessories).

Test facility	Tested element			Advantages	Limitations
	Reinforcement	**Support/Retaining**	**Accessories**		
CSIR - TERRATEK	Shortened bolts up to 1.6 [m] and their anchoring mechanism.	-	Accessories. There are no more details.	• Low-cost tests. • Shorter test cycle than for any equipment, up to 15 tests per day. • The only equipment with the ability to apply dynamic compression, tension or shear load. It is only necessary to reconfigure the equipment. • It can also carry out quasi-static tests.	• The speed used in the test is independent of the load transfer capacity of the tested reinforcing element. • The force applied to the bolt is not related to the input energy provided by the hydraulic system. • The force used in the test could exceed the energy that a rockburst can apply to the element. • The method by which load is applied does not take into account the energy absorbed by the reinforcement system, which, if effective, reduces the rate of rock ejection.
CSIR- Rock support	-	1.6 [m] x 1.6 [m] mesh and fibercrete panels	-	• The equipment boundary conditions are probably configured to represent rock mass fracturing around an excavation.	• The results obtained are sensitive to the distribution device used. The use of multiple block geometries and the use of multiple layers increases the complexity of the equipment. • A complex distribution device introduces variation when the tests are repeated, which makes it difficult to test different elements using the same methodology. • A recent variability in

Test facility	Tested element			Advantages	Limitations
	Reinforcement	Support/Retaining	Accessories		
					results was observed with increasing input energy.
SIMRAC	-	3 [m] x 3 [m] mesh	Props up to 2 [m] (with extensions)	• Well-designed equipment and experienced testing personnel. • Ability to repeat tests under the same conditions.	• Reinforcing elements cannot be tested. • The instrumentation in some cases is insufficient (video and recording of measurements). • It has been used primarily for commercial purpose testing on block support, accessories and connectors.
CSIR- Reinforcement Elements	Bolts and cables	-	-	• Appropriate use of thick-walled pipes to simulate the confinement that the rock mass provides to a borehole. • The load is applied to the outer surface reasonably representing the load applied by the ejected rock to a hole, but not to the surface accessories (nut, plate). • The equipment is comparatively cheaper to build. • The trial rate should be high considering the ease of setting them up.	• Minimal instrumentation: Load cells are not considered to measure the load distributed between the pivot bar and the bolt. No strain gauges were installed to measure the deflection and energy loss of the bolt and the oscillating beam. • The calculation methodology used to establish the energy absorption capacity of the tested element is basic. • The beam does not load the retaining element on the surface of a reinforcement system.
GRC- Support elements	-	1.2 [m] x 1.2 [m] mesh, diamond pattern.	-	• Installation time is short. • After the equipment is installed, the tests on	• The energy is described in terms of the maximum impact energy rather than

Test facility	Tested element			Advantages	Limitations
	Reinforcement	Support/Retaining	Accessories		
		Shotcrete panels 1.5 [m] x 2.75 [m]		supporting elements are relatively low. • The size of the elements is reasonable to represent the boundary conditions.	calculating the energy absorbed by the mesh and shotcrete combinations. • A bolt spacing of 0.72 [m] is considered very fair, and is only applicable for analyzing Canadian operations.
GRC- **Impact test**	2.44 [m] steel bars	-	-	• Cheap to build. • Quick to run tests on multiple systems. • The use of rubber plates in changing the transfer of stress by softening the reinforcement system has practical references.	• The installation of the reinforcing element is not divided into anchoring and drilling. However, the drilling is simulated. • The equipment was designed to test tensioned bolts, although the initial tension was not reported.
KBN	There is no general description of the bolts tested.	-	-	• Well designed equipment with sufficient instrumentation to measure and record results. • Ability to repeat tests. • Well established energy calculation methodology.	• The bolts tested are not brought to failure. • The calculations assume that the equipment frame acts as a rigid construction.
SRK/Duraset	Bolts and cables up to 5 [m] long.	-	-	• Relatively inexpensive test preparation. • The configuration of the equipment is consistent and allows to repeat tests under the same conditions. • The test facility could perform multiple tests on the same surface support element and use a simple	• The system has presented limitations with the instrumentation used in the tests and no effort has been made to quantify the energy losses of the system. • The results of the available trials are limited.

Test facility	Tested element			Advantages	Limitations
	Reinforcement	Support/Retaining	Accessories		
				load distribution system. • Ability to test bolts / cables longer than other equipment.	

2.1.3 Published dynamic test results

The ASTM standard describes how to analyze and report the results of conducting dynamic tests on reinforcing elements (especially Cone Bolt type) in order to determine their anchoring capacity to the rock (ASTM, 2008), these are shown below:

Table 5 Parameters to measure during impact dynamic test.

Parameter	Measurement unit
Drop number	Un
Drop height	m
Input energy	KJ
Impact velocity	m/s
Incremental displacement of the plate	m
Frame displacement. Potentiometer.	m
Cone displacement	m
Cumulative cone displacement	m
Steel plastic stretch	m
Steel elongation	% Deformation
Cumulative deformation	%
Cone total displacement	% In relation to total
Maximum load	Kg
Average load	Kg
Maximum load on the plate	Kg
Average load on the plate	Kg

Without prejudice to being the only established standard regarding the presentation of results from this type of test (ASTM standard), several authors have presented the product of their research according to the parameters they consider relevant. In the following paragraphs, a summary of the most relevant results will be presented.

The results obtained from dynamic tests to reinforcing elements can be presented in terms of displacement, velocity, acceleration and the variation of stress with respect to time for all the components involved in the test and the response in terms of load-displacement and load energy absorption capacity for the analyzed element.

When it is needed to determine the absorbed energy or its loss that could occur in the testing machine / tested element interface, the load - displacement curves should be used (Villaescusa et al., 2015). The area under the load-displacement curve represents the energy consumed by the reinforcing element in order to dissipate the input kinetic energy. It is possible that this dissipated energy is greater than the input kinetic energy due to the change to potential energy of the mass just after impact.

It should be noted that currently only two facilities perform rockbolt tests, the WASM and CANMET-MMSL. Therefore, the results of these test programs have been summarized in a database, in terms of the load-displacement curves and the energy

absorbed by the elements tested. In some cases, the results have been collected until the element reaches failure or the point where the mass stops.

However, there are difficulties for compare the results obtained from the use of each of the mentioned equipment, mainly due to the fact that different test configurations, load modes and tested reinforcement elements can be used.

2.1.1.3 Absorbed energy by rock bolts from dynamic testing

In Figure 22 a compilation of the impact results made to conventional and dynamic bolts is presented. Also is presented on which facility the tests were carried out, for some test there is not information about the used rig. The absorbed energy was plotted as a function of displacement. The information plotted has been taken from the publications cited in Table 6.

It is important to note that the best performance in terms of the mentioned parameters is presented in the dynamic Threadbar and D-Bolt bolts, because, although in some cases the Durabar and Yield-lok type bolts absorb around 60 KJ, they present a high rate of deformation compared with the rest of the dynamic bolts. This behavior is undesirable when expecting to counteract the effects of a rockburst.

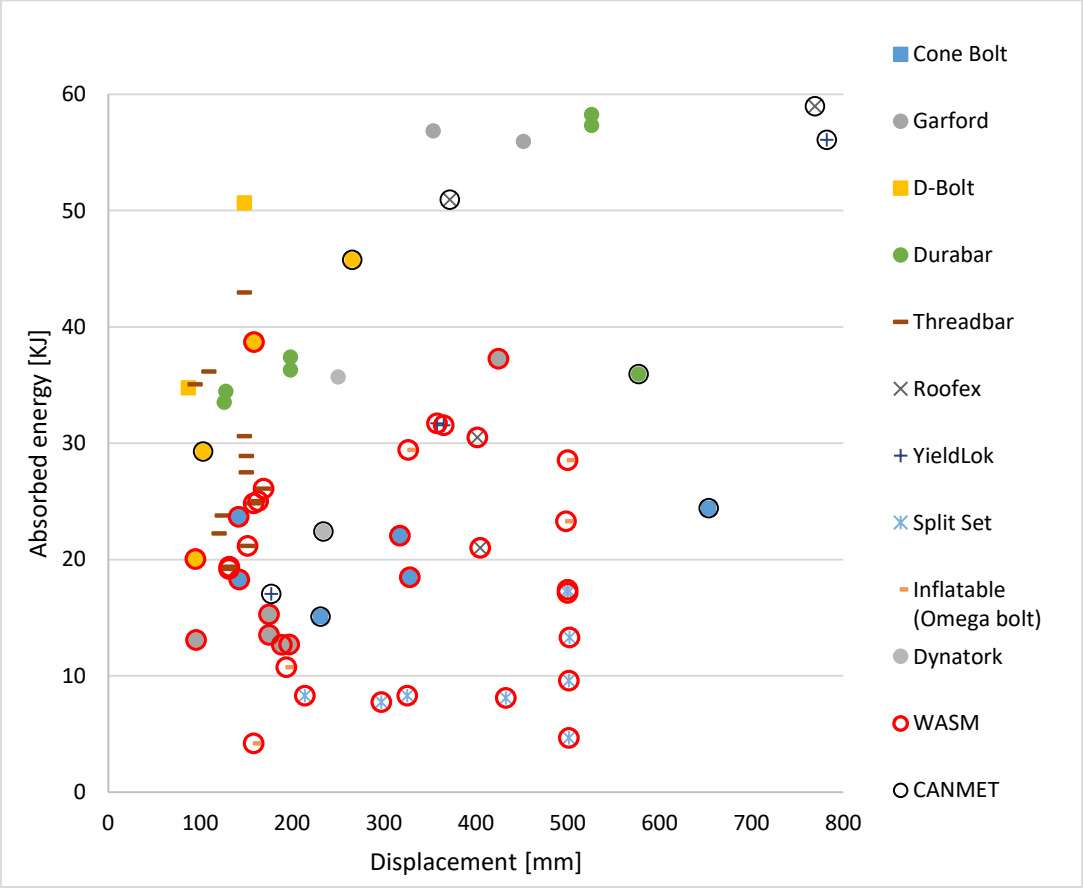

Figure 22 Absorbed energy Vs. Displacement. Rock bolt tests under dynamic loading.

2.1.1.4 Dynamic response analysis

Now, a detailed analysis of the dynamic behavior of the reinforcement elements is presented. According to the collected database, the Threadbar and D-bolt bolts present better performances as they absorb more energy with less final displacement than any other type of bolt featured. Considering this, Figure 23 shows a detail of the results collected for the chosen bolts.

Table 6 Dynamic test results references

Bolt type	Test facility	Reference
Cone bolt	WASM	Varden et al. (2008) Villaescusa et al. (2005b)
Modified cone bolt (MCB)	-	Cai et al. (2010)
	CANMET	Doucet & Voyzelle (2012)
Threaded Cone Bolt	-	McKenzie (2002)
Garford	WASM	Varden et al. (2008) Villaescusa et al. (2005b) Hadjigeorgiou & Potvin (2008)
D-Bolt	CANMET	Li & Doucet (2012)
	WASM	Doucet & Voyzelle (2012)
Durabar	CANMET	Doucet & Voyzelle (2012)
Threadbar	WASM	Villaescusa et al. (2005b)
	-	Muñoz (2016)
Roofex	WASM	Villaescusa (2012)
	CANMET	Doucet & Voyzelle (2012) Galler et al. (2011)
Yieldlok	-	Wu et al. (2010)
	WASM	McKenzie (2002) Villaescusa (2012)
Splitset	WASM	Player et al. (2009)
Inflatable bolt (Omega)	WASM	Player et al. (2009)
Dynatork	CANMET	Kabwe & Wang (2015)
	-	Oler (2012)

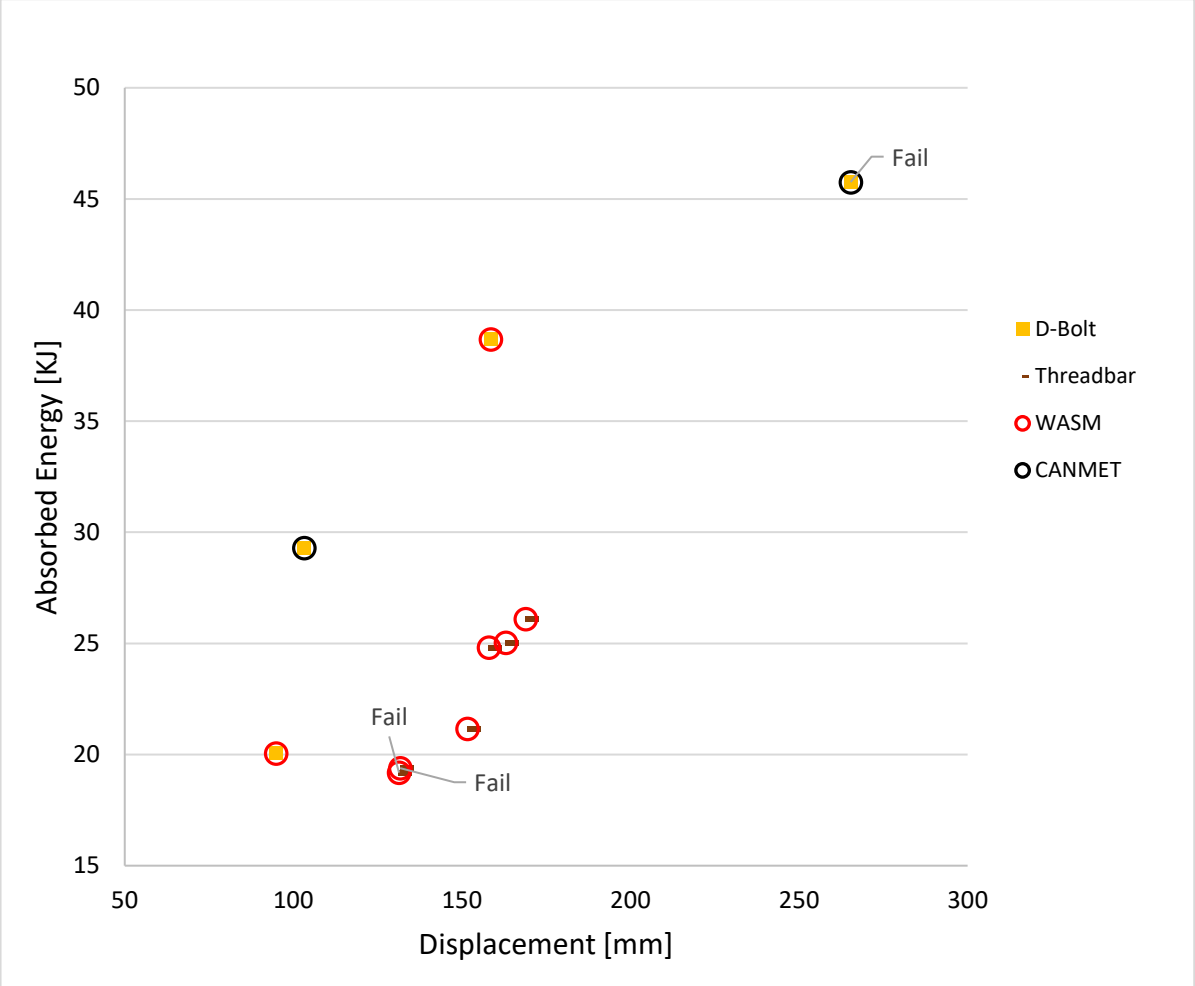

Figure 23 Absorbed energy Vs. Displacement, D-Bolt y Threadbar bolts. Bibliography results.

As expected, the greater the displacement, the greater the energy absorption for both elements, but only one test leads the D-Bolt to failure (Li & Doucet, 2012). It is important to clarify that the dynamic load that causes D-Bolt to fail was applied using the CANMET-MMSL equipment under the conditions described in Table 7

Bolt diameter [mm]	Bolt length [m]	Drop mass [Kg]	Drop height [m]	Velocity [m/s]	Impact Energy [KJ]
22	1.5	2897	1.97	6.2	56

Table 7 CANMET D-Bolt test characteristics

If the other results of D-Bolt bolts are analyzed, in one of the tests, the diameter changed (20 mm) and its length was shortened (0.9 m), while the drop height and mass decreased. The remaining tests were carried out with the WASM equipment, maintaining the diameter of the bolt (22 mm), but reducing the throw mass (200 Kg).

When the results of the threadbar bolts are analyzed in terms of their energy absorption capacity the best performance was obtained when carrying out the tests with the WASM

equipment. The testing was carried out under ideal conditions regarding bolt encapsulation with 0.4 – 0.45 water/cement ratio grout. The grout was allowed to cure in excess of 28 days prior to testing (Player J. , 2012).

Only tests where dynamic energy was transferred to the bolt were considered, it means that after impact is observed that stretch of the threadbar at the simulated discontinuity, no movement at the toe and minor to null deformation to the surface hardware occurs.

It was observed that the failure mode in all cases corresponds to the extension of the bolt and slippage of the anchor between 146.4 mm and 156 mm, this displacement was measured in the simulated discontinuity in the steel tube that confines the sample (for more details see Page 9). Bolt characteristics and test setup are presented in Table 8.

Table 8 WASM threadbar test characteristics

Bolt diameter [mm]	Bolt length [m]	Drop mass [Kg]	Drop height [m]	Velocity [m/s]	Impact Energy [KJ]
22	3.2	1964	1.8	5.94	35.6

The other tests were performed by decreasing the length of the bolt (2.3 m) and the drop height was slightly increased (1.85 m). In such cases the bolts presented failure.

2.1.1.5 Discussion about tests results

D-Bolt bolts failed with input energy equal to 56 KJ, while threadbar bolts with maximum input energy equal to 35.6 KJ did not fail. The curves in Figure 24 show the response of these elements when they are subjected to dynamic events of great magnitude.

When the load-displacement curves are compared, it is observed that the yield load, hardening and maximum loads are higher in the D-Bolt test and that the maximum displacement is around 36% over the displacement of the threadbar bolt. The maximum load is approximately equal to the final load in both cases. In the case of the D-Bolt, its increase is justified due to the hardening of the steel as the sample is subjected to several impacts (Li & Doucet, 2012). This behavior is not observed for the threadbar bolt.

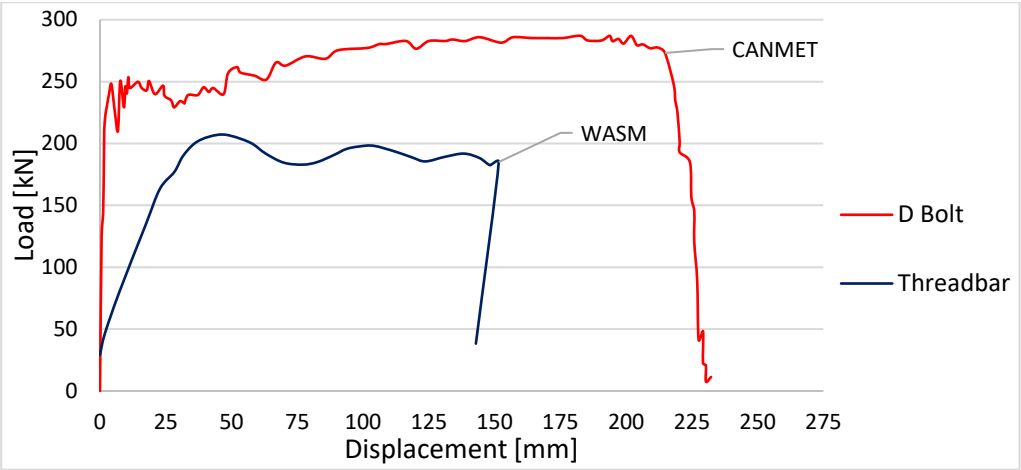

Figure 24 Load Vs. Displacement curves D-Bolt and Threadbar.

From the load-displacement curves obtained from dynamic testing is possible to determine the energy absorbed by the D-bolt and threadbar in the elastic or plastic region of deformation. The scheme in Figure 25 shows which area under the curves represents the energy absorbed by the steel bars before and after reach the yield load.

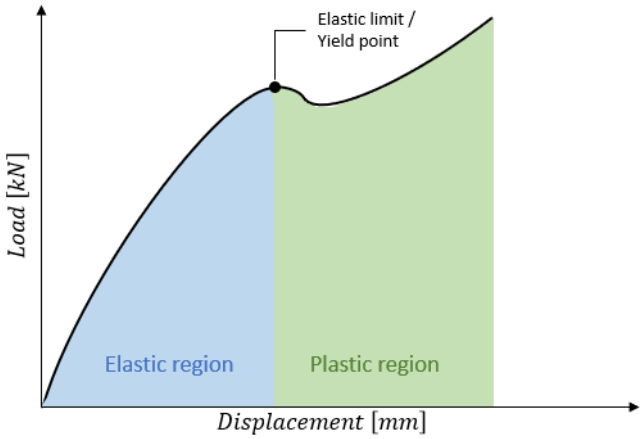

Figure 25 Elastic and plastic region of deformation

In Figure 26 is presented the energy absorbed in the elastic region versus the energy absorbed in the plastic region for the test results from the bibliography. Is observed that the threadbar absorbs around 18% of energy through elastic deformation, while the D-Bolt only absorbs 10%. This indicates that the D-Bolt absorbs more energy after reach irreversible deformation.

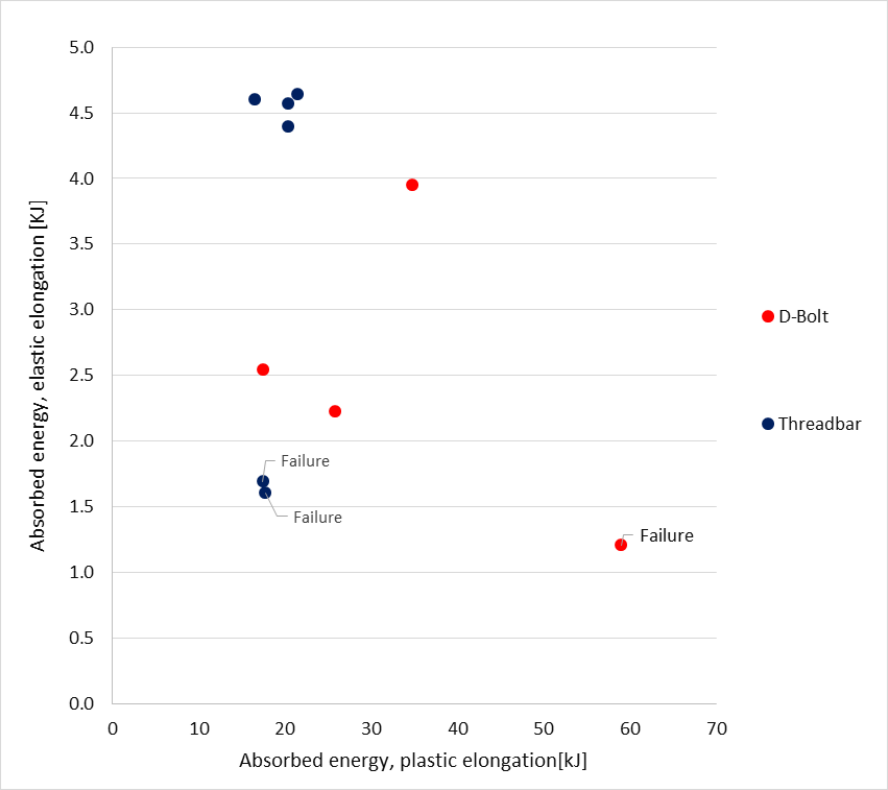

Figure 26 Absorbed energy in the range of elastic and plastic deformation.

In the case of dynamic bolts, it is desirable that all of them have a low coefficient of stiffness. Due to the threadbar stiffness, all the test results showed it had a better performance. Figure 27 shows a comparison of this parameter.

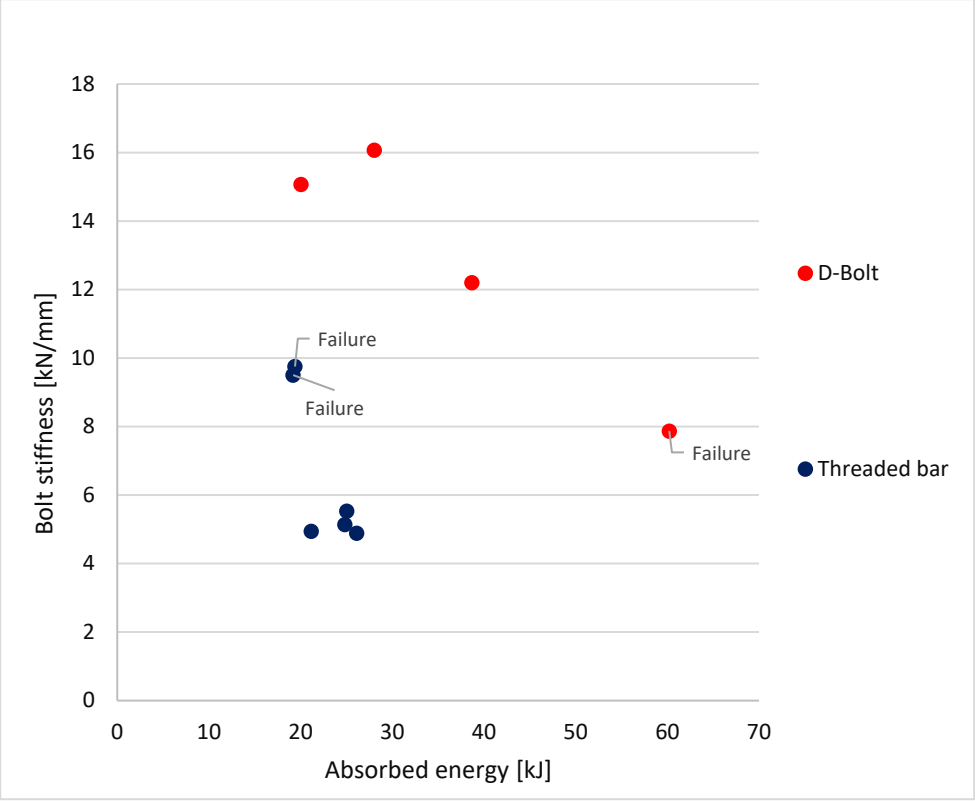

Figure 27 Bolt stiffness Vs. Absorbed energy.

2.1.1.6 Conclusions

All the dynamic test facilities have significant differences, which makes the comparison of results difficult. In addition to this, in most cases the results presented by different authors do not contain further details about the tests. However, from the results collected in this document, it was possible to identify the bolts with the best performance under dynamic stress.

When it comes to dynamic bolts, a good performance is characterized by a high energy absorption capacity with the least possible displacement. Considering this characteristic, the D-Bolt type is the best option. However, it is important to note that the results collected do not show the total absorption capacity of the threadbar (second best performance), so this characteristic is not conclusive.

The energy absorption capacity is proportionally related to the cross-sectional area, as well as to the tensile strength and maximum deformation of the bolt steel. The tests presented in the review show that for a D-Bolt with a diameter of 22 mm and a length of 1.5 m, the absorbed energy is 60 KJ before reaching failure. In the case of the threadbar, whose dimensions are 22 mm in diameter and 3.2 m long, it absorbed 26.11 KJ without reaching failure, this indicates that it could absorb more energy with an elongation of more or less than 11% before failing.

Fully grouted threadbar presents a stiffer behavior and can fail when reach its peak strength, without prejudice to this it is not correct to assume thar thereadbar is not suitable as rock reinforcement when dynamic load is imposed. Cai & Kaiser (2018) have concluded this before.

The conclusions presented here are subject to the condition that the results collected were obtained using different equipment, the characteristics of the bolts are not the same and the configuration of the tests is not standardized. Hence the need to carry out new tests to correct these irregularities.

2.2 Dynamic rock support design methodologies

The support selection for rockburst conditions is based on the load–displacement characteristics of the individual support components as well as the support capacities exceeding the calculated load, displacement, and energy demands imposed by the rockmass (Cai & Kaiser, 2018). According to Mikula (2012), the design of a support system can be approached from:

- **Analytical proposal:** Define equations that represent the expected response mechanism. These methods have not been adapted for dynamic conditions.
- **Empirical proposal:** Interpret the expected behavior of the fortification system from information collected in situ.
- **Numerical proposal:** Design numerical models that try to simulate the behavior of a reinforcement system in the event of a seismic event.

To execute the design of a fortification system using any of those proposed, the methodology to follow includes the following fundamentals:

1. **Source characteristics and location of the seismic event must be established:** This is necessary to have an idea of the nature and character of the sources of the dynamic event. Normally, this definition is obtained from the interpretation of information collected through seismic monitoring, but the potential for unexpected events or landslides in larger structures must also be considered.

2. **A rock movement relationship must be established for the mine:** It is necessary to define how the dynamic event propagates through the rock and how the vibrations will affect the excavations. Usually this behavior is determined from relating the PPV (maximum particle velocity), distance and magnitude of the event. PPV is widely used as an input parameter for calculations related to seismicity.

3. **Define damage criteria:** Determination of what level of vibration will cause the worst damage to the rock and the fortification system. This is not a simple labor, because the fortification interacts with the rock influencing both the damage pattern and the damage of the rock mass.

2.2.1 Analytical methodologies

Analytical design methodologies include that established in the CRH (Canadian Rockburst Support Handbook) and based on the demand for potential and kinetic energy (Kaiser et al., 1996; Heal, 2005; Scott, Penney, & Fuller, 2008).

These methodologies make various assumptions about the mechanisms of occurrence of dynamic events in order to carry out the calculation of the requirements of the adequate support system.

There are disadvantages when using deterministic approximations for the selection of fortification systems subjected to dynamic stresses, mainly due to insufficient understanding of the control mechanisms and the shortage of valid information to describe them. To the extent that the approaches do not match the unknowns and complexities, confidence in their results is reduced, which means that these methodologies must be applied with caution and knowing their limitations.

2.2.1.1 Methodology described in the Canadian Rockburst Support Handbook

It is a modified method from CHR (Kaiser, 1996) that can be used to calculate energy absorption, load capacity and displacement requirements. This method was applied at the Beaconsfield mine, but the seismic fault model was built with information from the Creighton mine.

2.2.1.2 Kinetic / potential energy methodology based on maximum particle velocity (PPV)

It is a widely used methodology based on the basic mechanics of a block of rock that is ejected from the walls or ceiling of an excavation. The design methodology follows the sequence described below:

1. Determine the maximum particle velocity (PPV) that can be generated on the gallery surface and the expected displacement on the walls (d_s). This is done by applying the named generalized ground motion relationships developed in order to capture the attenuation effect on ground motion measured from the source of the seismic event.
2. Calculate the total kinetic energy of the possible rock block to be ejected, that is, the demand energy (E_d) to which the installed fortification system will be subject.
3. Determine an integrated fortification system that combines several reinforcement, retention and support elements (support elements / bolt pattern) in order to achieve an energy absorption capacity (E_a) that exceeds the energy demand (E_d). As a basis for selection, the table presented by (Kaiser, McCreath, & Tannant , Canadian Rockburst Support Handbook 1996, 1996) can be used, where the energy absorption capacity for different support elements usually used in mining is indicated.
4. Determine the factor of safety FS.

2.2.1.3 Evaluation of kinetic energy in ejected rock during rockburst using compression test images

As with the methodology proposed in section 2.2.1.2, it is possible to estimate the stress in terms of the kinetic energy released to which a reinforcement system will be subjected, from the proposal made by Bravo-Haro et al. (2018). This study presents a way to determine the rock ejection energy from the deformation energy of the rock in situ together with an empirical coefficient obtained from compression tests on samples of the same rock mass.

The ejection velocity of the particles was estimated from videos recorded during compression tests of cylinders extracted from the rock at site, therefore, the kinetic energy of the ejected rock was obtained. Image recognition technique was used to meet this objective. The elastic deformation energy of the samples per unit volume was obtained from the deformation and applied load measured in the tests.

After the kinetic energy (E_k) and the strain energy (W) are defined, a factor k is calculated with the ratio E_k/W. It is assumed that a similar mechanism occurs in situ. Then, the kinetic energy presented by the ejected rock inside the excavation can be calculated from the multiplication of the deformation energy of the rock by the factor k.

2.2.1.4 Deformation based fortification system selection foundation

In 2013, Kaiser and Cai (2013a; 2013b) presented an analysis of the design methodology proposed in the CRH critically evaluating the underlying assumptions and consequences of the application of some of the dynamic support design principles adopted to date. Some problems identified are:

- Assuming that there is a direct relationship between the ejection energy and the demand to which the dynamic fortification system will be subjected is simplistic approach and, in many situations, incorrect. In some cases, the ejection velocity may be small and if the energy criterion is assumed, the demand on the fortification system would be small. This does not imply that yielding rock bolts are not necessary, as it may be necessary to control large instantaneous deformations due to a violent increase in rock volume as a result of the occurrence of a dynamic event.
- The assumed standard rock movement patterns are unacceptably flawed.
- Rock movements related to the energy transfer mechanism are rarely the only source of stress for the fortification system.
- Rock mass subjected to dynamic stresses fail in a brittle extensional type, which causes the convergences in the excavation not to be proportional to the deformation of the reinforcement system.

Based on this review, Kaiser (2014) proposed a support selection process for tunnels in rockburst-prone environments considering the deformation expected.

The deformation-based design approach seeks that the fortification system fulfills the functions of stabilizing the fractured rock due to stress (retention and volume control), controlling the convergence by reducing the damaging tangential and radial displacements of the fortified rock and minimizing its increased volume. Finally, it seeks to confine the rockmass that surrounds the excavation by increasing the radial stress thus raising the resistance of the rockmass further away from the excavation.

A reinforcement system designed to accommodate large deformations has to control the convergence between the roof and the floor to minimize the tangential deformation of the walls; it must also support fractured rock in the damage zone near the excavation walls. In addition to controlling tangential deformation, the fortification maintains the integrity of the excavation, for example, it retains fragments of reinforced rock to stop displacement before reaching the acceptable operational limits of radial displacement.

It is for this reason that an effective fortification system for rock fractured due to stress requires elements that are ductile as a result of the use of ductile steel (D-Bolts) or by sliding mechanisms with high creep capacity (Cone bolts) or by elastic stretching (Uncoupled cables).

Deformation controlled damage

There are several factors that affect the damage that occurs from a rock burst through a sudden increase in volume. Reinforcement system must be designed in such a way that it survives the violent and sudden process of volume increase so that the maximum wall velocity or ejection velocity (V_e) is equal to zero.

As already indicated in section 2.2, capacity of the fortification can be defined from load, energy or displacement. However, it is the demand in terms of displacement that is the most relevant aspect in terms of controlling the increase in volume. If the displacement capacity is greater than the demand, the excavation will be stable after the dynamic event has occurred and the ejection velocity will be equal to zero.

The stress coming from the displacement can be defined by multiplying the anticipated failure depth (d_f) by a factor representative of the increases in rock volume, Bulking Factor (BF), (Kaiser et al.,1996). For rockbursts from dynamic loads, the effect of dynamic deepening on anticipated failure depth should be evaluated so that the related volume increase can be added.

The depth of failure (d_f) can be obtained from the semi-empirical relationship presented by Kaiser et al. (1996) and that was redefined by several authors (Martin et al. (1996); Diederichs et al. (2010)). The depth of failure, but not the lateral extent of the failure, can also be defined from elastic models using the Hoek-Brown strength envelope based solely on cohesion, which in terms of theHoek-Brown parameters implies that m = 0 (Martin et al., 1996).

The volume increase factor of can be obtained from radial extensometer measurements. This factor depends on the confining pressure or radial pressure imposed by the support, the reinforcement effect caused by the use of fortification, as well as the deformation imposed on the fractured rock. Taking these factors into account, typical values have been proposed for the BF, Table 9.

It is also important to identify the factors that increase the deformation potential of the excavation (EDP) such as the geological structures that intersect the excavation (Kaiser, 2014).

Table 9 Recommended rockmass bulking factors (Kaiser et al.,1996)

Fortification location and condition	**Average load capacity** $\left[kN/m^2\right]$	**BF Recommended**	**Severely of the anticipated damage**
Floor heave	0	$30 \pm 5\%$ $> 50\%$	Low to moderate High
Walls and backs Standard bolt pattern, light mesh	< 50	$10 \pm 3\%$	Low to moderate

Fortification location and condition	Average load capacity $\left[{}^{kN}/_{m^2}\right]$	BF Recommended	Severely of the anticipated damage
Yielding support (assignable)	< 200	$5 \pm 1\%$	Low to high
Highly fortified rockmass	> 200	$1.5 \pm 0.5\%$	Low to high

Deformation control of the rock mass when failing as a result of a dynamic event

The maximum deformation capacity of a rock bolt δ_{max} cannot be assumed as a realistic design parameter, because on some occasions the operating or performance restrictions of the support system justify adopting a lower displacement capacity δ_{all}.

For example, a yielding bolt can have $\delta_{max} = 700\ o\ 800\ mm$ with an energy absorption capacity $E_{max} = 40\ o\ 50\ kJ$, but if it is installed along with shotcrete arches it could only tolerate a displacement of $\pm 100mm$. Also, if it is assumed that operations will be interrupted when the convergence is greater than 300 mm, it could be said that the design limits in terms of deformation are given by $\delta_{all} = 100\ a\ 300\ mm$ and the energy dissipation capacity is much less than that initially defined.

Fortification system design steps

The design steps to follow are described below (Kaiser, 2018):

1. Define the required accumulated displacement threshold δ_{all}, considering operational and economic aspects, including the expectations of quality of the fortification.
2. Select compatible components that connect well and can survive the travel threshold with a set static FS.
3. Calculate the energy absorption capacity of the selected system (accumulated capacity).
4. Define the maximum deformation capacity δ_{ult} for the fortification system (based on in situ performance monitoring).
5. Evaluate the distribution of energy use, the expected displacements and speeds on the walls.
6. Evaluate FS in terms of deformation capacity and energy absorption.

2.2.1.5 Fortification design methodology for rock mass subject to high stress

Villaescusa and Player (2014), describe the fortification design methodology proposed in Thompson et al. (2012), this methodology includes the steps to follow in order to:

- Identify the stress imposed by the rockmass.
- Select the reinforcement and support system with appropriate response characteristics.
- Specify the layout and installation of the elements that make up the fortification.

The generic procedure consists of the following steps (Thompson et al., 2012):

1. Identify a failure mechanism.
2. Estimate the stress per unit area.

3. Estimate the length of the reinforcement, the stress related to load and deformation.
4. Estimate the stress related to energy.
5. Select the appropriate reinforcement and support elements.
6. Propose the arrangement of the reinforcement and support elements, install them and evaluate them.
7. Specify the complete scheme of the fortification system.

This procedure may need to be applied to the possible failure mechanisms. In most cases, formal designs might be difficult to establish since the variables of the rock mass, which define the demand imposed in the reinforcement, cannot be quantified with a high degree of confidence. However, the stress can be defined qualitatively in terms of low, medium, high, very high and extremely high reaction pressure, surface displacement in the event of failure and energy demand per square meter, Table 10.

Table 10 Fortification design solicitation (Modified from Thompson et al., 2012).

In order to enhance the fortification design that survives dynamic loads, the stress of the rock mass regarding displacement and energy presented in Table 11 has been combined

Demand category	Reaction pressure (kPa)	Surface displacement (mm)	Energy (kJ/m²)
Low	< 100	< 50	< 5
Medium	100-150	50-100	5-15
High	150-200	100-200	15-20
Very high	200-400	200-300	25-35
Extremely high	> 400	> 300	> 35

with the database of dynamic reinforcement capacity established by the WA School of Mines (Player, 2012). The results of this design methodology are presented in Figure 28.

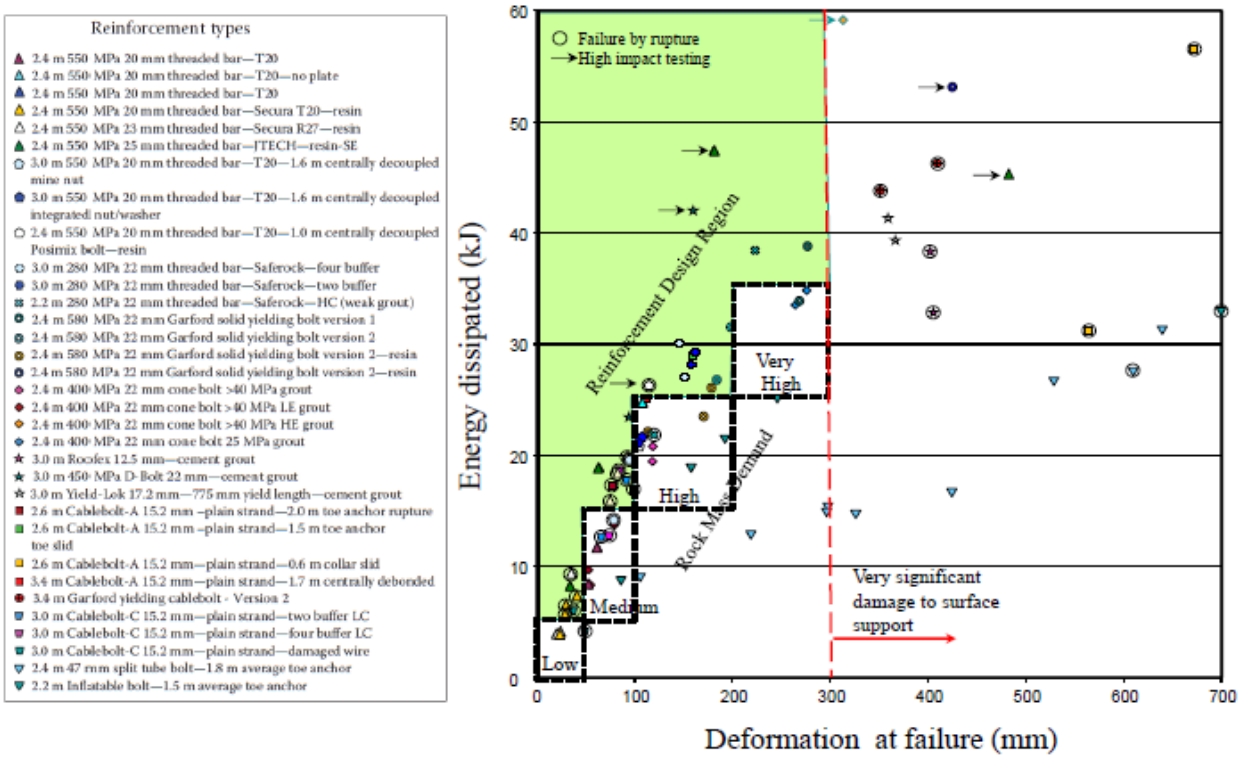

Figure 28 Fortification design under dynamic load (Player, 2012).

For each category of stress, the corresponding ranges of displacement are indicated, establishing a region that is labeled as low, medium, high and very high as appropriate. For each of these regions, the type of bolt that is compatible in displacement and that provides a greater energy dissipation capacity must be selected, these characteristics would be met by selecting the reinforcement within the green region (Reinforcement design region).

2.2.2 Empirical methodologies

Fortification design for permanent excavations in underground mines is generally based on empirical and intuitive approaches. These design methodologies are based on the rating assigned to the underground structures found in the analyzed project. The assigned rating is the result of the estimation of the rock resistance, analysis of the discontinuities, presence of water, etc. It should be noted that much of the information needed to assess the condition of the rock mass can only be collected after the excavation has been carried out.

There are many classification systems available, all of them well documented by various authors (Palmström, 1995; Singh & Goel, 1999). The use of rock mass classification systems for the selection of a fortification system is recommended only when there is insufficient geotechnical project data available, particularly during the initial stages.

Not all classification systems are designed in a way that allows the selection / design of fortification systems, since their main objective is the characterization of the rock mass. In this review, only empirical systems that allow the selection of fortifications for underground excavations will be mentioned (Guntumadugu, 2013).

Table 11 Empirical methodologies for fortification systems design.

Methodology	Type	Most common use	Detailed information
The rock quality designation (RQD)	Numerical form functional type	Based on drillhole analysis: Used in other classification systems.	Deere et al. (1988)
The rock mass rating (RMR) classification	Numerical form functional type	Tunnels, mines and foundations design.	Bieniawski (1974)
The 'Q' classification system	Numerical form functional type	Fortification design in underground excavations	Barton, Lien, & Lunde (1974)
The Geological Strength Index (GSI)	Numerical form functional type	Fortification design in underground excavations and used as input data in numerical modeling.	Hoek et al. (1995)
The Rock Mass index (RMI) system	Numerical form functional type	For general characterization, fortification design, TBM preview.	Palmström (1995)

Some of the methodologies analyzed consider the design of fortification systems based on empirical formulas based on basic rules combined with similar past experiences. These methodologies present a series of graphs and tables that make their use convenient. After analyzing some cases where empirical design methods were adopted, Syed (2004) determined that the two methodologies that provide the best guidance regarding the selection of a fortification system are the named RMR and Q, however they should not be assumed as definitive design methodologies.

2.2.3 Numerical methodologies

This proposal is not the same as that applied to develop the conventional numerical stress analysis model necessary to carry out the mine design. In this case, the model seeks to determine important information for the selection of the fortification system, such as the depth of the fault and the volume of rock that could be expelled before a dynamic event.

Numerical models are commonly used in the data analysis process before, during, and after excavation construction. These models allow complex systems of equations to be solved that in turn can be used to predict the evolution of stresses and strains in geomaterials as an excavation sequence progresses.

Because these methodologies are based on fundamental principles of mechanics and materials models, they are widely applicable in comparison to empirical analysis

methods. In other words, numerical analyzes are not as limited to a specific kind of geology and / or application as many empirical methodologies.

Numerical analysis methods also have an advantage over analytical methods as analytical methods can only be used for a limited range of conditions defined by a set of assumptions used in their development (i.e. isotropy, homogeneity, hydrostatic stresses, constitutive model perfectly plastic, excavation geometry, etc.) (Bobet, 2010).

In analytical models, the system is continuous, has an infinite number of degrees of freedom, and is governed by a differential equation. Numerical models work on the principle of dividing the model domain into discrete components, limiting the system to a finite number of degrees of freedom. Each component in the model must satisfy the governing differential equations and the continuity conditions associated with its neighbors (Jing L. , 2003).

The most difficult part of creating a numerical model is translating a practical problem into a representative input data set and understanding how to relate the results of the model to actual behavior. The process of determining representative inputs (particularly constitutive models and relevant parameters) is generally quite difficult, and if done incorrectly, it can render a given model useless. Even in relatively simple cases, the interpretation of model results is still highly dependent on experience (Jing & Hudson, 2002; Carter, et al., 2000; Bobet, 2010).

2.2.3.1 Continuous methods

Some of the oldest and most widely used numerical methods are based on the assumption that materials behave as a continuum. This assumption results in the restriction that the materials cannot be broken into pieces. This means that all material points remain in the same point neighborhood throughout the deformation process. Another interpretation is that the displacement field must be continuous (Jing, 2003).

As Jing (2003) pointed out, all systems are discontinuous at a certain scale. The distinction between continuous and discontinuous in general is quite uncertain, and depends on determining the scale to which a continuum can approximate observed behaviors. Depending on the information that is desired, a given material can often be modeled as continuous or discontinuous.

Continuous models are more commonly used than discontinuous models in rock mechanics (even when they are not necessarily appropriate), although the inability of continuous models to accurately reflect certain behaviors observed in situ, such as macroscopic separation of blocks fractured under high stress (Bobet, 2010).

Continuous models are more appropriate for representing rock masses that are intact or that are poorly fractured, and when failure is not expected to be structurally controlled (for example, such models are not intrinsically suitable for modeling a wedge fall by gravity). Altered rock tends to have enough freedom of movement along small-scale discontinuities that it can be represented as a pseudo-continuum. Only massifs with structures such that movement / failure is dominated by moderately spaced discontinuities between relatively strong or rigid blocks cannot be modeled by a continuous method.

The most common types of continuous modeling are the Finite Element Method (FEM), the Finite Difference Method (FDM), and the Boundary Element Method (BEM).

Because BEM codes are typically used for purely elastic analysis, only FEM and FDM will be discussed (Jing, 2003).

Finite elements method (FEM)

The finite element method has emerged as perhaps the most prominent method of continuous analysis in engineering applications (Jing, 2003; Bobet, 2010; Carter et al., 2000). Some examples of FEM programs are ABAQUS (Hibbit, Karlson and Sorensen, Inc.), PENTAGON-2D and -3D (Emerald Soft), Phase2 (Rocscience) and PLAXIS (Plaxis BV) (Bobet, 2010)

Finite differences method (FDM)

The Finite Difference Method was the first numerical method used to approximate the solutions to complicated partial differential equations (Jing, 2003). The differences between FEM and FDM are subtle, and are generally more a matter of habit than some fundamental difference in the nature of the methods themselves (Itasca, 2011) :

- Meshes with finite differences were originally intended to be square grids, while FEM meshes can be composed of irregular polyhedra. The development of the Finite Volume Method (FVM), which is considered a subset of FDM, allowed FDM codes to be as flexible as FEM codes with respect to heterogeneity and mesh generation.
- In FDM, quantities are not defined within elements, whereas FEM formulations use shape functions within elements as part of minimizing error / energy terms in the solution.
- FEM programs generally use an implicit solution method that brings together a global system of equations, which is solved simultaneously to find equilibrium. FDM programs generally use an explicit solution method (that is, dynamic or time running) that repeatedly solves the finite difference equations over the course of time steps.

For practical purposes, selecting one FDM over FEM is similar to selecting one FEM code over another; it is a matter of preference. The two methods ultimately solve the same system of equations. Individual preferences may exist between companies or researchers based on the effectiveness of the solution method, ease of use, or flexibility.

The most commonly used FDM programs in Geomechanics are FLAC and FLAC3D (ITASCA Consulting Group, Inc.) (Bobet, 2010). Although known as FDM programs, these codes actually use an FVM solution, allowing them to handle irregular mesh geometries.

Advantages and disadvantages

Below is an analysis of the identified advantages and disadvantages of using FEM or FDM

Table 12 Advantages and disadvantages of using FDM and FEM

	Advantages	**Disadvantages**
Finite element method FEM	• It is flexible in terms of handling heterogeneity and anisotropy. Heterogeneity is only modeled at the	• Discretization of the problem domain can cause problems in terms of memory usage. Because some constitutive models cause

	Advantages	Disadvantages
	macroscale through the definition of zones of different material properties. Simple cases of anisotropy can be modeled by modifying the stiffness matrices. • Staged models can capture the evolution of a system over time, including modeling excavation sequences and fortification installation. • A wide range of practical experiences with FEM codes have been developed in the geotechnical community, making the method relatively accessible.	the response of the model to depend on the mesh used, obtaining an optimal discretization can be difficult and can result in the execution of a computationally intensive model. • The need to store large arrays increases memory requirements relative to other modeling methods. • Sophisticated algorithms are needed to implement constitutive softening / hardening models. • Discrete fractures are difficult to accurately model.
Finite difference method FDM	• The mapping of non-linear behavior (i.e. plasticity) is carried out by direct solution of equations, instead of using complex return mapping algorithms as occurs in FEM. • The explicit solution method avoids the need to assemble massive arrays. • Easy accommodation of large displacements / deformations. • The fictional time variable can, in some cases, be calibrated to observe relevant results in terms of how physical systems evolve in real time. • The computational scheme allows to model dynamic problems and physical instability. • With regard to FLAC and FLAC3D in particular, one of the greatest strengths relative to other number codes is the existence of the integrated programming language, FISH, which allows users to define new variables and functions. This language, while less intuitive for some users than graphical user interfaces, adds great flexibility to the program, such as allowing users to define their own constitutive models.	• It is relatively inefficient at solving linear systems (that is, elasticity problems). • For static problems, the equilibrium solution is given as a function of the damping method and the parameters used; it also assumes that the user's "convergence" judgment is adequate (based on factors such as unbalanced forces, velocity field, etc.).

2.2.3.2 Published Numerical models of reinforcement elements

After identifying the deficiencies of the procedures for determining the energy absorption capacity of reinforcing elements used during the last decades, the use of laboratory test results has become a useful design tool, because they provide the means for a comparative analysis of the performance between different types of elements, as well as their behavior under static and / or dynamic load. However, it is observed that, for practical reasons, most laboratory tests only use a loading mechanism and under defined edge conditions, in addition, in the case of dynamic tests it implies a high investment in terms of economic resources, personnel and time.

The challenge then centers on how numerical modeling can eventually provide a more robust reinforcement / support element design tool and in turn provide feedback on laboratory results.

Although numerical models have been developed in an attempt to capture the mechanical processes that dominate the deformation or failure of fortification systems / elements, when tested under different loading conditions, the exact resistance mechanism of the elements is difficult to determine, even more so when they are tested in the laboratory.

This is mainly due to: a) the presence of several different materials (bolt, grout or resin, confining medium) with radically different stiffness and mechanical behavior, b) the three-dimensional appearance of the system that is difficult to simulate, i.e. bolt type and geometry, c) loading conditions and d) the way in which the test equipment applies the latter.

In this context, a model that functions as a simulation tool must in principle discriminate the structure to be analyzed into small elements and propose constitutive equations that describe the response of each of these individual elements and their interactions. Finally, these numerous equations are solved together using a computational application. The results of this procedure include the distribution of stress on the elements that make up the model and the displacement pattern of the fortification system within a structure.

A series of software has been developed for the modeling of civil and geotechnical problems. Some of them can be used to design and analyze fortification systems. Note that the use of 3D software is necessary to simulate all the features of a model, such as joints, failure planes, contact interface, and failure criteria.

Several numerical methods are used in rock mechanics to model the response of fortification elements and in most cases the response of the rock to loading and unloading. These methods include the finite element method (FEM), border element method (BEM), finite difference method (FDM), and discrete element method (DEM).

With these considerations in mind, several studies have been conducted on the behavior of bolts in the FE field, including those by Coates & Yu (1970), Hollingshead (1971), Aydan (1989), Saeb & Amadei (1990), Aydan & Kawamoto (1992), Swoboda & Marence (1992), Moussa & Swoboda (1995), Marence and Swoboda (1995), Chen et al. (1994, 1999, 2004), and Pal & Wathugala (1999).

One of the first attempts to use standard FE to model the bolt and grout was made by Coates & Yu (1970), this study defined from an FE model the stress distribution around a

cylindrical hole in tension or compression. It was found that the stress distribution is given as a function of the modulus of elasticity of the bolt and the rock.

The presence of grout between the bolt and the rock was not considered and there was no margin to define the creep state. The analysis was carried out only assuming a linear elastic behavior with two material phases, which limits the scope of the model.

Hollingshead (1971) integred grout in a model using three material phases (bolt-grout and rock) allowing one zone to flow into the grout, using a perfectly plastic elastic criterion, according to Tresca's failure criterion, for the three materials, how the interfaces behave was not considered in the model.

John and Van Dillen (1983) developed a new one-dimensional element that crosses a cylindrical surface, to which elements representing the surrounding material are attached. Three important modes of failure were considered, for fully grout bolts, a bilinear elastoplastic model for the axial response, perfectly plastic elastic and residual plastic for the binder material.

Although the last model eliminated many of the limitations presented by the previous proposals and its results are consistent with laboratory results, it did not consider the stiffness of the rock and the stresses in situ around the drilling. It was also stated that critical shear stress occurs at the grout-rock interface, which does not always occur either in the laboratory or in the field.

Aydan (1989) presents a one-bolt FE model. He assumes that a cylindrical bolt and a grout ring are connected to the rock by 8 three-dimensional nodes. Two nodes connect to the bolt and six to the rockmass.

The use of edge elements and FE techniques to analyze stress and strain along the bolt was carried out by Peng & Guo (1992). The slab effect was replaced by an edge element. The effect of the reinforcing element was overestimated due to the assumption of perfect union between the different components.

Stankus & Guo (1996) determined in horizontal and laminated rock strata, fully slurry bolts anchored to one point are very effective, especially if they are installed quickly at high tension after excavation. They used three bolt lengths of 3300, 2400 and 1500 mm and three tensions 66, 89 and 110 kN, finding that:

- Bolts with higher pretension induce smaller deflection
- The longer the bolt, the greater the load
- In bolts with the same length and high tension, there is a small deflection
- High deflection was observed for long bolts and small deflection for short bolts

They developed a method to achieve the optimal transmission effect (OBE). However, there are some assumptions in their methodology, such as, for example, the problem with the separating element they use, since it is not flexible for any type of mesh, especially with thin grout. Many relevant parameters of the contact interface cannot be defined in the separator element. All materials were modeled in the plastic region of deformation.

Marence and Swoboda (1995) developed the cross joint bolt (BCJ), an element that connects both sides of a shear joint. It has two nodes, one on each side of the

discontinuity. The model cannot predict the spacing length along the grout-bolt interface, and the hinge point position.

When it comes to modeling of laboratory tests to fortification systems / elements Ferrero (1995), Grasselli (2005), Aziz & Jalalifar (2007), Chen & Li (2015), and Tatone et al. (2015), have simulated laboratory tests on various types of bolt.

Ferrero (1995) used a three-dimensional (3D) code of finite elements to simulate in a cutting test a system of rock discontinuities reinforced by steel segments, also performing a back analysis of the elements to define the evolution of the stress in them. For both rock and steel, a perfectly plastic elastic behavior was assumed.

Grasselli (2005) used a 3D finite element code to simulate rebar and Swellex bolts shear tests. He assumed an elastic material model to simulate the bolts and a perfectly plastic model for an interface that represents the joint that separates the two blocks. This simulation provided some insight into bolt failure mechanisms under shear loading conditions.

Aziz and Jalalifar (2007) also proposed a 3D finite element code to simulate the laboratory tests performed on rock joints traversed by bolts subjected to shear load, they investigated the yield stress and the variation in the deformation of the bolt at the intersection of joint/rockbolt. The steel was simulated using a bilinear hardening model.

Chen & Li (2015) used the continuous code FLAC3D software to simulate laboratory tests performed on rebar and D-Bolt bolts by varying the anchor displacement angles. They used a trilinear material model to capture the hardenable behavior of steel. They also used different models to represent the grout-rock and grout-bolt interfaces in order to explicitly simulate the different adhesion mechanisms. In the case of the rebar bolt, the adhesion between the steel and the rock was defined by the high shear strength at the bolt-grout interface.

In the simulation of the D-Bolt, the bolt cohesion was defined by the shear resistance that was assumed equal in two anchor positions and with shear resistance equal to zero in the section of the bolt between them. Using this model, it was possible to realistically simulate the response of the D-Bolt and rebar in terms of load and displacement under conditions of pure shear load, pure traction and combined load.

Tatone et al. (2015) simulated pull test laboratory tests on reinforcing elements using the material and structural elements model approximations using the two-dimensional (2D) Y-Geo code, which is based on a hybrid finite-discrete element method. The results of both proposals are consistent in terms of the load-displacement response and damage propagation. They also demonstrated the effectiveness of reinforcing elements represented by structural elements in reducing the amount of damage around excavations.

Zhang et al., (2018) proposed a model based on the discrete element method (DEM) in 3D that investigates the micro and macro behavior at the grout bolt interface, taking into account the effects of bolt profile and particle size. Results were validated with measurements carried out in the laboratory; however, this model only considers the response to load in shear and under static conditions, nor does it consider the type of grout used.

Some of the most popular commercially available codes, such as FLAC, FLAC3D, UDEC and 3DEC developed by Itasca Consulting Group Inc, allow the use of structural

elements to simulate the use of different components of a fortification system. Indeed, two models of reinforcing elements can be used, the cable and the rockbolt, to consider both the properties of the bolt and the grout.

For practical purposes, the main difference between the two approaches is that the "cable" element does not provide flexural strength, making it more suitable for simulating cables, while the rockbolt element provides flexural strength, which makes it suitable for simulating other reinforcing elements such as fully milled rockbolts.

A review of the technical literature suggests that cable type elements are in more popular use than the rockbolt element, even for element simulation of rock reinforcements other than cables. This is mainly due to the complexity of the rockbolt element compared to the cable element, in terms of input parameters and calibration process.

For example, Vardakos et al. (2007), Malmgren & Nordlund (2008), Jiang et al. (2009), Li et al. (2012), Gao et al. (2015), and Shreedharan & Kulatilake (2016) used the cable element for the simulation of pull tests or excavation support, even in cases where cables were not used for the real reinforcement.

Ruest & Martin (2002) also used the cable element in FLAC2D but for the laboratory pull test simulation of instrumented cables and grouts inside steel tubes. The calculated loads along the cable element were compared with the loads measured for several tests where the grout properties were varied. The results showed very good agreement with those of laboratory tests.

Only, Nemcik et al. (2014), Ma et al. (2014), Marambio et al. (2018) and Vallejos et al. (2020) have reported the use of the rockbolt element for the simulation of completely gritted bolts subjected to tension.

Nemcik et al. (2014) ignored the forces perpendicular to the rockbolt element and subsequently its flexural strength, since they were only dealing with tensile load. In his analysis, the rockbolt. behaved similarly to the cable element. Similarly, Ma et al. (2014) used the rockbolt element in FLAC2D to simulate laboratory pull tests in order to determine the interaction between the bolt and the rock mass in a road tunnel.

When talking about the simulation of laboratory tests that apply dynamic load to reinforcing elements Vallejos et al., 2020) presents a numerical model based on the finite difference method (FDM) that represents the behavior of the threadbar bolt (commonly used in Chilean mining) when tested under a mechanism similar to that of the Canmet-MMSL's test.

Although the results obtained are consistent in terms of load-deformation with laboratory results, the bolt was modeled as rockbolt, in addition, the response of the grout or the interfaces that make up the test were not explicitly modeled.

3 Properties and elements that compound the numerical model

3.1 Introduction to FLAC3D

FLAC3D is a commercial geotechnical finite difference software. It uses an explicit Lagrangian calculation scheme and the mixed-discretization zoning technique (Itasca, 2012) to ensure that plastic failure and flow, as well as elastic behavior, are modelled accurately.

The calculation scheme used by FLAC3D takes a large number of calculation steps, each progressively redistributing an unbalanced force caused by changes to stress or displacement boundaries through the mesh (Itasca, 2011).

The unbalanced force is the algebraic sum of the net nodal-force vectors for all of the nodes within the mesh. The model is considered to be in equilibrium when the maximum unbalanced force is small compared with the total applied forces within the problem. If the unbalanced force approaches a constant non-zero value, this normally indicates that failure and plastic flow are occurring within the model.

By default, the model is assumed to be in equilibrium when the maximum unbalanced force ratio (i.e. the ratio between the magnitude of the maximum unbalanced force and the magnitude of the average applied mechanical force within the mesh) falls below $1x10^{-5}$ (Itasca, 2012).

There are several reasons why FLAC3D was selected for the analyses. One of the main aims of the numerical study was to model situations in which plastic flow may occur. As mentioned earlier, FLAC3D is suitable for simulating this type of problem.

By default, FLAC3D operates in small-strain mode; that is, nodal coordinates are not changed even if the computed displacements are large compared with the typical element size. In large-strain mode, nodal coordinates are updated at each step according to computed displacements. In large-strain mode, geometric nonlinearity is possible.

The intrinsic FISH language is one of the most useful features in FLAC3D. FISH can be used to include conditional 'if' statements and loops for repetitive tasks within a code and to carry out mathematical operations, define new variables or functions, and extract stresses and displacements from the analysis.

3.2 Components of numerical model

As explained earlier, there are two active facilities that test rock bolts under dynamic load, the WASM and CanMet-MMSL. It is important to clarify that it is known that New Concept Mining team has developed the new Dynamic Impact Tester (DIT) to study the behavior of reinforcement and retainment elements under dynamic loads, but the results are recent and by the time the explicit model was calibrated they were not available, therefore, the operation of this equipment was not studied.

A new facility developed by the University of Chile and MIRARCO with a loading mode similar to the CanMet-MMSL has been developed in recent years, the operating

mechanism was selected considering that some authors have questioned the effect of the other modes of dynamic loading on rock reinforcement elements (Vallejos et al., 2020). Considering the above and hoping that the proposed numerical model will serve as support for the tests to be carried out in the Chilean facility, the model to be described in this thesis is developed.

When talking about the reinforcement element to be modeled threadbar was chosen (known also as rebar or gewibar), due to its wide use in Chilean underground mining and its possible globalization.

The numerical model to be proposed is composed by four main elements: test facility structure, rock bolt, grout and confinement medium (steel tube). Three different geometries of FLAC3D meshes were created for the three first components. the steel tube is represented by DKT-CST hybrid structural element (Shell element). The dimensions of the model are the same as the ones used in CanMet laboratory testing. Model configuration is shown in Figure 29.

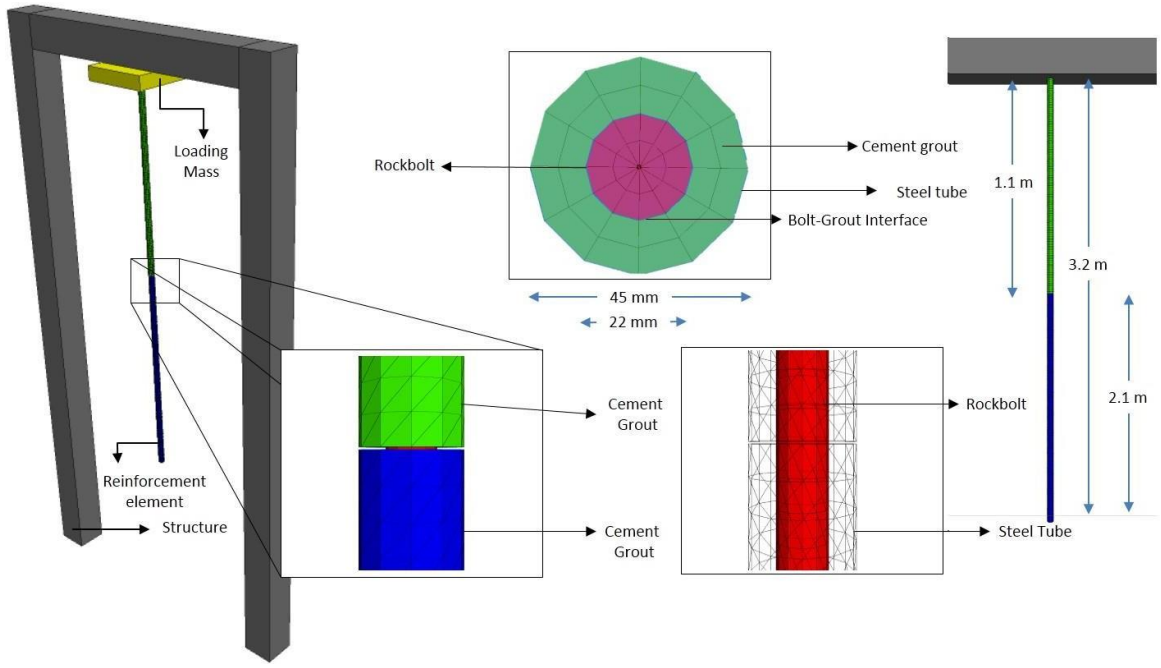

Figure 29 Model geometry and configuration

3.2.1 Properties and mechanical response of components

3.2.1.1 Rockbolt (Threadbar)

A rockbolt is represented in the model by an explicit element with a cylinder shape that responds to the tension through an elastic- plastic constitutive model. The element is modeled with Mohr-Coulomb criterion, controlled by bolt stiffness (K_b) and yield limit, as shown in Figure 30.

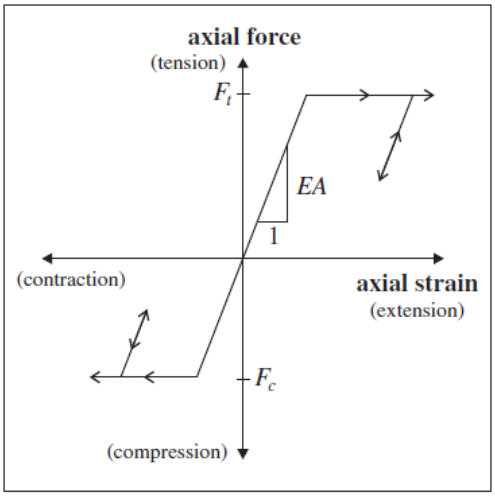

Figure 30 Mohr-Coulomb constitutive model. Taken from Itasca Consulting Group (2012)

Rockbolt properties are well known, and each manufacturer shows the properties of the material of its specific rock reinforcement element in their catalogues. Table 13 presents the mechanical properties corresponding to the threadbar.

Table 13 Threadbar mechanical properties

Property	Value
Bar diameter	22 mm
Yield limit	167.258 KN
Tensile strength	440 MPa
Young Modulus [E]	210 GPa
Poisson ratio [v]	0.27
Density	7,850 Kg/m3
Elongation	10 %

However, it is known that steel changes its yield limit and ultimate strength under dynamic loading conditions. According to Malvar & Crawford (1998), these magnitudes can be estimated by the elastic properties of steel scaling through a dynamic increase factor (DIF).

DIF depends on strain rate ($\dot{\varepsilon}$) in s^{-1} (1/second), and a coefficient (α). α is a function of rockbar static yield strength (σ_y) and allows the calculation of dynamic yield limit and dynamic ultimate strength of steel. See Equation 1.

$$DIF = \left[\frac{\dot{\varepsilon}(t)}{10^{-4}}\right]^{\alpha}$$

Equation 1 Steel Dynamic Increase Factor **(Malvar & Crawford, 1998)**

$$\alpha_{fy} = 0.074 - 0.040\frac{\sigma_y}{414}$$

$$\alpha_{fu} = 0.019 - 0.009\frac{\sigma_y}{414}$$

Where:

DIF	= Dynamic increase factor
$\dot{\varepsilon}$	= Strain rate
σ_y	= Yield limit of steel in static condition in MPa
α_{fy}, α_{fu}	= Coefficients for yield limit and ultimate strength of steel

The use of the DIF is recommended for steel bars with yield strengths varying from 290 to 710 MPa and strain rates between 10^{-4} and 225 s^{-1}. Threadbar static test results meet the yield strength condition mentioned above and dynamic tests has shown strain rates around 12 s^{-1}. Therefore, this formulation can be applicable to the rockbolt mechanical response model.

3.2.1.2 Grout

A group of explicit elements that envelops the threadbar, forming a ring with a defined thickness, represents the grout in which the rockbolt is inserted in the laboratory-scale dynamic tests.

However, the grout presents a complex mechanical response that must be studied and modeled in order to obtain a completely explicit model. The analyses performed are described below.

Grout strength degradation

Cement grout exhibits the phenomenon of strain softening under compressive loads. This behavior can be modeled by using a Strain-hardening/softening constitutive model. The constituve model is controlled by variations prescribed to the properties of the Mohr-Coulomb model (cohesion, friction, dilatation, tensile strength) as a function of plastic strain (Itasca, 2012). Figure 29.

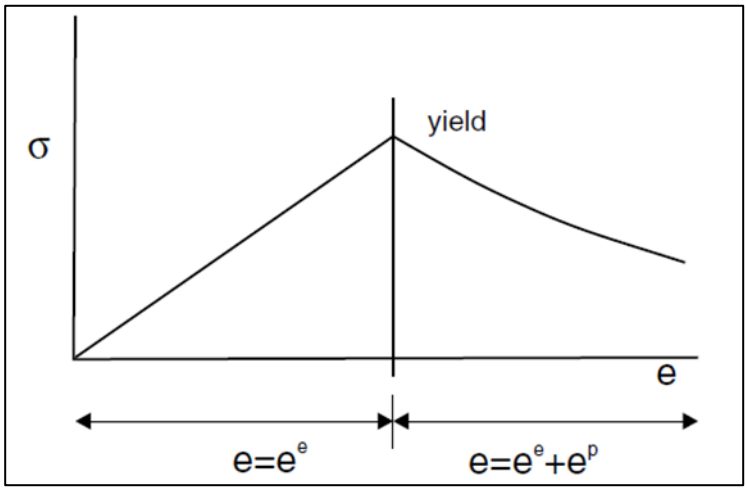

Figure 31 Strain-hardening/softening constitutive model. Taken from Itasca Consulting Group (2012)

Non-linear strength degradation of grout is highly stress dependent, as documented by triaxial test results from Hyett et al. (1992) and Xie & Shao (2008). The confining pressure and the water: cement (w:c) ratio of the grout strongly influences the shape of

the strength degradation as well as the value of residual strength. Strength degradation decreases with increasing confinement pressure. Finally, under high confinement pressure the grout becomes nearly ductile, and no degradation occurs.

Such behavior is observed in published results. With the aim of modeling the grout response, load-strain curves from triaxial tests on grout samples (0.4 and 0.44 water: cement ratio) under various confinements were extracted from bibliography and are presented in Figure 32.

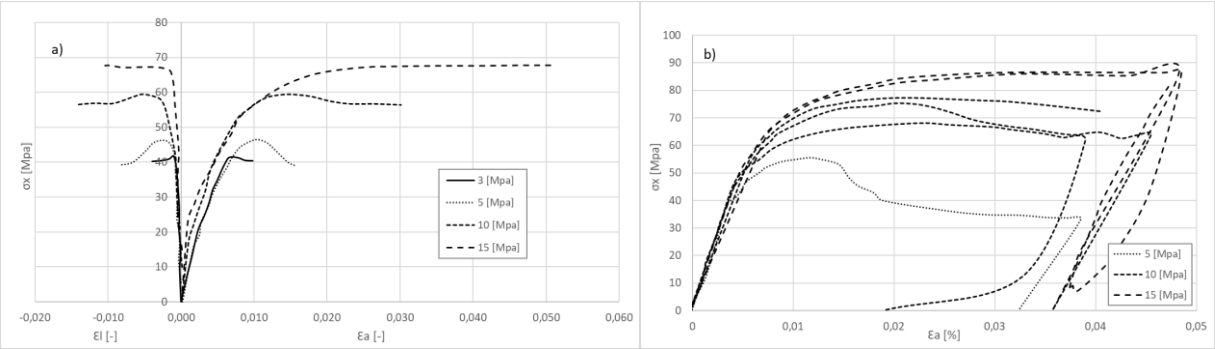

Figure 32 Stress — strain curves of cement grout in triaxial compression tests with different confining pressures a) 0.44 (modified from Xie & Shao, 2008) and b) 0.4 (modified from Hyett et al.,1994) water: cement ratio

The Cohesion Weakening Friction Strengthening (CWFS) model proposed by Renani and Martin (2018) allows to define the variation of the degradation behavior in relation to the confining pressure. This proposal was enhanced to respect the nonlinear nature of damage and to avoid sharp changes in the rate of cohesion degradation and friction mobilization, as is the case of the proposal by Hajiabdolmajid et al. (2002) proposal.

Considering the smooth form of plotted triaxial curves, CWFS model is adequate to represent the grout strength degradation response due to compressive load. The following empirical equations were used to describe cohesion degradation and friction mobilization of grout as smooth functions of plastic strain:

$$c = c_{ult} + (c_{ini} + c_{ult})\left[2 - \frac{2}{1 + \exp(-3.66\frac{\varepsilon^p}{\varepsilon_c^{p*}})}\right]$$

Equation 2 CWFS model cohesion degradation (Hajiabdolmajid et al., 2002)

$$\varphi = \varphi_{ini} + (\varphi_{ult} - \varphi_{ini})\left[\frac{2}{1 + \exp(-3.66\,\frac{\varepsilon^p}{\varepsilon_\varphi^{p*}})} - 1\right]$$

Equation 3 CWFS model friction mobilization (Hajiabdolmajid et al., 2002)

Where:

c_{ini} and c_{ult}: Initial and degraded values of cohesion.

φ_{ini} and φ_{ult} : Initial and mobilized values of friction angle.

ε_{c*}^{p} and $\varepsilon_{\varphi*}^{p}$: Plastic strains at cohesion and friction angle are within 5% of their ultimate values, respectively.

Based on the information gathered from bibliography and Equation 2 and Equation 3 the estimated parameters of the CWFS model for 0.4 and 0.44 w:c grouts are given in Table 14.

Table 14 Estimated parameters of the CWFS model for 0.4 and 0.44 w:c rate grouts. *Values taken from Hyett et al., 1994.

w:c	σ_{ini} [MPa]	σ_{ult} [MPa]	E [Gpa]	$\boldsymbol{\nu}$	ε_{c*}^{p}	$\varepsilon_{\varphi*}^{p}$	φ_{ini} [°]	φ_{ult} [°]	$\boldsymbol{C}_{ini}$ [MPa]	$\boldsymbol{C}_{ult}$ [MPa]	Density [g/cm3]*	Shear strength [Mpa]*
0.44	36.12	30.19	10	0.25	0.017	0.005	21.4	28.50	12	7.6	1.98	3.8
0.4	45.92	12.98			0.03	0.006	24	37	13	3	1.97	3.9

The variation of cohesion and friction for each strain and the corresponding stress-strain curves under triaxial compression resulting from the application of the CWFS model are depicted in Figure 33 and Figure 34.

The triaxial test data was analyzed in order to deduce the main geomechanical features of the grout for implementation in strain-softening/hardening constitutive model in FLAC3D. Peak and residual Hoek–Brown (H–B) failure criteria were fitted to the peak and residual strength values obtained as a result of CWFS implementation. These fits, together with the original test data and data from CWFS model are presented in Figure 35 Such comparation shows good agreement in terms of maximum and residual strength of grout at different confining stresses.

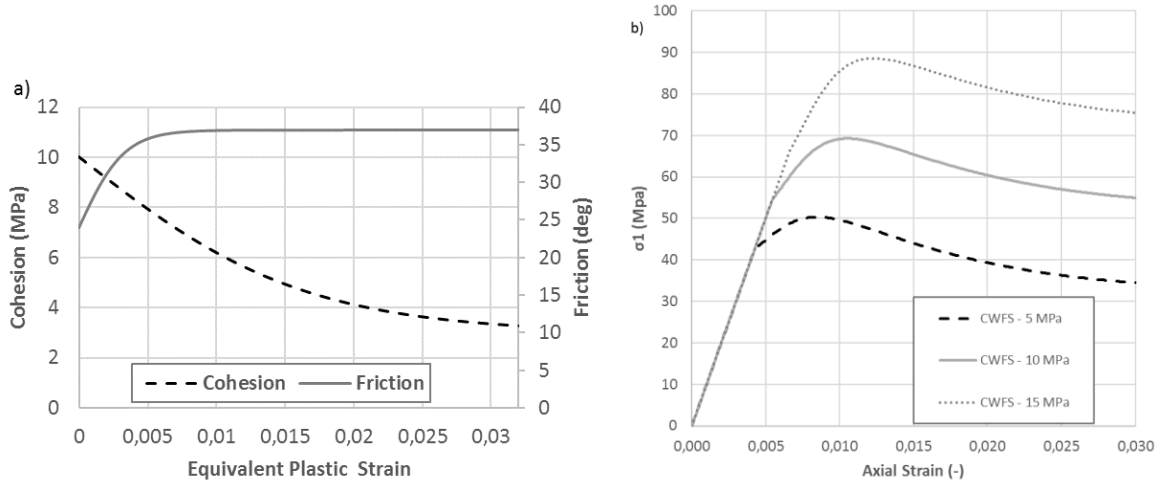

Figure 33 CWFS model for 0.4 w:c rate grout a) cohesion loss and friction mobilization, and b) stress-strain curves under triaxial compression

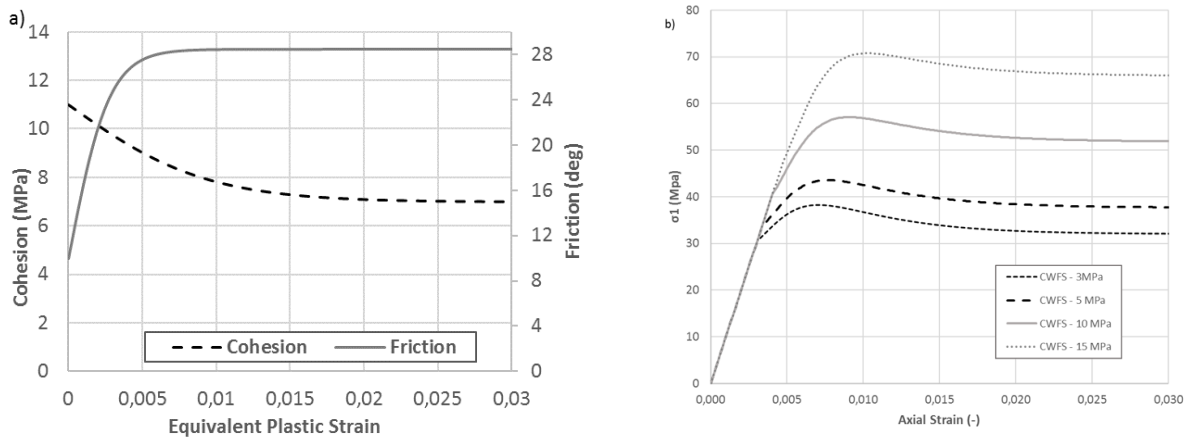

Figure 34 CWFS model for 0.44 w:c rate grout a) cohesion loss and friction mobilization, and b) stress-strain curves under triaxial compression

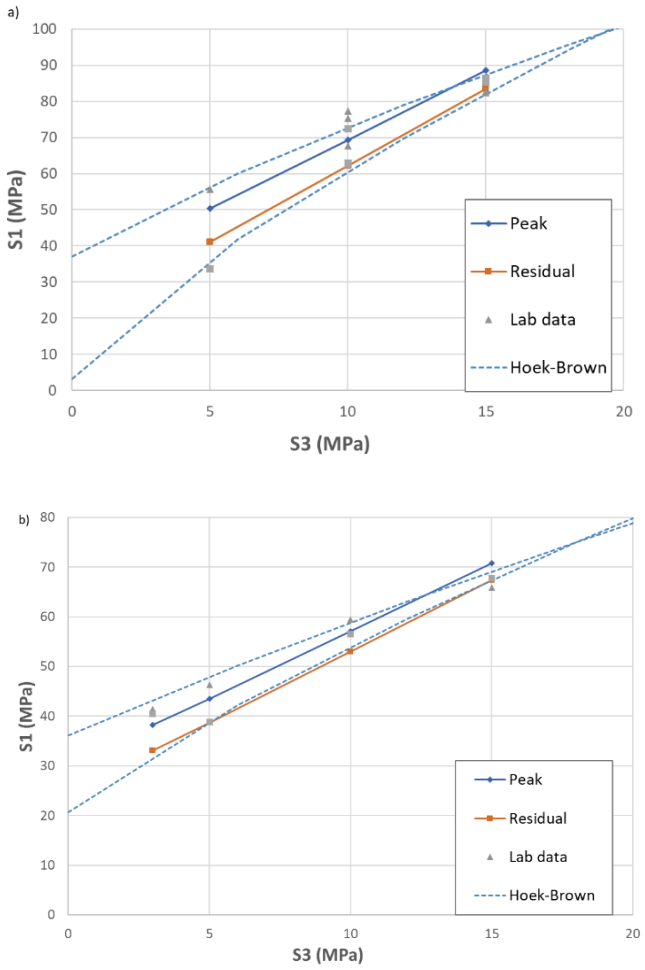

Figure 35 Peak and residual strength test results and fitted to Hoek–Brown failure criteria, laboratory data and CWFS model. (a) 0.4 (b) 0.44 w:c rate grouts.

Dilation angle variation

In addition to cohesion and friction, the dilation angle (ψ) for 0.44 w:c ratio grout was evaluated, considering that radial and axial stress-strain curves are available only for such grout samples (Xie & Shao, 2008).

The model that allows to calculate the dilation angle is divided into two parts: one referring to the peak dilation (ψ_{peak}) angle and the second part related to dilation angle decay with plasticity (K_ψ). Formulation is presented in Equation 4 and Equation 5 (Alejano and Alonso, 2005).

$$\psi_{peak}(\sigma_3) = \frac{\phi_{peak}}{1 + \log_{10}\sigma_c}\log_{10}\frac{\sigma_c}{\sigma_3 + 0.1}$$

Equation 4 Peak dilation **(Alejano & Alonso, 2005)**

$$K_\psi = 1 + (K_{\psi peak} - 1)^{e^{-\gamma^p / \gamma^{p*}}}$$

Equation 5 Dilation angle decay **(Alejano & Alonso, 2005)**

$$\gamma^{p,*} = \frac{\gamma^p}{\ln\left[(K_\psi - 1)/(K_{\psi,peak} - 1)\right]} \qquad \gamma^p = \left|\varepsilon_1^p - \varepsilon_3^p\right|$$

Where:

$\gamma_{peak}, \phi_{peak}$ = Peak dilation angle and peak friction angle, respectively.
$K_\psi, K_{\psi peak}$ = Dilation angle decay with plasticity and dilation angle decay peak, respectively.
γ^p, γ^{p*} = Shear plastic strain and plasticity parameter constant, respectively.
$\sigma_c, \sigma_3, \varepsilon_1^p, \varepsilon_3^p$ = Uniaxial compressive strength, confinement pressure, major and minor principal plastic strain, respectively.

Using the above-mentioned approach and fit coefficients presented in Table 15 dilatancy angle for cement grout with 0.4 w:c ratio was estimated for confinement pressures of 0, 5, 15 and 20 MPa.

Table 15 Approach and fit coefficients for dilation angle variation

Coefficient	Value
K_ψ	σ_3=0 20 σ_3=3 21 σ_3=5 28 σ_3=10 30
γ^p	25[$mstrain$]
$\gamma,^*$	20 [$mstrain$]

For mentioned confinements, point clouds for dilation angle of grout, calculated from triaxial tests, were depicted. The Figure 36 also shows curves of ψ as a function of the

plastic parameter γp and confinement pressure. The model fits the laboratory data in terms of peak friction angle and the process of dilation decay.

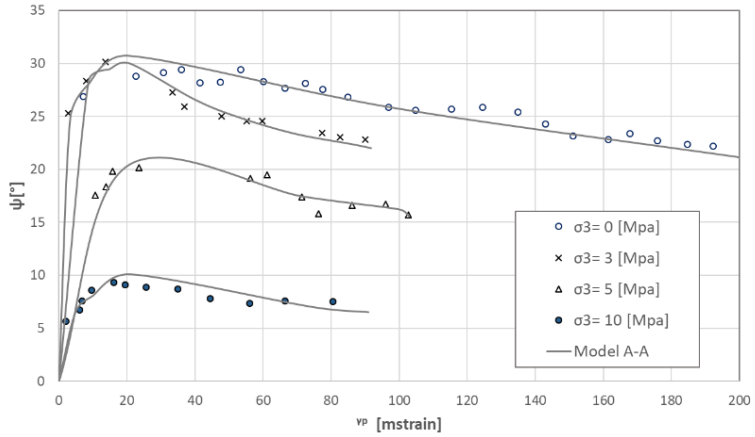

Figure 36 Dilatant behavior for cement grout of 0.44 w:c ratio. Dilatancy from triaxial test compared with the model proposed by Alejano & Alonso (2005)

Previous figure reveals the expected behavior: dilation angle dependencies as pointed out by Alejano & Alonso, 2005, that is, the dilation angle depends, first, on confining pressure (i.e., as confining pressure grows, the dilation angle diminishes) and second, on plastic shear strain (i.e., as plastic shear strain develops, the dilation angle decay).

Validation of grout mechanical properties

After defining the values to use as mechanical properties of grout (said cohesion, friction and dilation) in strain-softening/hardening constituve model, validation was carried out.

A series of 3D numerical simulations of triaxial compression tests of a Mohr-Coulomb strain-softening material were conducted with FLAC3D. The model has a height of 100 mm and a diameter of 50 mm. The mesh contains 96,000 elements and 100,521 grid-points. A constant grid-point velocity of 5 e^{-8} m/step was applied at the top and bottom of the sample, respectively.

During the simulation of the triaxial loading process the elements deform and reveal degradation and dilation. Considering the strength heterogeneity, the elements undergoing degradation and dilation will coalesce and is expected the formation of macroscopic fractures. The simulated stress - axial strain curves under confining pressure of 3, 5, 10, and 15 MPa for 0.4 and 0.44 w:c rate grouts together with analogous results from actual tests are shown in Figure 37. The results reveal good agreement in terms of σ_c, σ_{res}, yield point and softening behavior.

Material softening, upon shear or tensile failure, was implemented in FLAC3D by tables relating friction angle, cohesion and dilatancy angle to plastic shear strain. The elastic parameters Young's modulus and Poisson's ratio used initially were those recovered from the tests. The implementation is the same for both the validation of grout model and the dynamic test model.

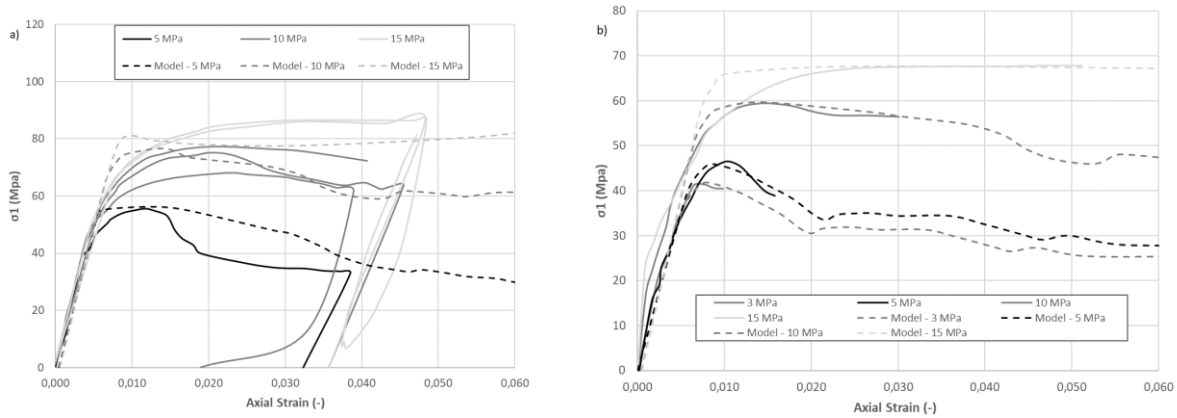

Figure 37 Complete set of stress strain curves for different confining pressures compared with lab results for a) 0.4; and b) 0.44 w:c rate grout

3.2.1.3 Steel tube

A shell structural element that envelops the grout represents the steel split pipe in which the grouted rockbolt is inserted in the laboratory-scale dynamic, the pipe tests apply confinement to the element tested and simulates the ground surrounding an excavation. During a seismic event, it constitutes both solid ground (steel pipe) and fractured plane (split), (Player et al, 2004).

In the numerical model the shell responds to the tension through an elastic constitutive model controlled by the Young modulus (E) and Poisson's ratio (v) of steel. This model is valid for homogeneous, isotropic and continuous materials that exhibit linear stress-strain behavior. Assigned mechanical properties are presented in Table 16.

Table 16 Steel tube mechanical properties

Property	Value
Inner diameter	45 mm
Thickness	5 mm
Young Modulus [E]	210 GPa
Poisson ratio [v]	0.27
Density	7,850 Kg/m3

The link between the shell (steel tube) and the grout (grid) was treated as rigid such that stresses develop within the shell as the grid deforms. The steel tube remains elastic and rigidly connected to the grout throughout the simulation.

The steel tube/grout interface can be allowed to fail in either tension or shear, such that gaps can form and slip can occur, but this behavior was not to considered to happen in the laboratory tests.

3.2.1.4 Interface between rockbolt and grout

Although it is considered that the model only consists of four main parts, it was necessary to use interface elements to allow relative movements between the rockbolt and the grout. Interface elements are used in two places in this numerical problem;

around the superior and inferior part of the rock bolt, the split tube length is not surrounded by the interface.

The interface properties play an important role in a rockbolt-grout model, governing whether a slip, or an opening of a gap between the rockbolt and the grout may occur, both of which are possibilities in the analysis. FLAC3D interface elements have properties of friction, cohesion, dilation, normal (k_n) and shear (k_s) stiffness, and tensile strength. Itasca (2012) recommends that the use of normal and shear stiffnesses be ten times that of the stiffest neighboring element.

The apparent stiffness (expressed in units of stress-per-unit length) of an element (or zone) in the normal direction (k_n) is:

$$k_n = 10\ x \max\left[\frac{K + \frac{4}{3}G}{\Delta Z_{min}}\right]$$

Equation 6 Normal stiffness **(Itasca, 2011)**

Where:

K = bulk modulus of the stiffest neighboring element
G = shear modulus of the stiffest neighboring element
ΔZ_{min} = smallest dimension of an adjoining element in the normal direction (see Figure 38)

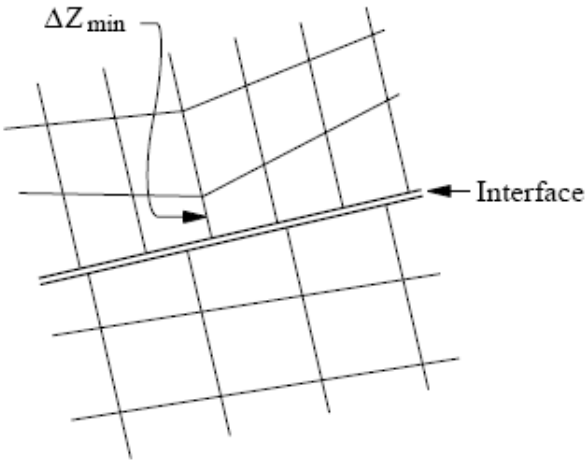

Figure 38 Element dimension used in stiffness calculation. Taken from Itasca (2012)

In the following analysis, the values were set Kn=Ks =210×10^3 (Pa/m), assuming the steel bar as the stiffer element. Friction angle, dilation angle, and tensile strength were set to zero, and cohesion value= 12 MPa.

3.3 Model implementation

Proposed model simulates the Impact Test equipment developed by CanMet-Mining and Mineral Sciences Laboratories (CANMET-MMSL). The facility transforms potential energy into kinetic energy through the fall of a mass from a given height that impacts the

lower end of a rockbolt embedded in a pipe with grout causing deformation and possible failure, simulating the in-situ conditions (Yi & Kaiser 1992; 1994b).

3.3.1 Equations to motion

In order to solve the numerical model, the dynamic system is divided into two scenarios as proposed and illustrated by Marambio et al. (2018) in Figure 39. The first scenario is described for the free fall of the mass used in the dynamic test until it impacts the plate (damping cushion in the current test) at a particular time of impact. The model developed here, does not include the explicit modeling of the external hardware (nut and plate), so the mass impacts the lower part of the steel tube.

The second scenario is in the interest of modelling, and it is after the moment of impact, when the mass begins to move along with the rockbolt, stretching it or sliding it until possible failure.

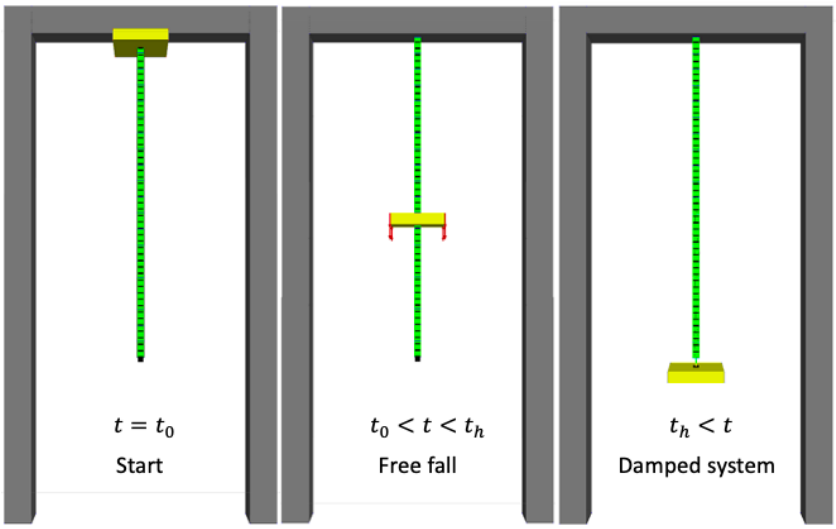

Figure 39 Solve scheme in FLAC3D Software; from left to right three temporal stages of the numerical model (Marambio et al., 2018)

Therefore, the system can be represented by two differential equations, in which the first describes the motion of the rockbolt and the second the motion of the grout, as presented in Equation 7 and Equation 8 respectively. St-Pierre (2007) has shown a similar scheme in the development of his model for the cone bolt reinforcement element.

$$m\ddot{x}_b + c_b(\dot{x}_b - \dot{x}_g) + k_b(x_b - x_g) - F_{fk} + mg = 0$$

Equation 7 Motion of rockbolt

$$m_g\dot{x}_g - c_b(\dot{x}_b - \dot{x}_g) - k_b(x_b - x_g) - c_g\dot{x}_g - k_g x_g + F_{fk} = 0$$

Equation 8 Motion of grout

Where:

m, m_g = Loading mass used in the dynamic test and grout mass, respectively.
g = Gravity constant.
k_b, k_g = Stiffness of rockbolt and grout, respectively.
c_b, c_g = Viscous damping of rockbolt and grout, respectively.

x_b, x_g = Displacement of rockbolt and grout, respectively.
$\dot{x}_b, \dot{x}_g$ = Velocity of rockbolt and grout, respectively.
$\ddot{x}_b, \ddot{x}_g$ = Acceleration of rockbolt and grout, respectively.
F_{fk} = Friction force representing the contact between rockbolt and grout.

The motion equations are solved by an iterative numerical method – explicit in time combined with the unbalanced force criteria from FLAC3D.

Notice that the mass of the rockbolt (m_b) in Equation 7 and grout weight (m_g) in Equation 8 are negligible in comparison with the loading mass of the dynamic test (m), where the loading mass is about 200 times higher than the mass of the rockbolt, and therefore not taken into account in motion equations. The stiffness of the rockbolt and the grout shown in Equation 7 and Equation 8 are approximated by their equivalent stiffness for systems connected in series (Rao & Yap 2011).

Furthermore, the viscous damping of the rockbolt and the grout are proportional to their respective masses, stiffness and a damping component (c_b, c_g) , commonly known as classical damping of Rayleigh (1877). See Equation 9 and Equation 10.

$$c_b = a_{0_b} m_b + a_{1_b} k_b$$

Equation 9 Rockbolt damping component

$$\boldsymbol{a_{0_b} = 2\omega_{1_b}\xi_{1_b} - a_{1_b}\omega_{1_b}^2}$$

$$a_{1_b} = \frac{2(\omega_{2_b}\xi_{2_b} - \omega_{1_b}\xi_{1_b})}{\omega_{2_b}^2 - \omega_{1_b}^2}$$

Where:

ω_{n_b} = n normal mode for rockbolt
ξ_{n_b} = n critical structural material damping

$$c_g = a_{0_g} m_g + a_{1_g} k_g$$

Equation 10 Grout damping component

$$a_{0_g} = 2\omega_{1_g}\xi_{1_g} - a_{1_g}\omega_{1_g}^2$$

$$a_{1_g} = \frac{2(\omega_{2_g}\xi_{2_g} - \omega_{1_g}\xi_{1_g})}{\omega_{2_g}^2 - \omega_{2g}^2}$$

Where:

ω_{n_g} = n normal mode for grout
ξ_{n_g} = n critical geological material damping

The damping components mentioned above depends on normal mode of vibration for rock bolt (Den Hartog, 1985) Equation 11, grout (Nilsson, 2009) Equation 12 and strain rate.

$$\omega_{n_b} = \frac{\mu_n}{2\pi L^2}\sqrt{\frac{EI}{\rho A}}$$

Equation 11 Rockbolt normal mode of vibration

Where:

L = Length of rockbolt
ρ = Desnsity of rockbolt
E = Young`s modulus of rockbolt
I = Moment of inertia of rockbolt
μ_n = Empirical coefficient for each mode

$$\omega_{1g} = \sqrt{k_g / m_g}$$

$$\omega_{2g} = \sqrt{3k_g / m_g}$$

$$\omega_d = \omega_n\sqrt{1-\xi^2}$$

Equation 12 Grout normal modes of vibration

Where:

k_g = Grout stiffness
m_g = Grout mass

Assumed damping parameters values are presented in Table 17.

Table 17 Damping parameters for rockbolt and grout

	Rockbolt	**Grout**
μ_1	3.52	-
μ_2	22	-
ξ_1	2	2
ξ_2	5	10

3.3.2 Model operation

The model defines the movement and the impact of the loading mass as explained in 3.3.1, the behaviour of the rock bolt and grout lies mainly in the following aspects:

- The dynamic test is represented by a mass that generate the impact. The input necessary to represent it is the loading mass in Kg. For initial modeling loading mass is = 2000 [Kg].
- Force at each node is calculated from stress, applied load, and body forces (stress and strain are constant within an element)

- The equations of motion are invoked to derive new nodal velocities, displacements and forces in each zone representing the rockbolt. In this sense, new strain rates are derived from nodal velocities to apply the dynamic increase factor proposed by Malvar & Crawford (1998) in a constitutive model elastic-perfectly plastic. This is repeated at every time step of calculation until the system reaches equilibrium. A visualization of nodes is presented in Figure 40.
- The strain rate of each element is determined from the velocity of each node.
- Whereas, in the split-tube configuration the monitoring point is located at the discontinuity of the encapsulating tube.
- The confinement imposed by the encapsulating tube is represented by a structural element type DKT- CSTH shell (Itasca Consulting Group 2012) being its constitutive behaviour elastic.

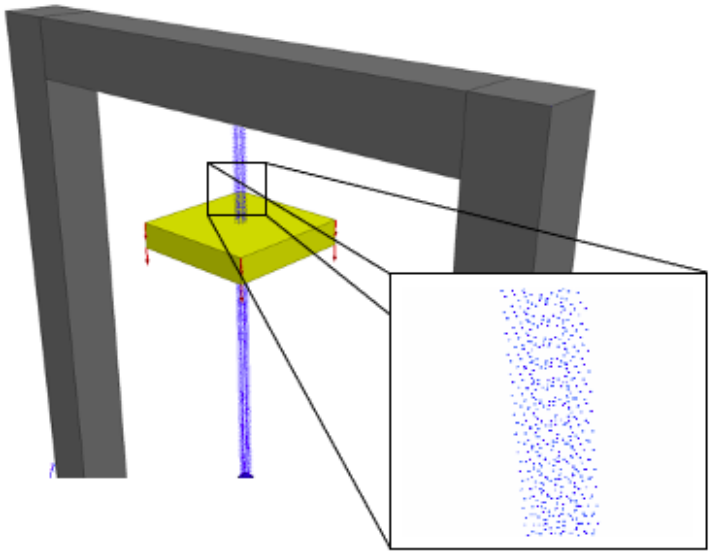

Figure 40 General view of nodes

3.4 Model results

3.4.1 Grout response

The view in Figures 41 and 42 allows a better visualization of the dynamic response of the grout, but it must be considered that the simulation represents the complete system. Obtained results are in terms of maximum (σ_1) and minimum (σ_3) principal stresses distribution along the grout. Grout properties for 0.4 w:c ratio stablished in 3.2.1.2 are implemented. As observed the failure of the element is located in the grout zone around the rockbolt debonded section, representing the laboratory results where the grout failed before the bolt after the impact.

When comparing the state of the model grout zones with images of the one sample after the dynamic test (Player & Cordoba, 2009), it is clear to see a correlation between the

failed zones, which indicate a good agreement of the model after the improvements made, in Figure 43.

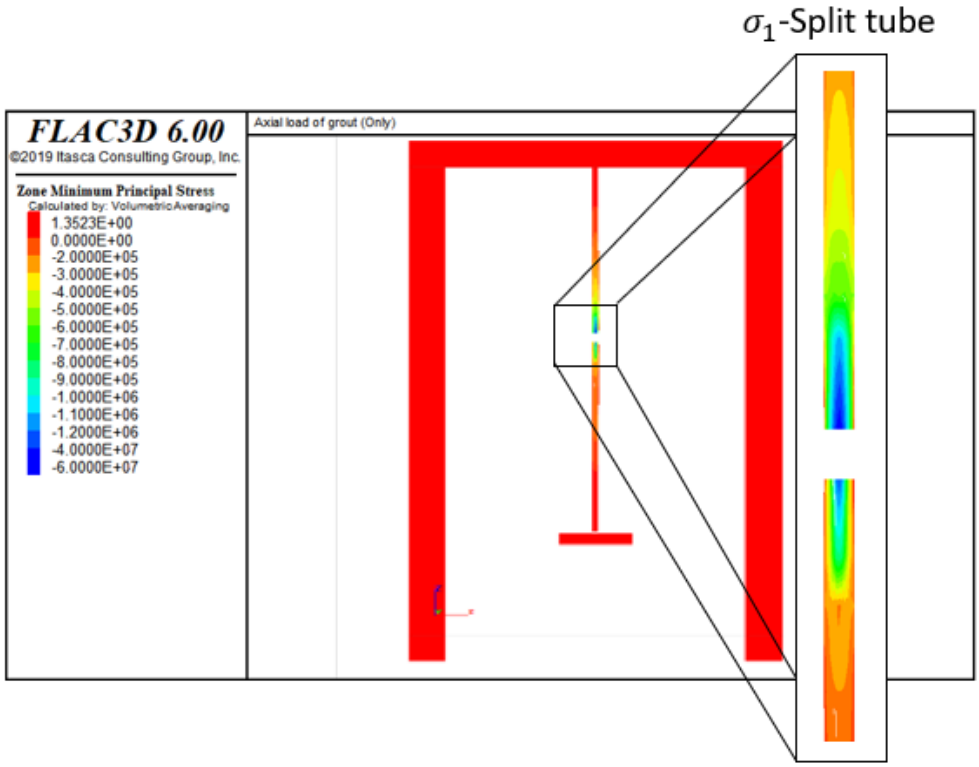

Figure 41 Grout maximum principal stress σ_1

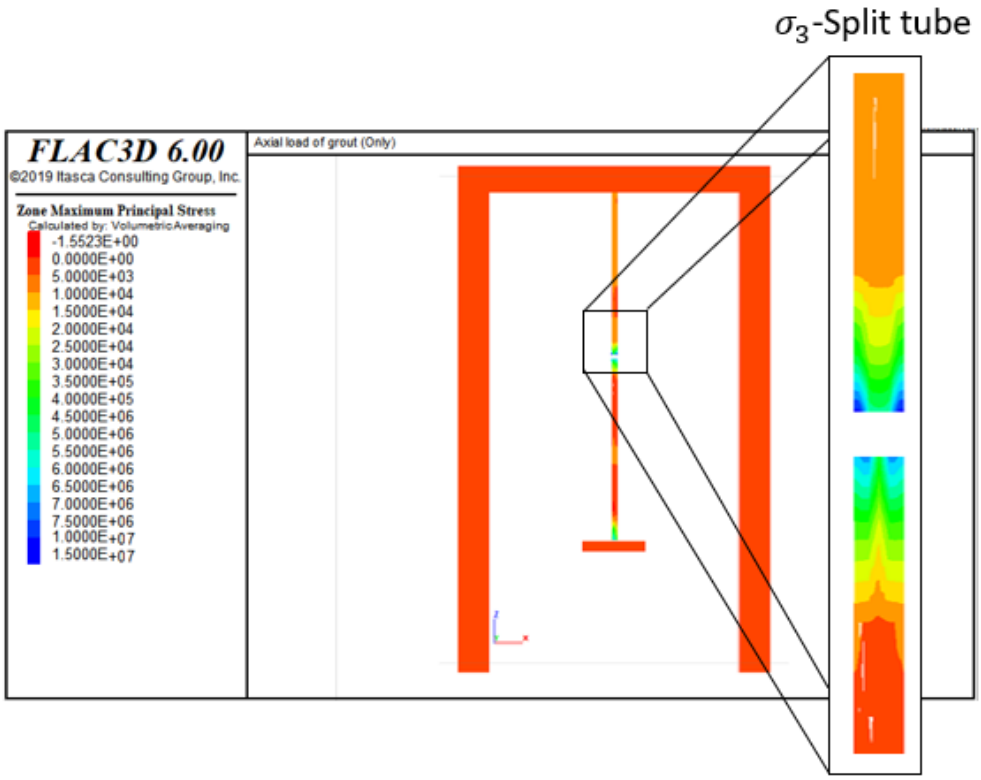

Figure 42 Grout minimum principal stress σ_3

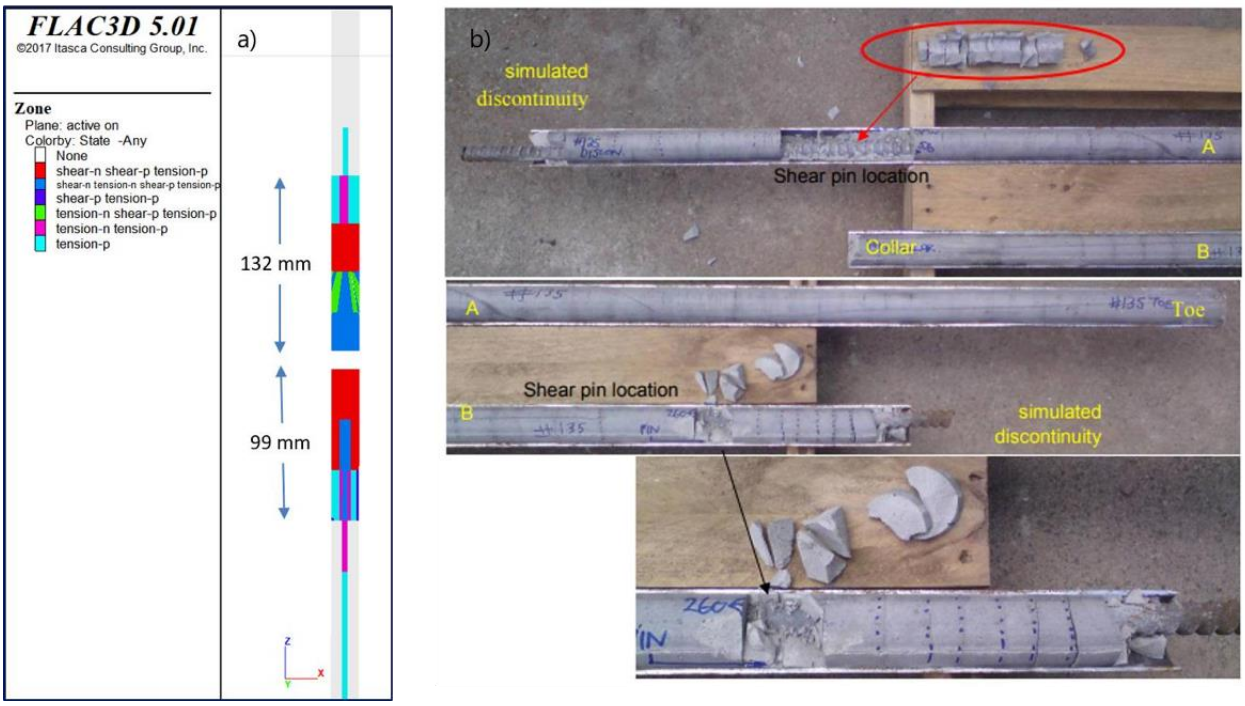

Figure 43 a) FlAC3D Grout zone state b) Grout state after dynamic testing, taken from Player & Cordova (2009)

The grout state zones indicated in Figure 43a indicate the final grout plasticity state for the zone as is indicated in Table 18.

Table 18 Model grout zone failure states

Failure state	Label
Failure in shear now	Shear-n
Failure in tension now	Tension-n
Failure in shear in the past	Shear-p
Failure in tension in the past	Tension-p
None	None

In laboratory testing the simulated standard boreholes included shear pins installed through the pipe wall penetrating approximately 5 mm into the grout to minimize or stop grout sliding (Player J. , 2012), this is the reason because in the simulation slip or opening gap is not allowed in the tube grout interface.

As can be observed in Figure 43b shear pins were installed as pairs above and below the simulated discontinuity, due to this the grout around these areas fails.

All disponible mechanical parameters of grout was considered in the simulations and the model responds as expected according to experience in dynamic conditions, showing failure all around the simulated discontinuity and near the grout bolt interface in the length where the system is less confined.

3.4.2 Rockbolt response

Not only an approach to grout behavior was obtained with numerical modeling, rockbolt response in terms of load and displacement was established. A monitoring zone was located along the free zone (split tube) of the reinforcement element as shown in Figure 44.

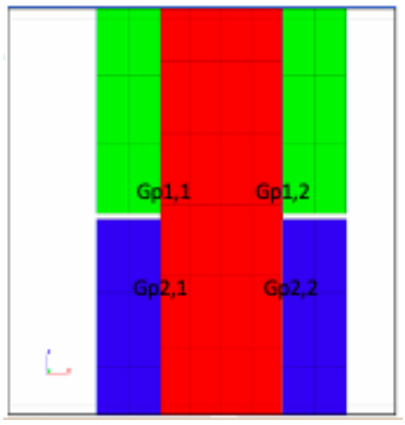

Figure 44 Rockbolt monitoring zone

Figure 45 illustrates a numerical example of the load Vs displacement curves of the rockbolt at a final time stage of the model, when equilibrium has been reached. It can be seen the comparison between the model (simulated curve) and laboratory-scale dynamic test results from WASM for threadbar (Player & Cordova 2009). In these graphs, the similarity between the numerical model and the laboratory testing results can be appreciated.

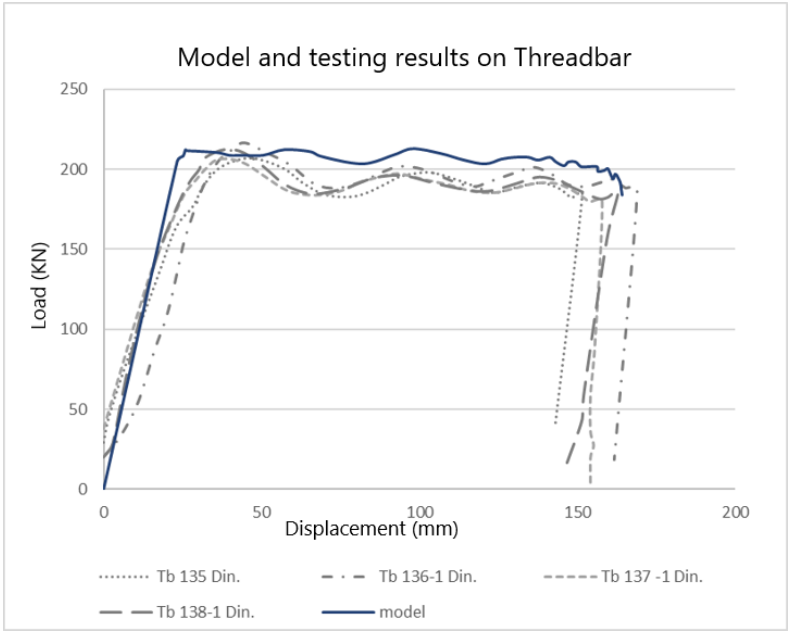

Figure 45 Load Vs. Displacement of dynamic test and numerical model of threadbar

The numerical model replicates the operation of the CanMet-MMSL rig, but the results are compared with the WASM tests results published (Player and Cordova, 2009; Player et al., 2009). This comparison, since there is a lack of published information, is relevant and correct, as shown in the analysis in 2.1.3, in which the results from both tests are similar in the elastic and plastic range of deformation.

4 Improvement and parametric analysis of numerical model

4.1 Improved geometry

The initial model is made up of elements explicitly represented from simple geometries: a cylinder for the rockbolt and an anulus for the grout. However, it is necessary to accurately show the surface of the bolt in order to make it fully representative of reality.

To achieve the real geometry of the threadbar inserted in grout, an external design software, Rhino3D, was used, as this allows to model complex geometries. Then, the obtained surface mesh was exported to ABAQUS, which fills the interior regions bounded by the surface meshes with tetrahedra or hex-dominant (hexahedra, prisms, pyramids and tetrahedral) elements. Finally, the solids are imported in FLAC3D.

The measurements that describe the threadbar are taken from the Saferock® catalog and are shown in Figure 46 and Table 19, 22 mm nominal diameter rockbolt is used as input for the model.

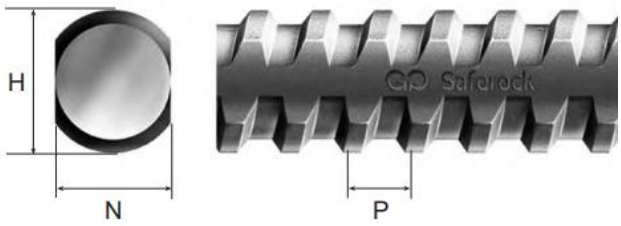

Figure 46 Threadbar. Saferock®

Table 19 Threadbar measurements

Nominal diameter [mm]	**Lineal mass** [kg/m]	**Rib pass** [mm] **P**	**Maximum Height** [mm] **H**	**Maximum width** [mm] **N**
16	1.52	9	18.2	14.7
19	2	9.9	21	17
22	**2.8**	**11.09**	**24.8**	**20.2**
25	3.6	12.5	28.2	22.8

Generated geometry in ABAQUS and imported in FLAC3D are presented in Figure 45. Parameters of rockbolt and grout are established in 3.2.1. The shell that represents the steel split tube implemented in the initial model is also considered and preserves its original parameters. Complete model geometry is presented in Figure 47 and geometrical components of each part of it are described in Table 20.

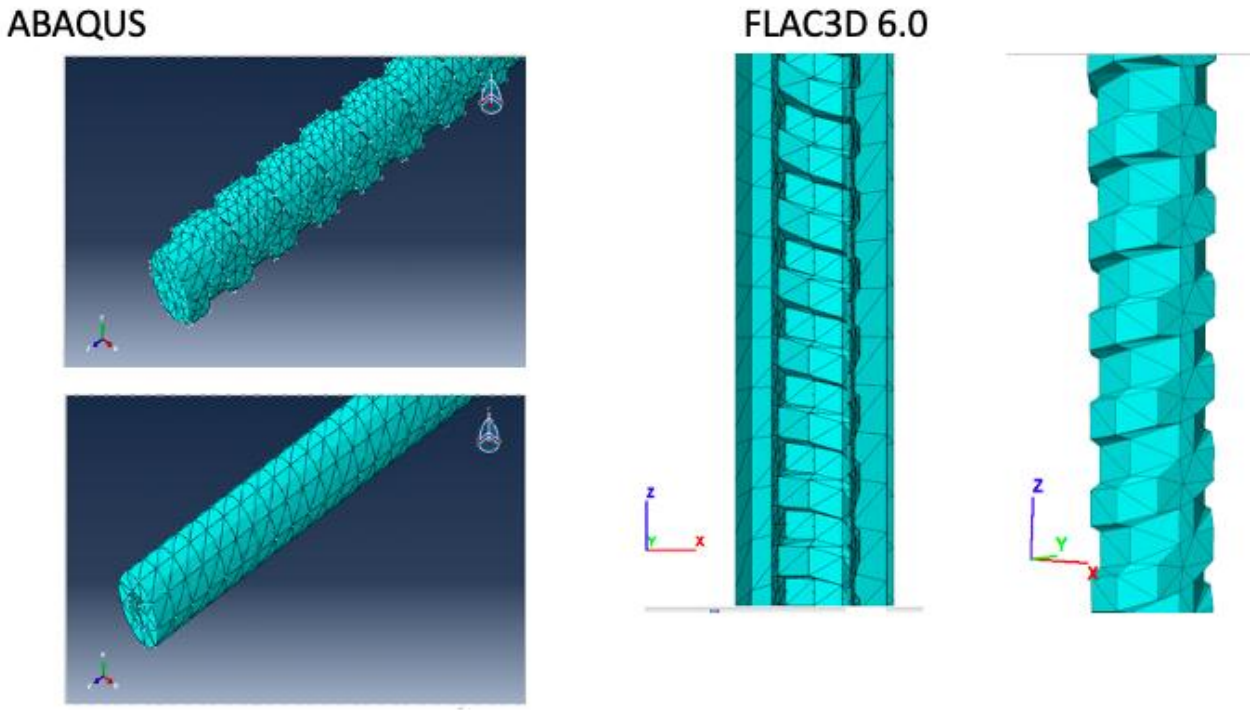

Figure 47 Geometry of threadbar in ABAQUS and FLAC3D

Movement and impact simulation are executed the same way as the first proposed model, but the time consumed in reach equilibrium is notably major, this is the product of the number of zones, elements and nodes, see Table 20, on which the procedure described in 3.3.2 is executed. This is the main disadvantage of representing the bolt rib on the model.

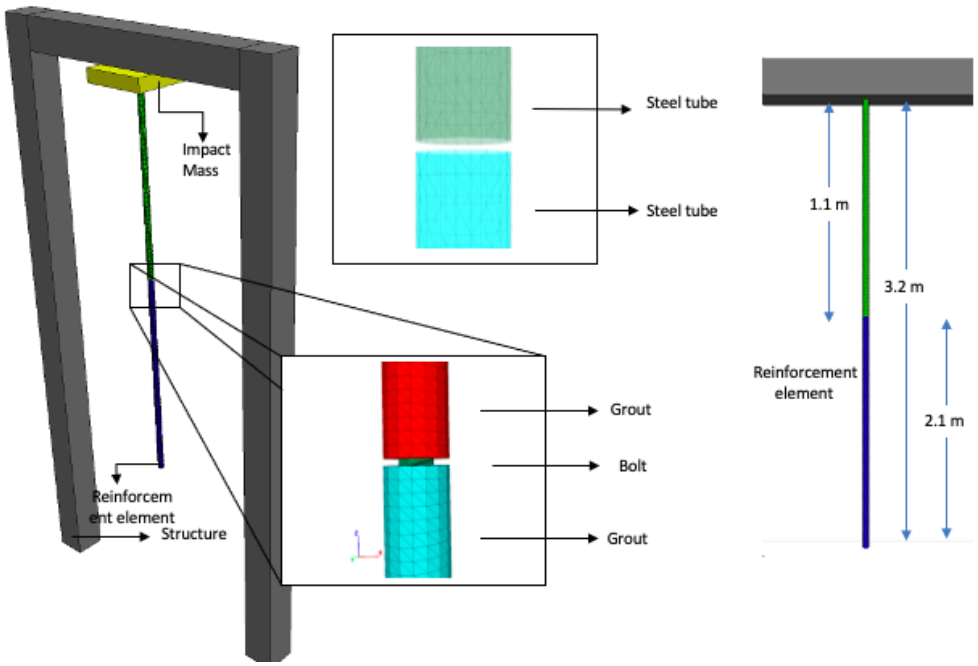

Figure 48 Complete geometry of improved explicit model

Table 20 Geometry zones and nodes

Geometry	Zones/ Elements	Nodes
Threadbar	80,899	35,890
Superior grout	23,980	10,697
Inferior grout	38,855	17,237
Superior steel tube	1,628	836
Inferior steel tube	2,200	1,122

4.2 Modeling results

The maximum and minimum stress at split tube for rockbolt and grout are shown in Figure 49 and Figure 50. It is important to note that stresses show variations with respect to the initial model in the area corresponding to the grout, indicating that the plow produced by the bolt when sliding affects the mechanical response of the grout increasing its strength.

In the case of rockbolt, the strength increases as the analyzed length moves away from the split tube zone, indicating that the bolt is more prone to failure in the confinement-free zone.

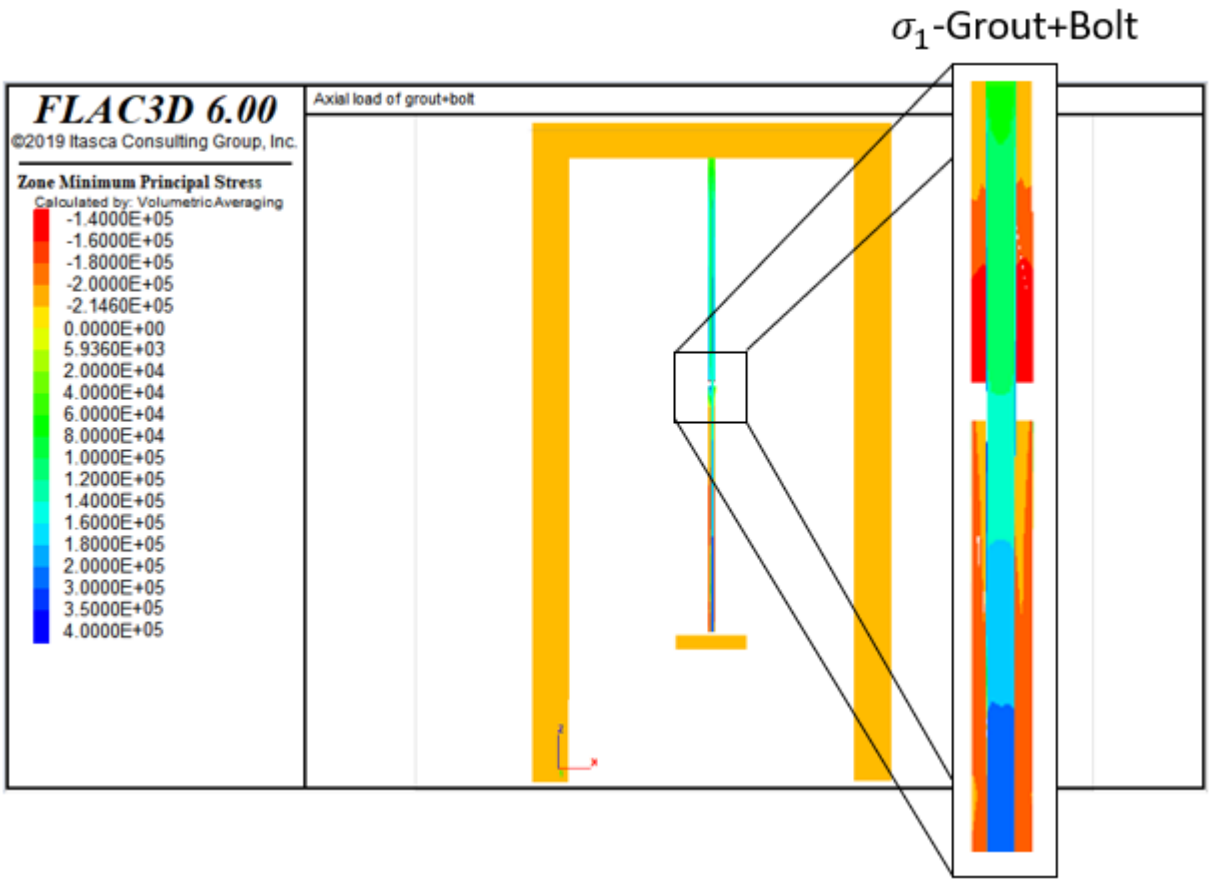

Figure 49 Principal maximum stress σ_1 at split tube zone for rockbolt and grout. FLAC 3D.

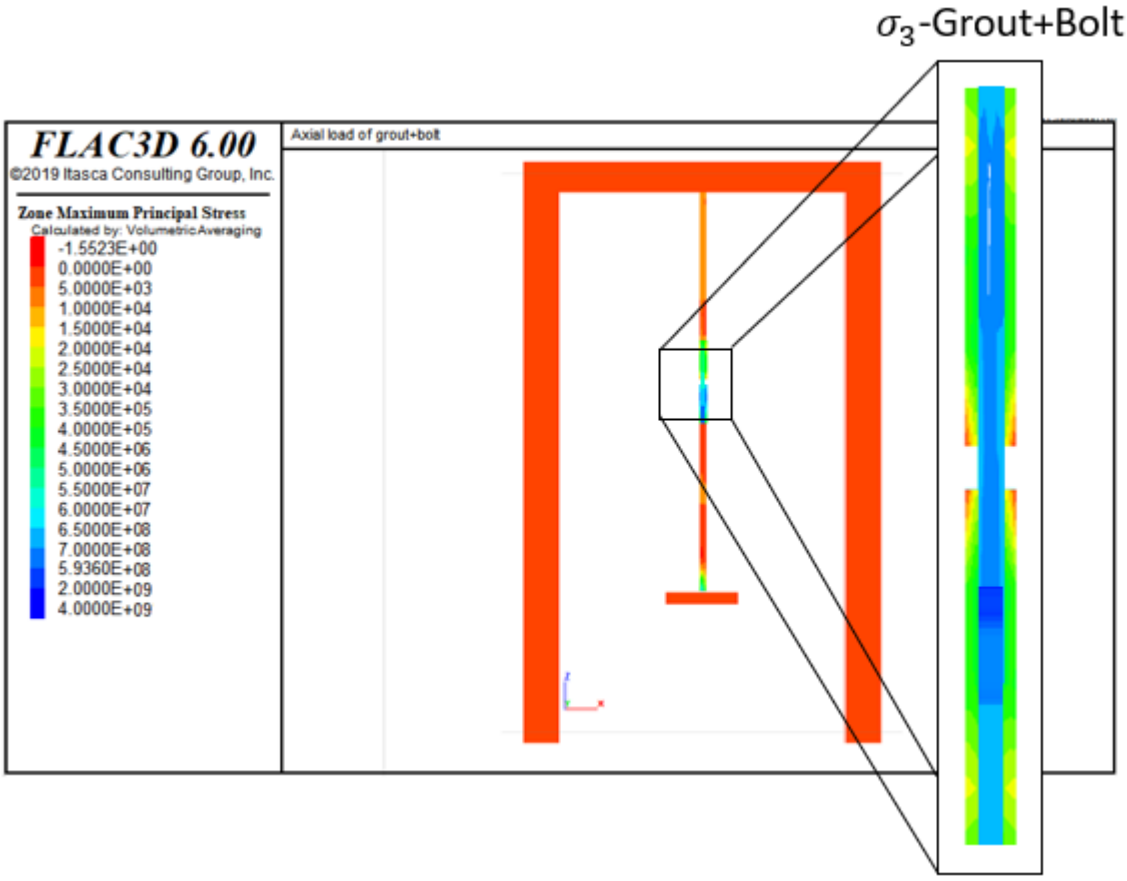

Figure 50 Minimum principal stress σ_3 at split tube zone for rockbolt and grout. FLAC 3D.

After considering that the improved model represents the real response of the reinforcement system under dynamic test a parametric study was executed. The parameters chosen to perform the analysis are those that can be modified in laboratory tests and that also have more influence on the system response.

4.2.1 Rockbolt response

At first, bolt length was modified from 3.2 m to 3.0 m and 2.3 m. These lengths were chosen because there are published results, (Player et al. 2009; Player and Cordova, 2009), that allows comparation with the numerical model. 1 [m] length was retained for the upper steel tube in the three sceneries.

In Figure 51 a comparation of the stresses obtained with the new lengths are presented. On the other hand, in Figure 52, bolt response is presented in terms of load Vs. displacement for both the model and for laboratory tests. It is considered that model results present good agreement with test results as difference of load and displacement does not exceed 5% in every point of the presented curves.

After carrying out a second validation of the model representativeness, other parameters were varied: Rockbolt diameter, impact mass and steel tube thickness. Model results in terms of load and displacement are presented in Figure 53.

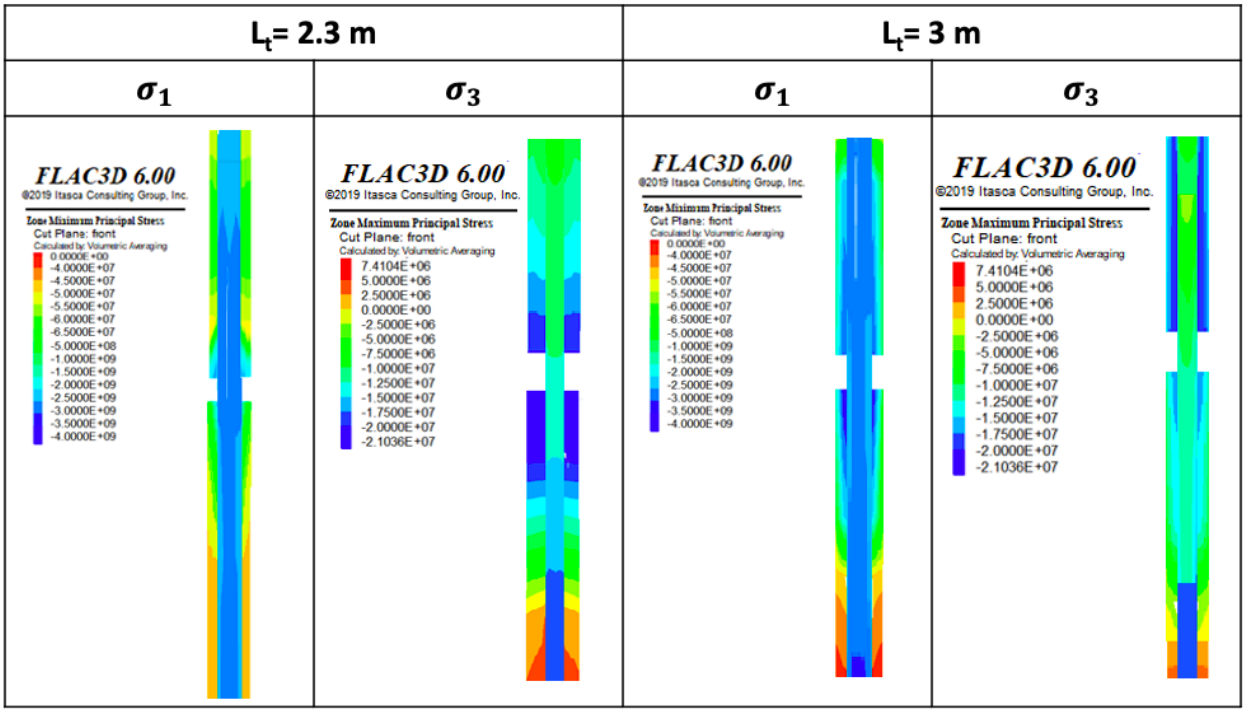

Figure 51 Stresses for 2.3 [m] and 3.0 [m]length rockbolt model

For diameter variation models a rockbolt length of 3.2 [m] and a 2000 [Kg] impact mass weight was implemented as inputs. It's observed a strong influence in terms of yield strength, increasing with a greater diameter. The same tendency is observed in terms of stiffness increasing as diameter increases. When displacement (and therefore deformation) is analyzed, a strong inverse relation regarding the diameter was seen.

Effect of mass impact variation is notorious only in terms of total displacement of rock bolt reaching a maximum with a 2200 [Kg] mass impact. Steel tube thickness has strong influence in rock stiffness and less influence in rockbolt deformation. For the last analyses 3.2 [m] rockbolt length and 22 [mm] diameter were fixed.

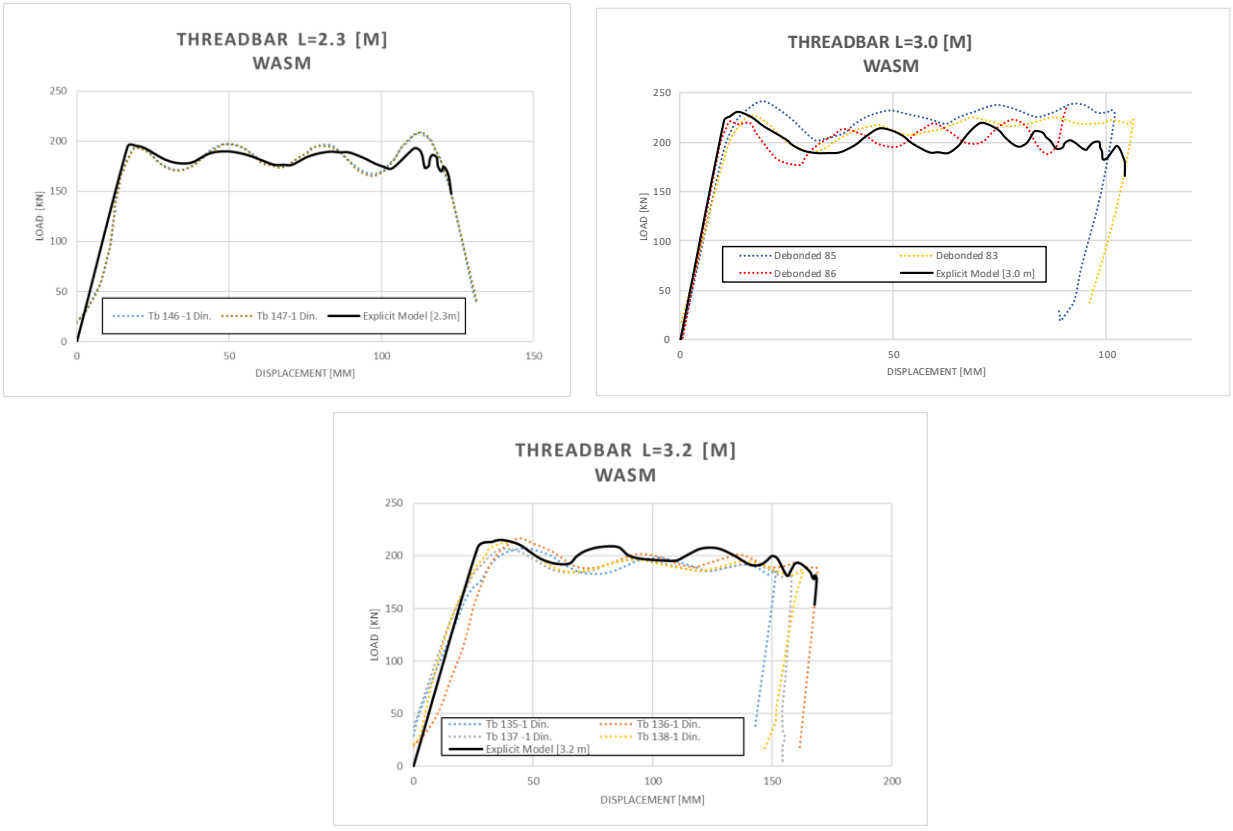

Figure 52 Load Vs displacement curves for various rockbolt lengths. Numerical model and test results.

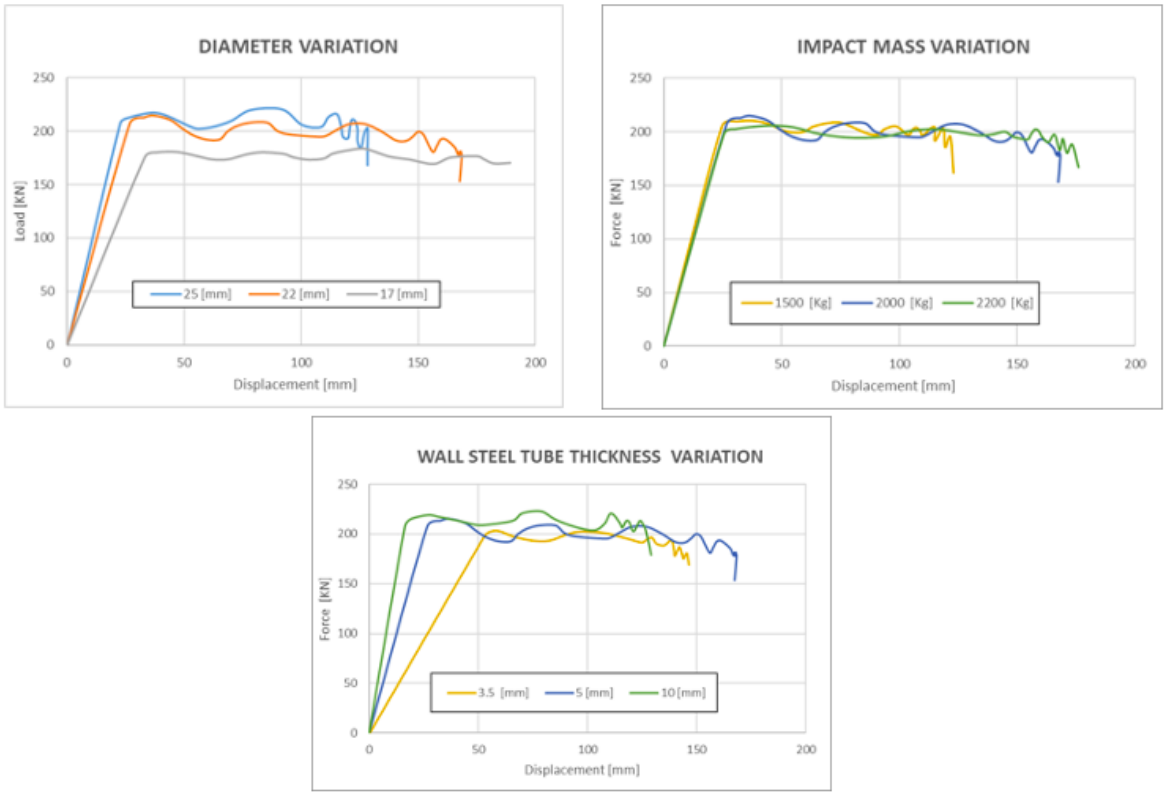

Figure 53 Load Vs. Displacement curves for parameters variation

4.2.2 Grout response

After evaluating the parametric analysis made in 4.2.1 was found that grout response is strongly influenced by the variation of the steel tube thickness, as confinement is directly related whit the inside and outside diameters of the pipe (Hyett et al.,1992). Modeling results are presented in Figure 54, grout yield load is incremented as thickness increases and displacement has the contrary effect, being major at less confinement.

The anchoring length was never modified; total bolt length and impact mass has not important effect on the mechanical response of grout.

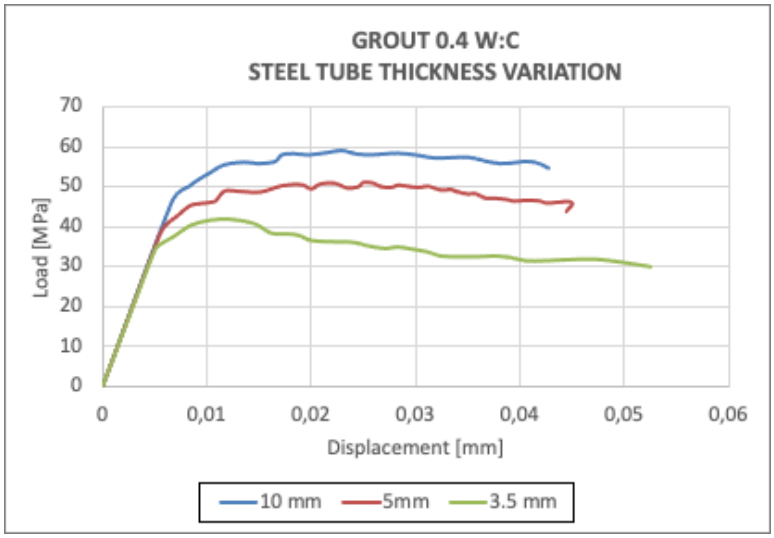

Figure 54 Load Vs. Displacement curves for various steel tube thickness

As there are no measurements about the resistance and deformation that affects the grout in the dynamic laboratory tests, the model results obtained will be compared with the Mohr-Coulomb failure envelope (Labuz & Zang, 2014) and the modified failure envelope presented by Shen et al., (2018), in terms of σ_1 and σ_3, since the latter criterion considers the variation in terms of friction and cohesion that the grout presents. See Figure 55. Results from laboratory triaxial and tensile tests (Hyett, 1992) and results from CWFS model presented in 3.2.1.2 are also depicted.

Results were also located in the τ Vs. σ_n plane. For this analysis, results from direct shear tests and the failure envelope proposed by Moosavi & Bawden (2003) are also compared.

Graphics show stress values that agree with the expected behavior of grout under axial loads.

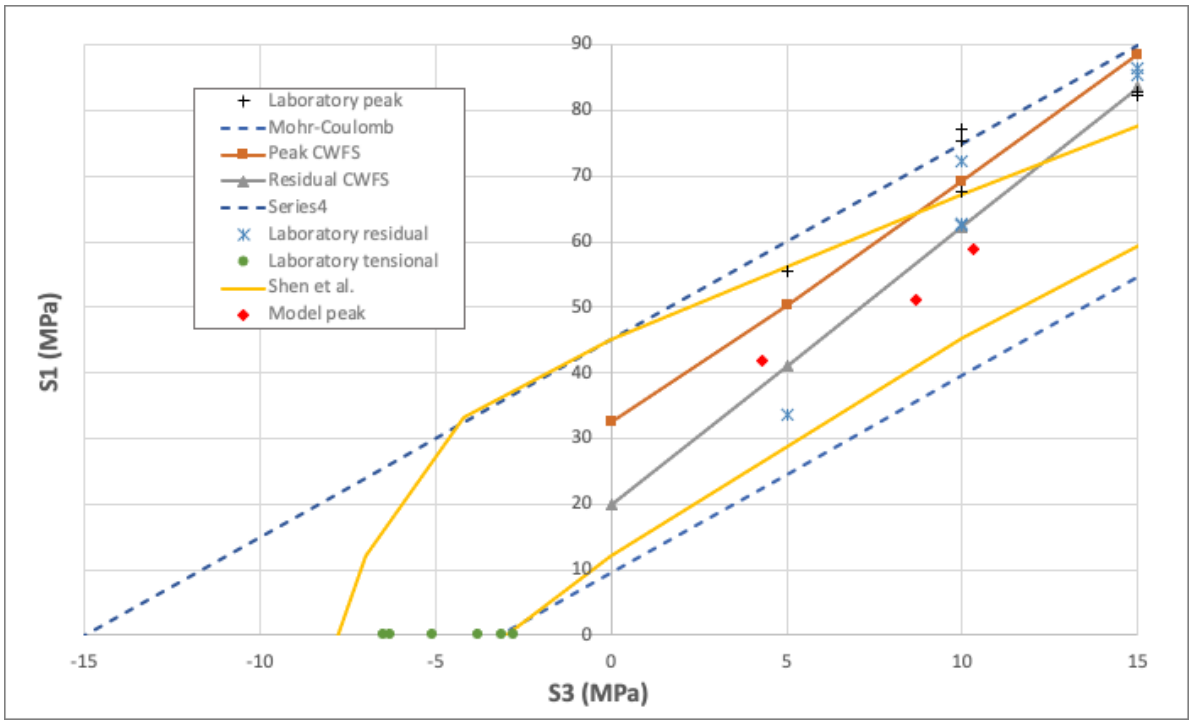

Figure 55 Grout σ_1 Vs σ_3 for various confinements

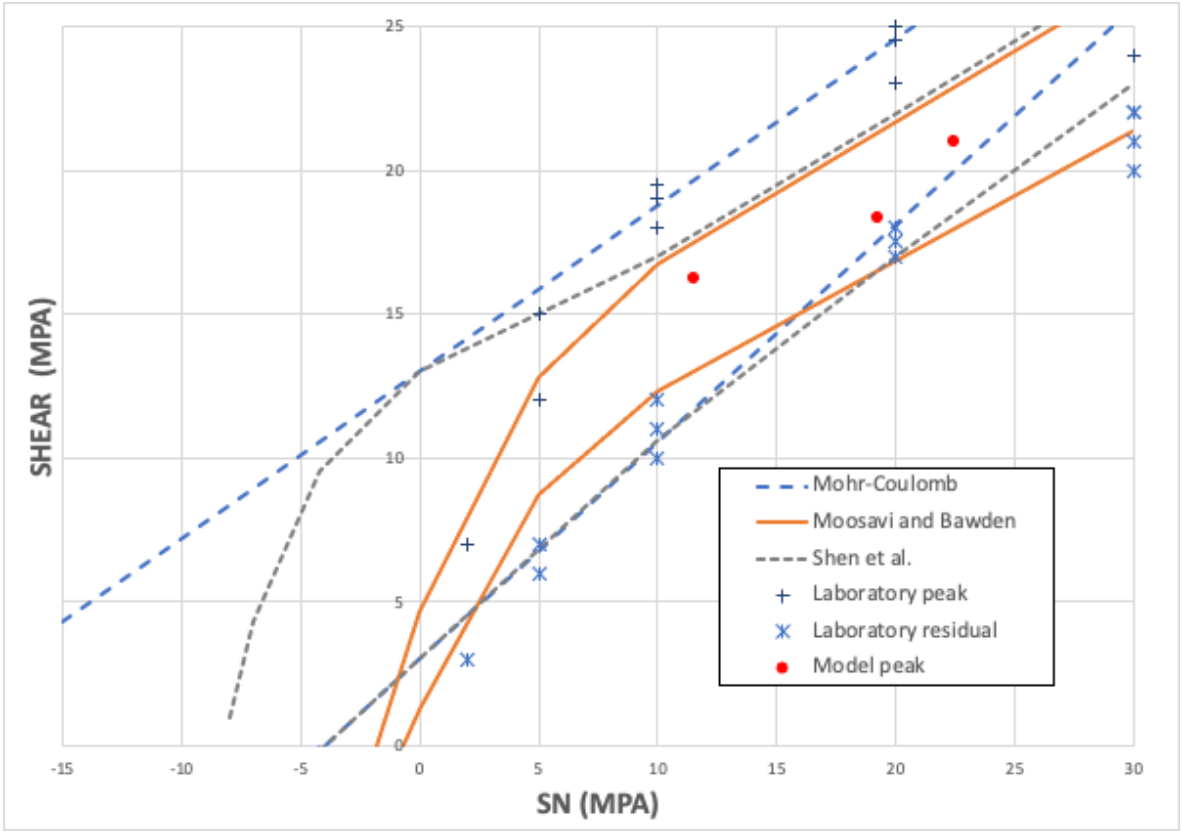

Figure 56 Grout τ Vs. σ_n for various confinements

4.2.3 Absorbed energy

As indicated in Chapter 2, energy absorption capacity of the reinforcement element is one of the main requirements at the time to design a support system. For this reason, Figure 57 to Figure 59 present the energy absorbed obtained from varying input parameters in the numerical modeling compared with energy absorbed in laboratory tests. From this information, it is seen that impact mass and rockbolt total length are the parameters that influence the most the energy absorption capacity of the threadbar.

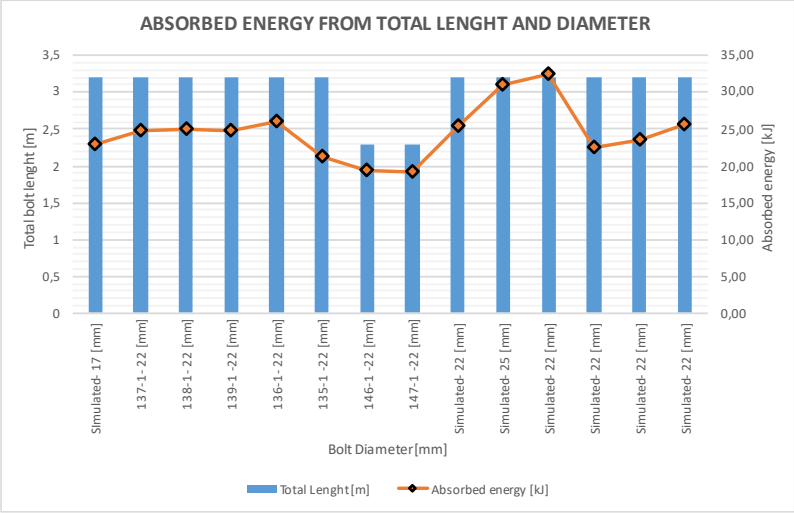

Figure 57 Energy absorbed, total length and diameter.

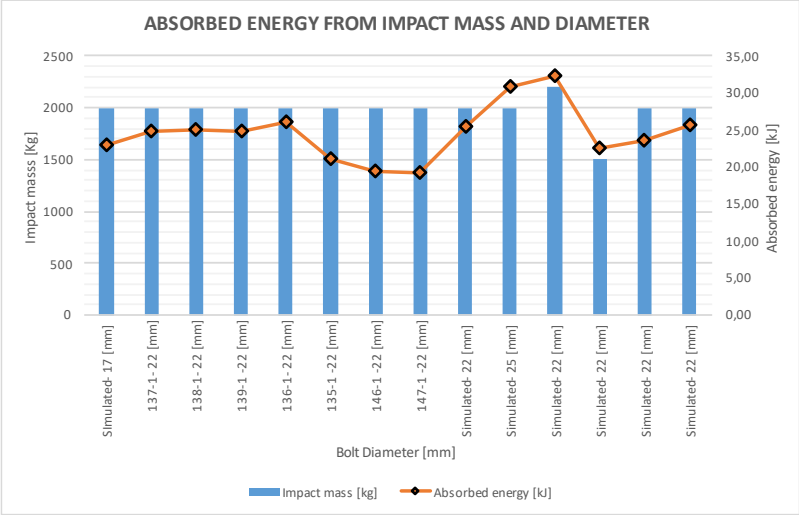

Figure 58 Energy absorbed, impact mass and diameter.

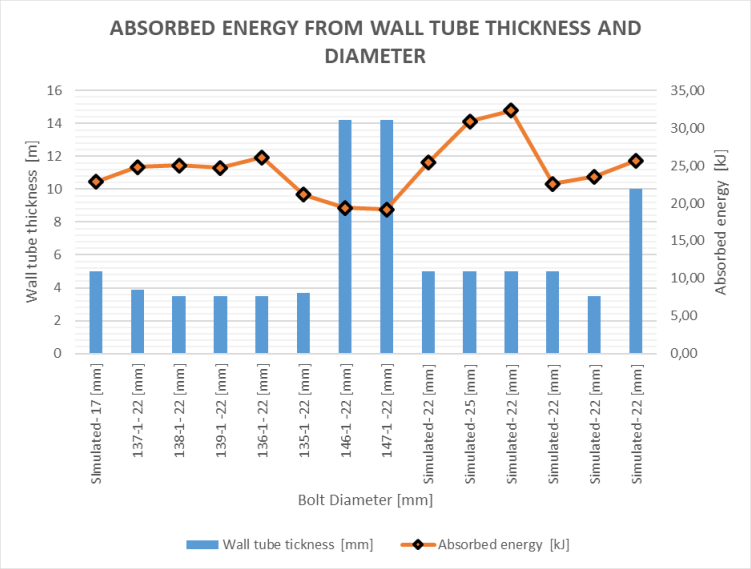

Figure 59 Energy absorbed, steel tube thickness and diameter

Figure 60 is a compilation of threadbar results from drop tests and simulations, where the total energy absorbed is plotted as a function of the displacement. The figure includes data grouped under 3 datasets, represented by different colors. Each dataset represents a variation in the diameter of the bolt and if it was tested in laboratory or simulated.

Considering that a wide variety of testing parameters was tested or modeled, the compiled datasets show some very clear “quasi-linear” trends. The yellow line indicates the behavior tendency for threadbars with 22 mm diameter, 3.2 m length, 2000 Kg impact mass and 5 mm steel tube thickness in both tests and simulations. The other trend lines indicate how the threadbar responds to the parametric variation implemented in the numerical model. The blue lines show what is observed when the parameters values are higher and green lines when are lower.

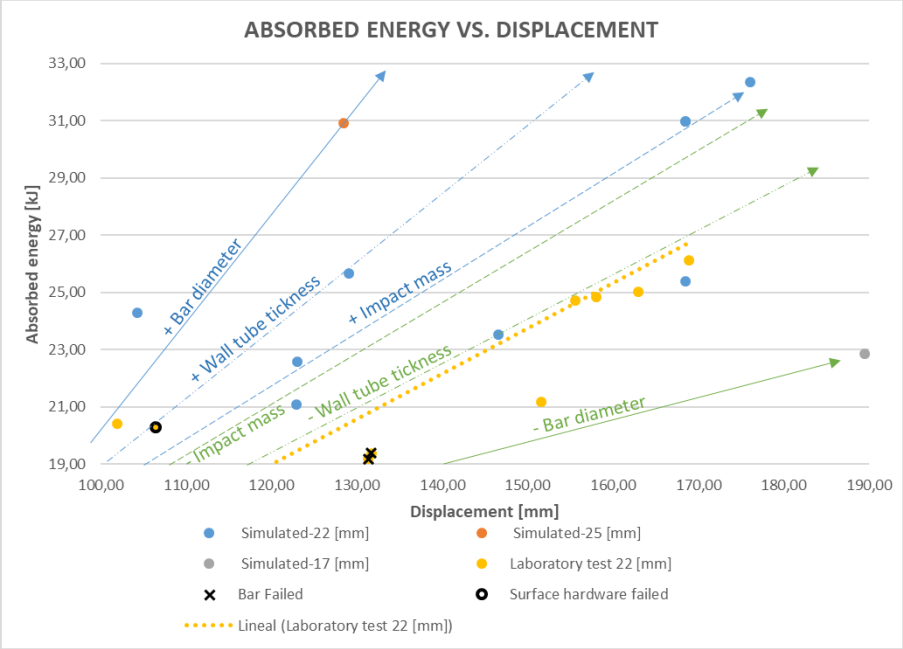

Figure 60 Absorbed Energy Vs Displacement trend

A large cloud of data plots in the area defined between 24 and 32 kJ of total energy absorption and between 150 and 175 mm displacement. The trend of energy increasing with displacement is to be expected as the energy is a product of the load capacity and displacement. In this specific zone of the graph are the data obtained from the higher mass impact implemented, in simulations was observed that bolt displacement increases as the impact mass increases.

The first half of the graph (say, energy between 20 and 31 kJ and displacement between 25 and 150 mm) is dominated by results obtained from the implementation of higher bar diameter or higher wall tube thickness. Results has shown that total displacement is inversely proportional to the mentioned parameters while load is directly proportional.

From this analysis, can be stablished that diameter has the biggest influence on bolt energy absorption capacity and stiffness.

5 Conclusions

In the present document, a model that simulates the behavior of threadbar subjected to dynamic laboratory tests is presented. The model configuration is based on CanMet-MMSL facility and was implemented in FLAC3D software.

An initial model describes where threadbar, grout and steel tube were explicitly implemented. Threadbar ribs were not modeled in this first stage. Grout role in the overall reinforcement system strength was determined. Grout inputs were correctly determined for 0.4 and 0.44 c:w ratio as shown by the similarity between the results of the model and the results of laboratory tests.

When analyzing the independent response of grout, it was observed that it fails partially along the rockbolt at the expected zones due to the mechanical parameters assigned. This shows that the constitutive model and parameters chosen are appropriate to describe the grout response including the post failure stage. The correct implementation of the grout in the numerical model is one of the main contributions of this work.

After reaching results from the initial model, an improved one was proposed. The principal improvement is the integration of threadbar real geometry (rib pass and form implemented) in the numerical model. When comparing the results of the dynamic test with the model results, good agreement was reached. However, the dumping at the final load/deformation stage is exaggerated in the model, and has no relevant influence in energy absorption capacity of the rockbolt.

The principal conclusion is that the presented model can be used as a support tool when determining the response of the threadbar in dynamic laboratory tests, it is a useful visualization tool that allows to identify the response of each component independently and of the complete reinforcement system.

5.1 Future work

It is important to clarify that results were monitoring at one zone located on split tube length. Monitoring on another zones along the system is recommended as test results are available to comparation and calibration if it is needed.

For the grout-bolt interface it is necessary to implement a model that represent accurately its behavior and implement it in the proposed test numerical model.

It is desirable to incorporate the heterogeneity of the materials, especially the heterogeneity of the grout, in the model as long as it does not affect the time it takes to reach the equilibrium of the system.

For this model to be useful to define the dynamic response of other reinforcing elements subjected to different test parameters, it is necessary to implement new geometries and validate and evaluate against laboratory results. Therefore, it is desirable to continue with the execution of laboratory tests under different facility configurations.

6 Bibliography

Alejano, L. R., & Alonso, E. (2005). Considerations of the dilatancy angle in rocks and rock masses. *International Journal of Rock Mechanics and Mining Sciences, 42*, 481-507.

ASTM. (2008). *ASTM D7401-08, Standard Test Methods for Laboratory Determination of Rock Anchor Capacities by Pull and Drop Tests (Withdrawn 2017)*. West Conshohocken, PA: ASTM International.

Aydan, O. (1989). *The stabilisation of rock engineering structures by rock bolts*. Nagoya: Geotechnical Engineering.Thesis.

Aydan, O., & Kawamoto, T. (1992). Shear reinforcement effect of rockbolts in discontinious rock masses. *Int.Sym. of Rock support in mining and underground construction*, (pp. 483-489.). Canada.

Aziz, N. I., & Jalalifar, H. (2007). Experimental and numerical study of double shearing of bolt under confinemen. *26th International Conference on Ground Control in Mining* , (pp. 242-249). Morgantown, WV, USA.

Barton, N., Lien, R., & Lunde, J. (1974). Engineering classification of rock masses for the design of tunnel support. *Rock mechanics, 6(4)*, 189–236.

Benmokrane, B., Chennouf, A., & Mitri, H. S. (1995). Laboratory evaluation of cement-based grouts and grouted rock anchors. *International Journal of Rock Mechanics and Mining Science & Geomechanics Abstracts. 32.*, 633 - 642.

Bieniawski, Z. T. (1974). Geomechanics classification of rock masses and its application in tunnelin. *in Proc. 3rd Int. Cong. Rock Mech*, (pp. 27–32).

Bobet, A. (2010). Numerical modelling in geomechanics. *The Arabian Journal for Science and Engineering, 35(1B)*.

Bravo-Haro, M., Muñoz, A., Rojas, E., & Sarrazin, M. (2018). Evaluation of kinetic energy on rocks ejected during rock bursting trough image processing of compression tests. "El Teniente" Mine case. In J. Vallejos (Ed.), *RaSim9*, (pp. 168-173). Santiago,Chile.

Cai, M., & Kaiser, P. (2018). *Rockburst Support Reference Book (I)*. Sudbury, Ontario, Canada: MIRARCO – Mining Innovation, Laurentian University.

Cai, M., Champaigne, D., & and Kaiser, P. (2010). Development of a fully debonded cone bolt for rockburst support. *Deep mining*, (pp. 342-392).

Carter, J. P., Desai, C. S., Potts, D. M., Schweiger, H. F., & Sloan, S. W. (2000). Computing and computer modelling in geotechnical engineering. *Geoeng2000*. Melbourne, Australia.

Carter, T. G., Diederichs, M. S., & Carvalho, J. L. (2008). Application of modified hoek-brown transition relationships for assessing strength and post-yield behaviour at

both ends of the rock competence scale. *6th International Symposium on Ground Support* .

Chen, S. H., & Pande, G. N. (1994). Rheological model and finite element analysis of jointed rock masses reinforced by passive, fully-grouted bolts. *International journal of rock mechanics and mining sciences & geomechanics abstracts (Vol. 31, No. 3)*, 273-277.

Chen, S., & Egger, P. (1999). Three dimensional elasto-viscoplastic finite element analysis of reinforced rock masses and its application. *International Journal for Numerical and Analytical Methods in Geomechanics, 23(1)*, 61–78.

Chen, S.-H. e. (2004). Composite element model of the fully grouted rock bolt. *Rock mechanics and rock engineering, 37(3)*, 193–212.

Chen, S.-H., & Shahrour, I. (2008). 'Composite element method for the bolted discontinuous rock masses and its application'. *nternational Journal of Rock Mechanics and Mining Sciences, 45(3)*, 384–396.

Chen, Y., & Li, C. C. (2015). Experimental and three-dimensional numerical studies of the anchorage performance of rock bolts. *13th ISRM International Congress of Rock Mechanics*. OnePetro.

Coates, D. F., & Yu, Y. S. (1970). Three dimensional stress distribution around a cylindrical hole and anchor. *Proceeding of 2nd Int. Cong. Rock Mechanics*, (pp. 175-182).

Deere, D. U., & Deere, D. W. (1988). The Rock Quality Designation (RQD) Index in Practice' in Rock Classification Systems for Engineering Purposes. *ASTM International,*, 91-91–11. doi:10.1520/STP48465S.

Den Hartog, J. (1985). *Mechanical vibrations. Dover Publications*. New York.

Diederichs, M., Carter, T., & Martin, T. (2010). Practical rock spall prediction in tunnels. *Proceedings of the 2010 World Tunelling Congress*. Richmond: Tunneling Association of Canada.

Doucet, C., & Voyzelle, B. (2012). *Technical information data sheets*. Technical report, CANMET.

Duenser, C., Thoeni, K., Riederer, K., Lindner, B., & Beer, G. (2012). New developments of the boundary element method for underground constructions. *International Journal of Geomechanics, 12(6)*, 665–675.

Dunham, R. (1976). Anchorage tests on strain-gauged resin bonded bolts. . *Tunnels and Tunnelling*.

Farmer, I. (1975). Stress distribution along a resin grouted rock anchor. *International Journal of Mechanics and Mining Sciences & Geomechanics Abstracts. 12*, 347–351.

Ferrero, A. M. (1995). The shear strength of reinforced rock joints. *International Journal of Rock Mechanics and Mining Sciences & Geomechanics Abstracts;32(6)*, 595-605.

Fu, H.-Y., Jiang, Z.-M., & Li, H.-Y. (2010). Physical modeling of compressive behaviors of anchored rock masses'. *International Journal of Geomechanics., 11(3)*, 186–194.

Galler, R., Gschwandtner, G., & Doucet, C. (2011). Roofex bolt and its application in tunnelling by dealing with high stress ground conditions. *ITA-AITES World Tunnel Congress*. Helsinki, Finland.

Gao, F., Stead, D., & Kang, H. (2015). Numerical simulation of squeezing failure in a coal mine roadway due to mining-induced stresses. *Rock Mechanics and Rock Engineering*, 1635-1645.

Garay, P., & Zepeda, R. (2012). *Informe de Avance: Evaluación de Pernos Cedentes División El Teniente (SGM-I-047/2012). Superintendencia de Geomecánica GRMD, DET, Codelco.*

Gaudreau, D., Aubertin, M., & Simon, R. (2004). Performance assessment of tendon support systems submitted to dynamic loading. PhD thesis. École polytechnique.

Graselli, G. (2005). 3D behaviour of bolted rock joints: experimental and numerical study. *International Journal of Rock Mechanics and Mining Sciences;42(1)*, 13-24.

Guntumadugu, D. R. (2013). 'Methodology for the design of dynamic rock supports in burst prone ground. McGill University.

Hadjigeorgiou, J., & Potvin, Y. (2008). Overview of dynamic testing of ground support. In Potvin (Ed.), *In Proceedings 4th International Seminar on Deep and High Stress Mining* (pp. 349-371). Perth, Australia: Australian Centre for Geomechanics.

Hadjigeorgiou, j., & Potvin, Y. (2011). A critical assessment of dynamic rock reinforcement and support testing facilities. *Rock mechanics and rock engineering, 44(5)*, 565-578.

Hadjigeorgiou, J., & Potvin, Y. (2011). A critical assessment of dynamic rock reinforcement and support testing facilities. *Rock mechanics and rock engineering, 44(5)*, 565-578.

Hagan, P. (2004). Variation in load transfer of a fully encapsulated rockbolt in International Conference in Ground Control in Mining. *Proceedings of the 23rd.*

Hajiabdolmajid, V., Kaiser, P., & Martin, C. (2002). *Modelling brittle failure of rock.* International Journal of Rock Mechanics and Mining Sciences. 39(6), 731-741.

Heal, D. (2005). *Ground support for rockbursting conditions.* Australian Centre for Geomechanics Course, (505).

Hoek, E., Kaiser, P., & Bawden, W. (1995). Support of underground excavatıons ın hard rock. Rotterdam: AA Balkema.

Hollingshead, G. W. (1971). Stress distribution in rock anchors. *Canadian Geotechnical Journal 8*, (pp. 588-592.).

Human, J., & Fernandes, N. (2004). Testing of temporary face support systems under rockfall conditions. *In International Platinum Conference 'Platinum Adding Value'*. The South African Institute of Mining and Metallurgy.

Hyett, A. B. (1992). The Effect of Rock Mass Confinement on the Bond Strength of Fully Grouted Cable Bolts. *International journal of rock mechanics and mining sciences & geomechanics abstracts, 29*(5), 503-524.

Hyett, A. J., Bawden, W. F., & Macsporran, G. R. (1995). A constitutive law for bond failure of fully-grouted cable bolts using a modified hoek cell. *International Journal of Rock Mechanics and Mining Science & Geomechanics Abstracts, 32*, 11-36.

ISRM. (1973). Rock Characterization, Testing and Monitoring. . Pergamon Press.

Itasca. (2011). FLAC version 7.0. Itasca Consulting Group.

Jhon, C. M., & Van Dillen, D. E. (1983). Rock bolts: A new numerical representation and its application in tunnel design., (pp. 13-25 (Cited in Moosavi 1994)). Texas A&M University.

Jiang, Y., Li, B., & Yamashita, Y. (2009). Simulation of cracking near a large underground cavern in a discontinuous rock mass using the expanded distinct element method. *International Journal of Rock Mechanics and Mining Sciences 46*, 97-106.

Jing, L. (2003). A review of techniques, advances and outstanding issues in numerical modelling for rock mechanics and rock engineering. *International Journal of Rock Mechanics and Mining Sciences, 40*, 283-353.

Jing, L., & Hudson, J. (2002). Numerical methods in rock mechanics. *International Journal of Rock Mechanics and Mining Sciences, 39*, 409-427.

Kabwe, E., & Wang, Y. (2015). Review on rockburst theory and types of rock support in rockburst prone mines. *Open Journal of Safety Science and Technology, 5(04)*, 104.

Kaiser, P. (2014). Deformation-based support selection for tunnels in strainburst-prone ground. In Y. Potvyn, & M. Hudyma (Ed.), *DeepMining 2014*. Sudbury, Canada: ACG.

Kaiser, P. K. (2018). Ground control in strainbursting ground-A critical review and path forward on design principles. *RaSim9*, 146-158. (J. Vallejos, Ed.) Santiago, Chile.

Kaiser, P. K., & Maloney, S. M. (1997). Scaling laws for the design of rock support. *Pure and applied geophysics, 150(3–4)*, 415–434.

Kaiser, P. K., McCreath, D. R., & Tannant , D. D. (1996). *Canadian Rockburst Support Handbook 1996*. Geomechanics Research Centre.

Kaiser, P., & Cai, M. (2013a). Critical Review of design principles for rock support in burstprone ground-time to rethink! *Ground support*, 3-38. (Y. Potvin, & B. Brady, Eds.)

Kaiser, P., & Cai, M. (2013b). Rockburst damage mechanism and support design principles. *RaSim8*, (pp. 349-370). Saint-Petesburg, Moscow,Russia.

Labuz, J., & Zang, A. (2014). Mohr–Coulomb failure criterion. In *SRM Suggested Methods for Rock Characterization, Testing and Monitoring: 2007-2014*. Springer.

Lei, X. Y. (1996). Formulation and application of 3D anchor bolt elements. *Engineering Mechanics, 2*.

Li, B., Qi, T., Wang, Z. Z., & Yang, L. (2012). Back analysis of grouted rock bolt pullout strength parameters from field tests. *Tunnelling and Underground Space Technology*, 345-349.

Li, C., & Doucet, C. (2012). Performance of d-bolts under dynamic loading. *Rock Mechanics and Rock Engineering*, 193-204.

Li, C., & Stillborg, B. (1999). Analytical models for rock bolts. *International Journal of Rock Mechanics and Mining Sciences. 36*, 1013 - 1029.

Ma, S. e. (2015). Numerical modeling of fully grouted rockbolts reaching free-end slip. (A. S. Engineers, Ed.) *International Journal of Geomechanics, 16(1),*, 4015020.

Ma, S., Nemcik, J., & Aziz, N. (2014). Simulation of fully grouted rockbolts in underground roadways using FLAC2D. *Canadian Geotechnical Journal ;51(8)*, 911-920.

Malmgren, L., & Nordlund, E. (2008). Interaction of shotcrete with rock and rock bolts: a numerical study. *International Journal of Rock Mechanics and Mining Sciences;45(4)*, 538-553.

Malvar, L. J., & Crawford, J. E. (1998). Dynamic increase factors for steel reinforcing bars. Orlando, Florida: Proceedings of the 28th Department of Defense Explosives Safety Board Seminar, Department of Defense Explosives Safety Board.

Marambio, E., Vallejos, J., Burgos, L., González Castro, L., Saure, J., & Urzúa, J. (2018). *Numerical modelling of dynamic testing for rock reinforcement used in underground excavations. Proceedings of the fourth international symposium on block and sublevel caving, pp 767-780*. Vancouver, Canadá.

Marence, M., & Swoboda, M. (1995). Numerical model for rock bolt with consideration of rock joint movements. *Rock Mechanics & Rock Enginnering 28.(3)*, 145-165.

Martin, C. D., Kaiser, P. K., & McCreath, D. R. (1996). Hoek-Brown Parameters for predicting the depth of brittle failure around tunnels. *Canadian Geotechnical Journal, 36,N°1*, 136-151.

McKenzie, R. (2002). Use of cone bolts in ground prone to rockburst. *Coal Operators' Conference* . The AusIMM Illawarra Branch.

Mikula, P. A. (2012). 'Progress with empirical performance charting for confident selection of ground support in seismic conditions'. *Mining Technology, 121(4)*, 192–203.

Moosavi, M., & Bawden, W. F. (2003). Shear strength of Portland cement grout. *Cement and Concrete Composites*(25(7)), 729-735.

Moosavi, M., Jafari, A., & Khosravi, A. (2005). Bond of cement grouted reinforcing bars under constant radial pressure. *Cement and Concrete Composites, 27*, 103-109.

Moussa, A., & Swoboda, G. (1995). Interaction of rock bolts and shotcrete tunnel lining. *Int.Sym. of Numerical models in Geomechanics*, (pp. 443-449).

Muñoz, A. (2016). *Criterios básicos de forticación.*

Nemcik, J., Ma, S., Aziz, N., Ren, T., & Geng, X. (2014). Numerical modeling of failure propagation in fully grouted rock bolts subjected to tensile load. *International Journal of Rock Mechanics and Mining Sciences, 71*, 293-300.

Nierobisz, A. (2006). The model of dynamic loading of rockbolts. *51(3)*, 453-470.

Nilsson, C. (2009). Master thesis. *Modelling of dynamically loaded shotcrete, Royal Institute of Technology*.

Oler, R. (2012). DSI new developments in yieldable rock bolts. *Technical report, Dynamic Ground Support Application Symposium.*

Ortlepp, W. (2000). *Realistic dynamic stope support testing GAP 611. Technical report*. Research Advisory Committee, SIMRAC.

Ortlepp, W., & Stacey, T. (1998). *Testing of tunnel support: dynamic load testing of rockbolt elements to provide data for safer support design. Final project report GAP 423*. Safety in Mines Research Advisory Committee, SIMRAC.

Ortlepp, W., Human, L., Erasmus, P., & Dawe, S. (2005). Static and dynamic load-displacement characteristics of a yielding cable anchor-determined in a novel testing device. *Rock Burst and Seismicity in Mines (RaSiM6)* (pp. 529-534). Perth: Australian Centre for Geomechanics.

Pal, S., & Wathugala, G. W. (1999). Disturbed state model for sand–geosynthetic interfaces and application to pull-out tests. *International journal for numerical and analytical methods in geomechanics, 23(15)*, 1873-1892.

Palmström, A. (1995). 'Characterizing the strength of rock masses for use in design of underground structures. *International conference in design and construction of underground structures.*

Pardo, C., & Villaescusa, E. (2012). Methodology for back analysis of intensive rock mass damage at the El Teniente Mine. *MassMin 2012, 6th Int Conf & Exhibition on Mass Mining,*. Sudbury.

Peng, S., & Guo, S. (1993). An improved numerical model of grouted bolt-roof rock interaction in underground openings. *Rock support in mining and underground construction*, (pp. 67-74). Canada.

Player, J. (2012). *Dynamic testing of rock reinforcement systems*. Curtyn University.

Player, J., & Cordova, M. (2009, June 18). WASM Dinamyc results-Reinforcement. Company El Teniente. WA School of Mines.

Player, J., Villaescusa, E., & Thompson, A. (2008). An examination of dynamic test facilities Mining and Metallurgy. *In Australian Mining Technology Conference*. Melbourne: Australasian Institute of Mining and Metallurgy.

Player, J., Villaescusa, E., & Thompson, A. (2009). Dynamic testing of friction rock stabilisers. *RockEng09, Rock Engineering in Difficult Conditions*, (pp. 9-15). Toronto.

Player, J., Villaescusa, E., & Thompson, A. G. (2008). An Examination of Dynamic Test Facilities. *Australian Mining Technology Conference*. Melbourne: Australian Institute of Mining and Metallurgy.

Rao, S., & Yap, F. (2011). *Mechanical vibrations*. Prentice Hall, Upper Saddle River.

Rayleigh, L. (1877). *Theory of Sound*. New York: Dover Publications.

Renani, H. R., & Martin, C. D. (2018). *Modeling the progressive failure of hard rock pillars*. Tunnelling and underground space technology. 74, 71-81.

Ruest, M., & Martin , L. (2002). FLAC simulation of split-pipe tests on an instrumented cable bolt. *Proceedings of the 104th Annual General Meeting of the Canadian Institute of Mining, Metallurgy and Petroleum*. Montreal: Canadian Institute of Mining, Metallurgy and Petroleum.

Saeb, S., & Amadei, B. (1990). Finite element implementation of a new model for rock joints. *Int. Symp. of Rock Joints*, (pp. 707-712).

Scott, C., Penney, A. R., & Fuller, P. (2008). Competing factors in support selection for the west zone of the Beaconsfield Gold Mine, Tasmania'. In AusIMM (Ed.), *Narrow Vein Mining Conf*, (pp. 173–178). Ballarat, Vic., Australia.

Shen, B., Shi, J., & Barton, N. (2018). An approximate nonlinear modified Mohr-Coulomb shear strength criterion with critical state for intact rocks. *Journal of Rock Mechanics and Geotechnical Engineering*(10(4)), 645-652.

Shreedharan, S., & Kulatilake, P. H. (2016). Discontinuum–equivalent continuum analysis of the stability of tunnels in a deep coal mine using the distinct element method. *Rock Mechanics and Rock Engineering, 49(5)*, 1903-1922.

Singh, B., & Goel, R. K. (1999). Rock mass classification: a practical approach in civil engineering. Elsevier.

Stacey, T. (2016). Addressing the Consequences of Dynamic Rock Failure in Underground Excavations. *Rock Mechanics and Rock Engineering 49(10)*, 4091-4101.

Stankus, J. C., & Guo, S. (1996). Computer automated finite element analysis-A powerful tool for fast mine design and ground control problem diagnosis and solving. *5th Conference on the use of computer in the coal industry*, (pp. 108-115). West Virginia-USA.

Stillborg, B. (1983). Research carried out within the Swedish Mining Research Foundation in relation to cables and cable bolting. In O. Stephansson (Ed.), *Proceedings of the International Symposium on Rock Bolting (Rock Bolting: Theory and Application in Mining and Underground Construction,Abisko, Sweden)*, (pp. 571-573). Balkema, Rotterdam.

St-Pierre, L. (2007). Development and validation of a dynamic model for a cone bolt anchoring system. PhD thesis. McGill University.

Swoboda, G., & Marence, M. (1991). 'FEM modelling of rockbolts. *Proceedings of Computer Method and Advances in Geomechanics* (pp. 1515–1520). Cairns (Australia): Balkema.

Syed, A. (2004). Studies on support design for Underground excavations. Bangalore University.

Tatone, B. S., Lisjak, A., Mahabadi, O. K., & Vlachopoulos, N. (2015). Incorporating rock reinforcement elements into numerical analysis based on the hybrid finite-discrete element method (DFEM). *Proceedings of ISRM Congress*. Montreal, Canada.

Thompson, A., Villaescusa, E., & Windsor, C. (2012). Ground support terminology and classification: an update. *Geotechnical & Geological Engineering, 30(3)*, 553-580.

Vallejos, J., Marambio, E., Burgos, L., & González, C. (2020). *Numerical modelling of the dynamic response of threadbar under laboratory-scale conditions*. Tunnelling and underground space technology.

Vardakos, S. S., Gutierrez, M. S., & Barton, N. R. (2007). Back-analysis of Shimizu Tunnel No. 3 by distinct element modeling. *Tunnelling and Underground Space Technology 22(4)*, 401-413.

Varden, R., Lachenicht, R., Player, J., Thompson, A., & Villaescusa, E. (2008). Development and implementation of the garford dynamic bolt at the kanowna belle mine. *In 10th underground operators conference*, (pp. 14-16). Launceston, Australia.

Villaescusa, E. (2012). *Static and dynamic laboratory testing of rock reinforcement systems - el Teniente mine.Technical report*. Western Australian School of Mines - Curtin University.

Villaescusa, E., & Player, J. R. (2014). A Reinforcement Desigh Methodology for Highly Stressed Rock Masses. *8th Asian Rock Mechanics Symposium*. Sapporo, Japan.

Villaescusa, E., Thompson, A., & Player, J. (2005a). *Dynamic testing of ground support systems. Technical report*. Minerals and Energy Research Institute of Western Australia (MERIWA).

Villaescusa, E., Thompson, A., & Player, J. (2005b). Dynamic testing of rock reinforcement systems. *CRCMining Australian Mining Technology Conference-New Technologies to Produce More with Less. .* Melbourne, Australia.

Villaescusa, E., Thompson, A., & Player, J. (2015). *Dynamic testing of ground support systems. Technical report*. Minerals and Energy Research Institute of Western Australia (MERIWA).

Walton, G. (2014). Doctoral dissertation. *Improving continuum models for excavations in rockmasses under high stress through an enhanced understanding of post-yield dilatancy*. Queen's University.

Wu, Y., Oldsen, J., & Lamothe, M. (2010). The yield-lok bolt for bursting and squeezing ground support. In M. Van Sint Jan, & Y. Potvin (Ed.), *Proc. 5th Int. Seminar on Deep and High Stress Mining* (pp. 301-308). Santiago, Chile: Australian Centre for Geomechanics.

Xie, S. Y., & Shao, J. F. (2008). Experimental study of mechanical behaviour of cement paste under compressive stress and chemical degradation. *Cement and Concrete Research, 38* , 1416-1423.

Yanyi, Y. (1994). Analytical model for evaluating reinforcement efficiency of bolts in layered rock masses . *Chinese Journal of Rock Mechanics and Engineering, 4*.

Zhang, C., Tahmasebinia, F., Varsar, O., Canbulat, I., & Saydam, S. (2018). A numerical and analytical study of the behavior of fully grouted rock bolts under shear dynamic loading. *10th Asian Rock Mechanics Symposium*.

Zhou, Y., & Zhao, J. (2011). In *Advances in rock dynamics and applications*. CRC Press.